Titre: Title:	Development of Biocomposites Based on Cellulosic Reinforcements
Auteur: Author:	Helia Sojoudiasli
Date:	2017
Type:	Mémoire ou thèse / Dissertation or Thesis
Référence: Citation:	Sojoudiasli, H. (2017). Development of Biocomposites Based on Cellulosic Reinforcements [Thèse de doctorat, École Polytechnique de Montréal]. PolyPublie. https://publications.polymtl.ca/2514/

UNIVERSITÉ DE MONTRÉAL

DEVELOPMENT OF BIOCOMPOSITES BASED ON CELLULOSIC REINFORCEMENTS

HELIA SOJOUDIASLI

DÉPARTEMENT DE GÉNIE CHIMIQUE

ÉCOLE POLYTECHNIQUE DE MONTRÉAL

THÈSE PRÉSENTÉE EN VUE DE L'OBTENTION
DU DIPLÔME DE PHILOSOPHIAE DOCTOR

(GÉNIE CHIMIQUE)

AVRIL 2017

UNIVERSITÉ DE MONTRÉAL

ÉCOLE POLYTECHNIQUE DE MONTRÉAL

Cette thèse intitulée:

DEVELOPMENT OF BIOCOMPOSITES BASED ON CELLULOSIC REINFORCEMENTS

présentée par : SOJOUDIASLI Helia

en vue de l'obtention du diplôme de : Philosophiae Doctor

a été dûment acceptée par le jury d'examen constitué de:

M. TAVARES Jason-Robert, Ph. D., président

M. CARREAU Pierre, Ph. D., membre et directeur de recherche

Mme HEUZEY Marie-Claude, Ph. D., membre et codirectrice de recherche

M. GRMELA Miroslav, Ph. D., membre

M. RODRIGUE Denis, Ph. D., membre

DEDICATION

To my parents and my sister

ACKNOWLEDGEMENT

First and foremost, I would like to express my sincere gratitude and thanks to my supervisor, Professor Pierre J. Carreau, and my co-supervisor Professor Marie-Claude Heuzey for their patience, extensive knowledge and motivation. Their guidance helped me in this research and writing of the thesis. I could not have imagined having better mentors for my Ph.D.

I would like to thank the rest of my thesis committee for accepting to evaluate my thesis: Professors Denis Rodrigue, Miroslav Grmela, and Jason Robert Tavares.

I gratefully acknowledge the Natural Sciences and Engineering Research Council of Canada (NSERC) for funding.

My sincere thanks also goes to Professor Bernard Riedl who helped me through part of this research. I would also like to express my deepest appreciation to my colleagues in rheology group who shared their knowledge during our interesting discussions and became some of my close friends.

I appreciate the help and kind cooperation of technical and administrative staffs of Chemical Engineering Department of Polytechnique Montréal for being great help during my PhD, especially Melina Hamdine, Guillaume Lessard, Martine Lamarche, Gino Robin, Claire Cercle, Evelyne Rousseau and Valerie Baudart.

Friends are the colors of life and I am so very blessed to have a colorful life. I would like to thank every single one of my great friends for being a part of my journey and supporting me during these years. I'm grateful to have you in my life and be able to count on you like family.

And finally, my most loving thanks to those who matter to me the most, Mark, my parents Mahin and Ali and my lovely sister, Nika. I would like to express my gratitude to them and tell them they are my dearests and I would not be able to accomplish my goals without their unconditional love and support.

RÉSUMÉ

Les renforts cellulosiques sont une ressource renouvelable, biodégradable et biocompatible et leur faible densité ainsi que leur abondance élevée ont favorisé leur insertion dans les matrices polymères. Cependant, ces charges hydrophiles sont généralement incompatibles avec les matrices thermoplastiques communes non polaires telles que le polypropylène (PP) ou le polylactide (PLA). Le but de cette thèse est de développer des biocomposites possédant des propriétés mécaniques améliorées, à base de renforts cellulosiques.

Dans la première phase de cette étude, les propriétés rhéologiques, mécaniques et morphologiques des composites polypropylène/fibres de lin ont été étudiées. Les polypropylènes greffés anhydride maléique (PPMA) ou acide acrylique (PPAA) ont été utilisés comme compatibilisants. Il a été montré que le malaxage à l'état fondu de ces composites entraîne une diminution de la longueur moyenne des fibres d'environ 70%. Par ailleurs, nous avons observé que l'ajout de compatibilisants, améliore l'interaction fibre/polymère et conduit à une plastification de la matrice. L'équilibre entre ces effets concurrents détermine le comportement rhéologique du composite. Le PPMA et le PPAA se sont avérés efficaces, mais leur efficacité dépend de leur indice de fluidité à chaud (MFI) et de leur teneur en groupements greffés. Les tests en traction ont montré que le module d'Young du composite contenant 30% en poids de fibres de lin est amélioré de 200% et que sa résistance à la rupture augmente de 60%, par rapport au PP. Le PPMA, ayant la teneur la plus élevée en groupements anhydrides maléiques, s'est avéré le plus efficace pour améliorer la compatibilité interfaciale entre la matrice PP et les fibres de lin, toutefois l'effet plastifiant de cet agent de couplage est significatif.

Dans la seconde partie de ce travail, les propriétés rhéologiques, mécaniques, morphologiques et thermiques des composites PP/nanocristaux de cellulose (CNC), préparés par malaxage à l'état fondu ont été étudiées. Le PPMA a été utilisé comme compatibilisant pour ce système. Les influences de deux températures d'élaboration et de deux PPs de poids moléculaires différents ont été étudiées. Il a été montré qu'en présence de CNC la dégradation du PP à une température d'élaboration élevée avait un effet significatif sur le comportement rhéologique de ces systèmes. Lors des tests en traction, le module d'Young des composites contenant 2% en poids de CNC est amélioré d'environ 30% et leur résistance à la rupture est augmentée jusqu'à 16%, par rapport aux matrices seules. En revanche, la contrainte à la rupture des composites diminue de 17% à 75% par rapport à la matrice, en fonction des conditions d'élaboration et du poids moléculaire du PP. Dans

le cas du PP de faible poids moléculaire, les composites élaborés à une température plus élevée ont montré de meilleures propriétés mécaniques. D'autre part, les meilleures propriétés mécaniques sont obtenues pour les composites à base de PP possédant un poids moléculaire élevé, élaborés à une faible température. L'extrusion bi-vis des composites à base de PP de faible poids moléculaire s'est avérée plus efficace que l'utilisation d'un mélangeur interne, pour l'élaboration de ces composites. Le module d'Young des composites PP/CNC peut être décrit par le modèle proposé par Nielsen, basé sur l'équation d'Halpin-Tsai. Enfin, il a été observé que les composites PP/CNC présentent une bonne ductilité, avec une augmentation de la contrainte à la rupture, par rapport au PP, comprise entre 43% et 73% PP, alors que les composites PP/fibres de lin sont fragiles, avec une contrainte à la rupture inférieure de 0,06 à celle de la matrice.

Dans la dernière partie de cette thèse, l'état de dispersion des CNC et CNC modifiés (mCNC) a été étudié dans du diméthyl sulfoxyde (DMSO). Les mCNC ont été modifiés par greffage d'un chlorure d'acide organique à la surface des nanoparticules. L'efficacité de cette modification de surface est confirmée par spectroscopie de photoélectrons aux rayons X (XPS). A température ambiante, les propriétés rhéologiques des suspensions de CNC restent quasiment inchangées au cours du temps, alors qu'à une température de 70°C un gel se forme après un jour, même à une très faible concentration de CNC (1% en poids). Pour les suspensions contenant 3% en poids de CNC, la viscosité complexe mesurée à 70°C augmente de près de 4 décades après une journée. Pour les mCNCs dans du DMSO, un gel faible est formé à partir du premier jour et la température n'a pas affecté la gélification et l'évolution de la viscosité complexe est faible, après un jour. Les propriétés rhéologiques des gels de mCNC à 70°C sont largement plus faibles que celles des gels de CNC. Enfin, l'ajout de 10% en poids de polylactide (PLA) au milieu ne prévient pas la formation de gels pour les suspensions CNC. De plus, la viscosité et le module de stockage réduits des suspensions de CNC et de mCNC dans un milieu PLA/DMSO sont considérablement inférieurs à ceux des échantillons sans PLA. Ce résultat a été attribué aux mauvaises interactions entre les nanoparticules et les chaînes de PLA et à la diminution du mouvement brownien des nanoparticules, due à l'augmentation de la viscosité du milieu de la suspension. Au meilleur de nos connaissances, c'est la première fois que la gélification des suspensions de CNC et de mCNC, avec une très faible teneur en solvant polaire non aqueux et non-toxique comme le DMSO, a été étudiée.

ABSTRACT

Interesting properties of cellulosic reinforcements such as their low density, renewability, biodegradability, absence of health hazard and high abundance have favored their use in polymer composites. The key issue for polymer composites based on cellulosic reinforcements is the incompatibility between these hydrophilic fillers and non-polar common matrices such as polypropylene (PP) or polylactide (PLA). The main objective of this dissertation is to develop polymer biocomposites with enhanced mechanical properties based on cellulosic reinforcements.

In the first phase the rheological, mechanical and morphological properties of flax fiber polypropylene composites were investigated. PP grafted maleic anhydride (PPMA) and PP grafted acrylic acid (PPAA) were utilized as compatibilizers. Compounding resulted in a decrease of the mean fiber length by about 70%. It has been observed that both compatibilizers, besides enhancing fiber/polymer interaction, can lead to plasticization and the balance between these competing effects determined the overall rheological behavior of the composite. PPMA and PPAA were effective compatibilizers for PP/flax fiber composites, but their efficiency depended on their melt flow index (MFI) and grafted group content. The tensile modulus of the composite containing 30 wt% flax fibers was improved by 200% and the tensile strength improved by 60% in comparison with the neat PP. The PPMA with the highest content of MA was found to be the most efficient in improving the interface between the PP matrix and the flax fibers, however the plasticizing effect of this coupling agent was significant.

In the second phase the rheological, mechanical, morphological and thermal properties of PP/cellulose nanocrystal (CNC) composites prepared in the molten state were investigated. PPMA was used as a compatibilizer for this system. The effect of two different processing temperatures with two different molecular weight PPs has been investigated. Degradation of the PP in the presence of CNCs at high processing temperature was shown to have a significant effect on the rheological behavior. The tensile modulus of composites containing 2 wt% CNCs was improved by about 30% and the tensile strength was increased up to 16%, in comparison with the neat matrices. The tensile strain at break of the composites decreased by 17% up to 75% with respect to the matrix, depending on the processing conditions and PP grade. For low molecular weight PP the composites processed at higher temperature showed better mechanical properties. On the other hand, better mechanical properties were obtained for the high molecular weight PP-based

composites processed at lower processing temperature. Preparing the low molecular weight PP composites via twin-screw extrusion was shown to be more efficient than using an internal batch mixer. The tensile modulus of the PP/CNC composites could be fairly well described by a model proposed by Nielsen based on the Halpin-Tsai equation. Finally, it was observed that the PP/CNC composites exhibited a good ductility, with their strain at break varying between 43 and 73% of the PP value in comparison to the PP/ flax composites, which were brittle and their strain at break was less than 0.06 of that of the matrix.

In the last phase, the potential use of dimethyl sulfoxide (DMSO) as a dispersing medium for CNCs and modified CNCs (mCNC) was investigated. Cellulose nanocrystals have been modified via grafting an organic acid chloride on the surface of the nanoparticles. The efficiency of surface modification has been confirmed by X-ray photoelectron spectroscopy (XPS). The rheological properties of CNC suspensions did not change significantly with time at room temperature, but the CNC suspensions at 70 °C underwent gel formation, even at a very low concentration (1 wt%) after one day. For suspensions containing 3 wt% CNCs, the complex viscosity at 70 °C increased by almost 4 decades after one day. For the mCNCs in DMSO a weak gel was formed from the first day and temperature did not affect the gelation and changes in the complex viscosity after one day were marginal. The rheological properties of the mCNC gels at 70 °C were found to be much lower than those of the CNC gels. Finally, the effect of adding 10 wt% of polylactide (PLA) to the solvent on the rheological properties of CNC and mCNC suspensions was investigated. PLA did not prevent gel formation for the CNC suspensions. However, the reduced viscosity and storage modulus of the CNC and mCNC suspensions in PLA/ DMSO were considerably lower than those of samples without PLA. This has been attributed to poor interactions between the nanoparticles and the PLA chains and the decreased influence of the Brownian motion due the increased viscosity of the suspending medium. To the best of our knowledge this is the first time that the gelation of CNC and mCNC suspensions at very low content in a polar non-aqueous, safe solvent like DMSO has been investigated.

TABLE OF CONTENTS

LIST OF TABLES

LIST OF FIGURES

CHAPTER 1 INTRODUCTION

Using short conventional fibers (glass, carbon, etc.) to improve the mechanical properties of polymers has been considered by many industries for past decades [1]. Recently the use of short natural fibers such as sisal, jute, hemp and flax in reinforced thermoplastics has triggered new investigations in a number of industrial sectors [2]. Aqueous suspensions of cellulose nanocrystals (CNCs) can be prepared by acid hydrolysis of the biomass such as bacteria, cotton, and wood pulp [1]. The resulting nanocrystals are rod-like particles or whiskers, and depending on the source, these nanocrystals offer a wide range of aspect ratios. The natural cellulosic fibers offer numerous advantages compared to "man-made" ones: low density, low cost, availability, biodegradability, absence of health hazard, high filling potential, high stiffness and good specific mechanical and acoustic insulation properties [3, 4]. Also the abrasive action of natural fibers to equipment is less severe compared to that of glass and carbon fibers [5].

Despite their interesting properties, the key issue for cellulosic fiber-reinforced polymers is the incompatibility between the hydrophilic particles and thermoplastic polymers such as polyprolylene (PP) and polylactide (PLA) [6]. This incompatibility generally results in poor particle wetting [7], presence of aggregates [1], and weak stress transfer at the interface of particle-matrix. Since the most effective ordinary solvent for dispersing cellulose nanocrystal (CNC) particles is water, mostly water-soluble polymers or water-based emulsions such as latex [8], polyvinyl alcohol (PVOH) [9] and polyethylene oxide (PEO) [10] have been studied for preparing CNC nanocomposites.

Melt processing is the most economical and environment-friendly method of preparing polymer composites. This technique has been used to produce biocomposites of cellulosic based fillers. Generally the dispersion of non-modified particles is worse in melt mixing in comparison to solvent-casting method. This can be attributed to the cellulosic reinforcements strong hydrogen bonds that needs a solvent or very high mechanical force to break.

Different chemical surface modifications of CNCs like acetylation [11], TEMPO-mediated oxidation [12], grafting [13-17] have been investigated. It is expected that surface modification of CNCs should improve the dispersion of the filler within a polymeric matrix by improving the interface between polymer and particles, but it may also decrease the hydrogen bonds between the nanoparticles. These bonds were reported to be the basis of the reinforcing effect of cellulose

whisker nanocomposites [18]. Besides chemical surface modification, compatibilizers like PPMA have been widely used to compatibilize cellulosic based fillers with hydrophobic polymers like PP [19-21]. The efficiency of these compatibilizers highly depends on their grade and content [21].

In this work common preparation methods were used to develop biocomposites with enhanced mechanical properties based on cellulosic reinforcement. The main contributions of this research are reported in three scientific articles that represent the core of the thesis.

The document consists of the following chapters:

- Chapter 1: Introduction
- Chapter 2: Literature review
- Chapter 3: Objectives
- Chapter 4: Organization of the articles
- Chapters 5 to 7: The three articles reporting the main results of this project
- Chapter 8: General discussion
- Chapter 9: Conclusion and recommendation

CHAPTER 2 LITERATURE REVIEW

2.1 Structure and chemistry of cellulosic fibers

Natural vegetable fibers, based on their origin, can be classified into different groups. Figure 2.1 presents the classification of vegetable natural fibers in more details.

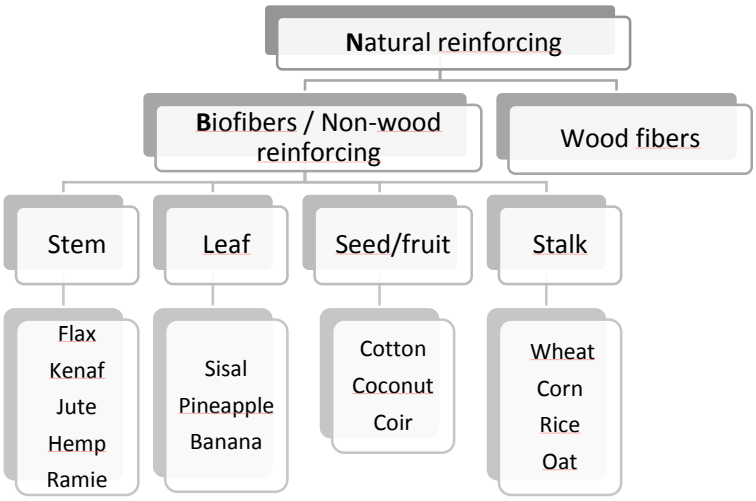

Figure 2.1 Classification of natural fibers based on their origin [22].

Jute, ramie, flax and sisal are the most commonly used fibers in polymer composites [5]. Natural plant fibers consist of helically cellulose micro fibrils, bound together by an amorphous lignin matrix. Lignin acts as a protection against biological attacks, which also keeps the water in fibers and gives stiffness to stems. Pectin and hemicellulose in natural fibers are polysaccharide matrices that act as compatibilizers between cellulose and lignin and keep different elements including fibers together [23]. Surface of most commercial grades of lignocellulosic fibers is covered with a wax which helps separating the fibers. Natural fibers, based on their origin, harvest and type of extraction may contain different components. In Table 2.1 the composition of different components for various natural fibers is presented.

Flax fibers are widely used in Europe and North-America. They exhibit a specific elastic modulus between 20 and 50 m^2/s^2 [24] and a very high tensile strength (up to 1500 MPa for elementary fibers and around 800 MPa for bundles) [6].

Table 2.1 Chemical composition of some natural fibers [25].

Fiber	Cellulose (wt%)	Lignin (wt%)	Hemicellulose (wt%)	Pectin (wt%)	Wax (wt%)	Moisture Content (wt%)
Jute	61-71.5	12-13	13.6-20.4	0.4	0.5	12.6
Hemp	70.2-74.4	3.7-5.7	17.9-22.4	0.9	0.8	10
Kenaf	31-39	15-19	21.5	-	-	-
Flax	71	2.2	18.6-20.6	2.3	1.7	10
Ramie	68.6-76.2	0.6-0.7	13.1-16.7	1.9	0.3	8
Sisal	67-78	8-11	10-14.2	10	2	11
Cotton	82.7	-	5.7	-	0.6	-
Coir	36-43	41-45	10-20	3-4	-	8
Banana	63-67.6	5	19	-	-	8.7

2.2 Cellulose

Cellulose, the world's most abundant natural, renewable, biodegradable polymer, is a classic example of reinforcing elements that animals or plants synthesize as a skeletal composite. This composite consists of a matrix reinforced by fibrous biopolymers, which exist as whiskers like microfibrils that are biosynthesized and deposited in a continuous fashion. The chemical structure of cellulose, seen in Figure 2.2, is a carbohydrate polymer made up of repeating β-D-glucopyranose units and consists of three hydroxyl groups per anhydroglucose unit (AGU) giving the cellulose molecule a high degree of functionality [26]. Cellulose can be regarded as a homopolymer containing 2000 or more glucose units in each chain [27]. Cellulose fibers contain regions in which the chain molecules have a highly ordered (crystalline) arrangement and some in which there is a disordered (amorphous) arrangement [27]. The configuration of the glucose units is ß and in the crystalline areas these units are organised in *trans* positions. Such configuration of the glucose unit results in a highly symmetrical and compact molecular chain.

Cellulosic fibers can be used to produce crystalline microfibrils that are almost defect-free. This quite "primitive" polymer can be used to create high performance nanocomposites presenting

outstanding properties. This reinforcing capability results from the intrinsic chemical nature of cellulose and from its hierarchical structure [28].

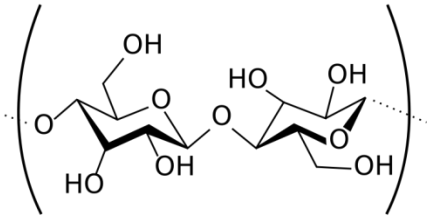

Figure 2.2 Chemical structure of cellulose

Cellulose has been recognised to exist mainly in two crystalline forms designated as Cellulose I and II. Cellulose I is the crystal structure of native cellulose. The average value of crystallinity is about 66.67%. Cellulose II occurs in regenerated materials (viscose, cellulose sheets) and when native cellulose is treated with strong swelling agents (e.g. sodium hydroxide used in mercerisation) [27].

2.3 Cellulose nanocrystalline (CNC)

CNC was discovered in 1949, but it was only in 1995 that Favier et al. [29] used them in nanocomposites. These particles were used to improve the mechanical properties of solution-cast films of poly(styrene-co-butyl acrylate) latex [29]. Two main factors causing diversity of CNCs are: cellulose source material, which can differ in the biosynthesis of microfibrils, and extraction process which can change the crystallinity, charge, shape and size of particles. Aqueous suspensions of cellulose nanocrystals can be prepared by acid hydrolysis of the biomass from different sources like natural fibers or tunicate. The aim of this process is to dissolve away the amorphous regions of low lateral order. By using different types of acids for hydrolysis, different charges can be formed on the surface of CNCs [30]. Following acid hydrolysis, the microfibrils in the original cellulose are swollen and separated into much smaller crystalline cellulose units. Cellulose nanocrystals composed of nanofibrils exhibited Cellulose I structure [31].

Cellulose nanocrystals can be produced in three forms: rods, spheres and porous network [32]. The most conventional type of cellulose nanoparticles is rod-like [4], and depending on the source, these nanocrystals offer a wide range of aspect ratios (*L/d*, *L* being the length and *d* the diameter), from 1 to about 100 [5]. Different terms are used to refer to CNCs in the literature: nanocrystalline cellulose (CNC), cellulose whiskers and cellulose nanowhiskers (CNWs).

As the nanowhiskers generated from cellulose fibers contain only a small number of defects in the crystalline structure, they have much higher mechanical properties than those of the initial fibers. This highly ordered structure produces not only unusually high strengths, but also significant changes in electrical, optical, magnetic, ferromagnetic, dielectric, conductive, and even superconductive properties. Since these whiskers contain only a small number of defects, their axial Young modulus is close to that derived theoretically from their chemistry and potentially stronger than steel and similar to Kevlar [28]. Because of their small size, it is not possible to measure directly the Young modulus and strength of CNCs. It was reported that the cellulose crystal regions exhibit a Young modulus up to 143 GPa [6], whereas the Young modulus of flax fibers has been reported to be about 28 GPa [7].

In many publications on reinforcement of polymer matrices, cellulose whiskers have been extracted from tunicate as this type of whiskers has higher aspect ratio even though the availability of these CNCs is restricted. Compared to ramie whiskers-based nanocomposites, the higher modulus values obtained for tunicin whiskers-based nanocomposites are mainly ascribed to both the higher aspect ratio of tunicin whiskers, of about 70 (only 30 for ramie whiskers) and the higher elastic modulus of the tunicin network [33].

2.4 Comparison with other fillers

Compared to inorganic fillers, the main advantages of lignocellulosic fillers are listed below [28]:

- Renewable
- Wide variety of fillers available throughout the World
- Absence of health hazard
- Non-food agricultural based economy
- Low energy consumption
- Low cost
- Low density
- High specific strength and modulus
- High sound attenuation of lignocellulosic based composites
- Comparatively easy processability due to their nonabrasive nature, which allows for high filling levels, resulting in significant cost savings
- Relatively reactive surface, which can be used for grafting specific groups.

Besides, the energy consumption for manufacturing non-woven natural fiber, including culture, harvesting and fiber separation, is only a third of the energy necessary for the manufacturing of glass-fiber mats [4].

Physical and mechanical properties of natural and manmade fibers and fillers are compared in Table 2.2. As it can be noticed here, a drawback of these fibers lies in their intrinsic variability. For example the modulus of flax fiber varies from 28 to 80 GPa. The behavior and the properties of natural fibers depend on many factors, such as harvest period, weather variability, quality of soil and climate of the specific geographic location as well as preconditioning [1, 34]. In addition, the natural fiber diameter distribution is much wider compared to glass fibers and the surface roughness of natural fibers is sensitive to the preparation technique [1, 34, 35].

Table 2.2 Properties of natural fibers and man-made fibers [23, 36].

Fiber	**Density (ρ) [g/cm^3]**	**Modulus *(E)* [GPa]**	**Strength (σ_u) [MPa]**
Flax	1.4 – 1.5	28 – 80	345 – 1500
Jute	1.3 – 1.5	13 – 30	393 – 800
Sisal	1.3 – 1.5	9 – 38	468 – 700
Ramie	1.5	44 – 128	400 – 938
Hemp	1.5	70	550 – 690
Glass fiber-type E	2.5	70	2000 – 3500
Glass fiber-type S	2.5	86	4570
Aramide	1.4	63 – 67	3000 – 3150
CNC	1.5	128	-

2.5 Polypropylene (PP)

Because of its low price, good mechanical properties, processability, relatively low melting temperature and widespread use in technical applications [6], polypropylene (PP) is one of the best candidates as a matrix for many industrial applications. This polymer was discovered in the early 1950s by Giulio Natta. PP is a macromolecule of hydrocarbons, composed of only carbon and

hydrogen atoms. Even though its hydrophobic nature can protect the cellulosic fibers [37], this characteristic nature of PP makes it highly incompatible with these fibers [38].

Three different stereochemical configurations of PP can be produced depending on the catalyst and the method of polymerization: atactic, isotactic and syndiotactic (Figure 2.3). Isotactic PP has a T_g in the range of −10 to 0 °C, melting point of 160-170 °C. Considering the wide use of PP, this material is mainly discussed in the following section on composites of cellulosic fibers.

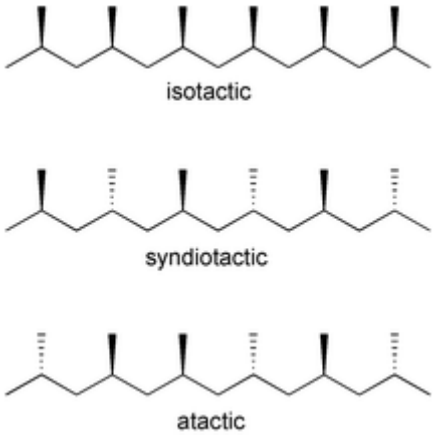

Figure 2.3 Different tacticities of polypropylene [39]

2.6 Composites of cellulosic fibers

The use of short natural fibers such as sisal, jute, hemp, coir (coconut fiber) and flax in reinforced thermoplastics has triggered new investigations in a number of industrial sectors, notably the automotive industry, construction, textiles, etc. [2]. Ford's materials engineering department in Cologne, Germany has done considerable development work in the area of injection mouldable flax/PP grades for radiator grills, front ends and engine shields for the new Ford Focus [27]. The main problem of natural fibers is their hydrophilicity, which will cause incompatibility hydrophobic polymers [6]. This incompatibility generally results in poor fiber wetting [7], presence of bundles [1], and weak fiber-matrix adhesion. The other consequence of these filler's hydrophilicity is their high water uptake and moisture adsorption tendency, which results in mechanical instability of final products and hinders the durability of these materials in outdoor usages [40]. Another important limitation of lignocellulosic materials is their relatively low degradation temperature, limiting the processing temperature to about 200 °C. This restrains the choice of polymers that can be used with natural fibers to polymers with relatively low processing temperatures such as polyethylene (PE), polypropylene (PP) and polyvinyl chloride (PVC) [3].

Rheological characterization provides knowledge essential both for process development and for fundamental flow characterization of filled thermoplastics. Generally, the rheological behavior of filled systems is quite complex, and the relationships between the fibers at the microstructural level and the macroscopic properties are still not fully understood [41]. Because of the great interest in cellulose and natural fiber composites, the rheological behavior of suspensions of these fillers in different polymer matrices has been examined by different investigators. The flow properties depend on fiber length, stiffness and strength, volume fraction of the filler, state of dispersion and fiber-matrix adhesion [35, 42-44]. Increasing the volume fraction of fibers can increase their entanglement and also resistance to flow with increases in viscosity [43, 45-48]. Besides shear viscosity, the addition of filler increases the storage and loss moduli of the polymer matrix, especially when the fiber aspect ratio (*L/D*) is significant. This behavior has been also observed by different authors in composites of natural fibers [19, 45].

It has been reported that shear thinning is more pronounced and the power-law index, *n*, decreased with increasing filler content, because of disentanglement, breakage and orientation of the fibers [47, 49]. Feng et al. [47] revealed that for composites of sisal fibers the decrease in the power-law index is a result of the aspect ratio reduction. In composites with larger contents of fiber, individual fibers are subjected to more stress from other fibers, which results in more fiber breakage.

Pre-shearing also was shown to decrease the complex viscosity due to orientation of fibers [43]. Kim et al. [44] noticed that the initial value of the complex viscosity was not recovered and was smaller for larger pre-shearing shear rates [50].

George et al. [48] studied the effect of length of pineapple fibers on rheological behavior of composite. They noticed that the viscosity marginally increased with increases of fiber length from 2 to 10 mm. Also this caused a poorer dispersion of fibers at the same time. Fibers of shorter length were more easily aligned and distributed along the flow direction than longer fibers and resulted in less flow resistance of the composite [47]. On the other hand, longer fibers were more easily broken down during processing as indicated by the decreasing ratio of weight average length to number average length (*Lw*/*Ln)* [43].

Arias et al. [51] used small amplitude oscillatory shear (SAOS) rheological measurements to investigate crystallization behavior of PLA/Flax composite. They observed that rheometry was a precise technique for analyzing the crystallization behavior of polymers in the temperature range which results in low to very low crystallization rates.

The effect of coupling agents on the flow properties of composites has also been studied by Hristov and Vlachopoulos [52]. They investigated different coupling agents (maleated polyethylenes, Polybond 3009, Polybond 3109 and Coesive F30) in maple wood flour composites based on high density polyethylenes (HDPEs) of different molecular weights (M_W) and molecular weight distributions (MWD). Using rotational and capillary rheometers combined with scanning electron microscopy (SEM) for morphological analysis, they found that low M_W and narrow MWD HDPEs led to larger viscosity increases with wood flour addition. They also showed that the presence of coupling agents led to significant interfacial adhesion improvements, as confirmed by scanning electron microscopy (SEM) analysis. Nevertheless, their investigation did not account for possible plasticizing effects of the coupling agents. Disregarding the plasticizing effect of the coupling agent, the viscosity of compatibilized composites may increase as a result of better wettability and high interfacial adhesion [7]. Crossover frequency of storage and loss modulus is used to calculate the average relaxation time of the sample. Twite-Kabamba et al. [19] reported an increase in the crossover frequency with hemp addition, with or without PP grafted maleic anhydride (PPMA), which revealed a loss of elasticity of the composites as the fibers were more rigid than the polymer chains. The crossover frequency increased with hemp concentration, indicating a decrease in the average relaxation time [19]. Le Moigne et al. [53] investigated the rheological behavior of flax and sisal-reinforced PP composites compatibilized with a PPMA. Even though they did not compare the properties of non-compatibilized samples with compatibilized ones, they observed a drastic decrease in the viscosity of the PP/PPMA blend in comparison with the neat PP, but this plasticization effect could have been counterbalanced by the effect of fibers to increase the viscosity. In general the studies on PP/flax composites focused on either mechanical or rheological properties of the composites.

2.7 Surface modification and compatibilization of lignocellulosic fibers

The most important factor for good fiber reinforcement in a composite is the strength of adhesion between the matrix polymer and the fibers [54]. Generally a strong interface allows effective stress transfer between the matrix and fibers, leading to a composite with high strength, but low toughness. Conversely, a weak interface would increase the incidence of crack splitting and delamination at the interface during fracture, thereby producing a composite with lower strength, but high toughness [27]. Lignocellulosic/thermoplastic composites usually have a high modulus, but suffer from low impact, tensile and bending strengths [55].

In order to overcome the problem of lignocellulosic fibers incompatibility with polyolefins, two methods have been proposed in the literature: impregnation and chemical modification. The former does not result in covalent bonding between the cellulosic material and the coupling agent. The latter, depending on the chemical reaction that occurs, can lead to different types of chemical bonds between the fibers and the matrix [56]. Two possible routes for chemical modifications are the grafting of molecules with functional groups compatible with the matrix, and the matrix modification by a surfactant or compatibilizer [2, 35, 57]. Compatibilizing and surface modification methods for cellulose reinforced composite can be classified as:

-Mercerization (alkaline treatment): This method includes surface treatment with NaOH solution to remove lignin, pectin and waxes covering the surface of natural fibers. This treatment can lead to the breakdown of fiber bundles into smaller fibers, increasing surface roughness and activating reactive groups on the surface, with consequently a better wetting of fibers by the polymer matrix.

-Chemical treatments such as esterification, etherification, graft copolymerization, permanganate treatment, acrylation, in-situ polymerization and etc. They include modifying the surface composition and creating chemical bonds with the polymer using different compounds such as silane, $KMnO_4$ and isocyanate.

-Surface treatments such as using cold plasma, corona, electron beam and photochemical approaches to functionalize either the surface of fiber or polymer.

-Heat treatment at temperatures higher than 180°C under inert atmosphere. This type of treatment affects the properties of hemicelluloses and lignin and the dimensional stability and durability of the composite.

-Using a compatibilizing agent as a treatment for both polymer matrix and filler. A coupling agent is a substance that functions at the interface to improve the compatibility of components by forming a chemical bridge between the reinforcement and matrix. Generally, one end of the molecule is tethered to the reinforcement surface and the functionality at the other end interacts with the polymer phase. Different types of coupling agents such as maleic anhydride grafted polyolefin, silane and titanate have been used to compatibilize natural fibers with polymers.

Although mercerization and chemical treatment of fibers have been reported in different investigations [23, 25, 46, 48, 56, 58-62] as effective methods for surface modification of natural

fibers, these methods are not favorable at industrial scales. In all the chemical surface modifications the usage of solvent is inevitable, which means an additional procedure is added to the process to evaporate and recover the solvent. In some cases the solvent is toxic and the procedure is time-consuming, besides the energy needed for solvent evaporation and recovery is noticeable. Therefore, in this literature review we will mostly concentrate on solvent free surface modifications for lignocellulosic fibers. Arbelaiz et al. [57, 63] and Cantero et al. [64] compared the effect of different surface modifications like silanation and alkalization and they observed that adding a maleated polypropylene (PPMA) was a more effective way to improve the tensile and flexural properties of PP/flax composites. Arbelaiz et al. [63] compared the effect of PPMA and MA treatment of fibers in PP composite reinforced by hybrid of glass and flax fiber. They revealed that PPMA-treated composite tensile strength values were higher than neat polypropylene [63], which indicated an improvement of stress transfer from the PP matrix to the flax fiber bundles [65]. Van de Velde and Kiekens [66] also confirmed that a matrix modification resulted in higher improvements in mechanical and adsorption characteristics than a fiber modification.

Maleic anhydride modification of polypropylene has often been used to make PP less hydrophobic and thus more compatible with polar fibers. The maleic anhydride polar groups form covalent and hydrogen bonds with the surface of the fibers, which improve the fiber–matrix adhesion. On the other hand, the PP segments of PPMA, through co-crystallization, form compatible blends with the bulk PP matrix [57]. Besides co-crystallization in the solid state, PP chains of PPMA may entangle with the chains of PP in the molten state, resulting in a better compatibility [54, 67]. Another advantage of matrix modification with a compatibilizer over fiber surface modification is the easier and more economical solvent-free processing, which is more environmental-friendly and less energy consuming.

As mentioned earlier, water uptake of natural fibers is another disadvantage of these fibers as it may affect the dimensional and environmental stability of their composites. Although PPMA must have the tendency to take up more water than normal PP (because of the presence of polar anhydride functions), composites with a PPMA matrix were shown to take up less water [66]. On the one hand sorption inside the matrix was in fact increased by the modification of the PP, but on the other hand this modification led to improved adhesion. This improved adhesion should prevent – to some extent – the flax fiber from taking up water. [66].

Paunikallio et al. [67] investigated the reactions between PPMA and viscose fibers via Fourier transform infrared (FT-IR) spectroscopy and proposed a two-step mechanism: 1) the activation of the copolymer by changing the carboxyl groups present in the PPMA to more reactive anhydride groups, which react more easily with hydroxyl groups at 150 – 160 °C and 2), the esterification of cellulose. The authors observed that the esterification, besides the creation of hydrogen bonds between PPMA and the surface of cellulosic fibers, led to a better adhesion of the fibers to the polymer chains. Unlike acrylic or methacrylic acid, maleic anhydride do not react with itself under typical industrial grafting conditions [68]. The decreased tendency to participate in side reactions makes maleic anhydride an appropriate moiety when grafting polar groups on PP [69].

According to Gauthier et al. [70] important parameters for the treatment using PPMA are the degree of grafting and the length of the grafted alkyl chains. When the hydrophilic group content is larger, the interactions between these groups and the surface of the fibers increase, but, on the other hand, the possibility of the existence of free MA in the material is higher. MA has been reported to react with the surface of cellulosic fibers and decreases their active sites [69]. Another key parameter is the length of the PP chains in PPMA compatibilizers. Long chains of PP will entangle with the matrix chains and cannot penetrate the fiber bundles. It has been also reported that the improved adhesion between the fibers and the matrix also prevented to some extent the flax fibers from absorbing water [66]. Often an optimum content of compatibilizer is needed. When the amount of compatibilizer is low (less than the critical concentration, ϕ_c), the limiting factor is the adhesive strength. With increasing compatibilizer concentration, the adhesive strength is improved through an increase in the number of polar interactions. However, at concentrations greater than ϕ_c, the cohesive strength (i.e. within the matrix) may be reduced due to the dense attachment of the polar molecular chains to the solid substrate and reduction in the chain entanglements of polar molecules with the bulk matrix. As a result, the cohesive strength can even be lower than the adhesive strength and the interface may fail cohesively instead of adhesively i.e. through the ‘interphase’ or bulk matrix, leading to a weaker adhesion [27]. This optimum content of compatibilizer for each system can be determined experimentally.

For the same fiber weight fraction, PPMA modified lignocellulosic fiber/PP composites exhibited similar or even superior specific mechanical properties than glass fiber/PP composites [63]. Twite-Kabamba et al. [19] revealed that PPMA can have dual effect as a compatibilizer and plasticizer depending on the content of fibers. At low contents of natural fibers, by keeping the ratio of

coupling agent to fiber constant, the added coupling agent would mostly remain in the matrix and the plasticizing effect would be dominant in that case. However, by increasing the content of hemp fibers, and accordingly coupling agent, the amount of PPMA and the interface of matrix-polymer interface would increase, resulting in a higher shear viscosity in comparison with the untreated composites.

2.8 CNC suspensions

Water is known as the best dispersing medium for CNCs. The nanoparticles are stabilized in aqueous suspension by negative charges of sulfate half-ester on their surface, which are introduced during the hydrolysis process [26, 71]. Derakhshandeh et al. [72] investigated yielding and flow of nanocrystalline cellulose (CNC) suspensions by rheological measurements and light scattering echo (LS-echo). Araki et al. [73] studied the rheology of CNC suspensions with the same size and particle shape with respect to their preparation methods. They found out that the rheological behavior of aqueous suspensions of CNCs hydrolyzed with H_2SO_4 is different from CNCs hydrolyzed with HCl. The HCl-treated CNC aqueous suspensions were thixotropic at high concentrations and anti-thixotropic at lower concentrations, whereas H_2SO_4-treated CNC aqueous suspensions showed no time-dependency for the viscosity. Even though both types of sample showed a shear-thinning behavior, the extent for the HCl-treated suspension was more important [73]. The flow curve of rod-like chiral nematic suspensions can be divided into three different flow regions: low, medium and high shear rates. Each region is attributed to different morphology of rod-like chiral nematic systems [74]. For this sample a plateau was surrounded by two shear-thinning regions. [75].

The first shear-thinning with a power law dependence of 0.5 refers to structured domains of the suspensions, which begins to deform at low shear rates. At intermediate shear rates the size of the domains decreases, which results in a viscosity plateau. At high shear rates the chiral nematic structure is distorted and particles start orienting in the flow direction, which causes the second shear-thinning region.

Bercea and Navard [75] studied the rheology of rigid cellulose whisker aqueous suspensions at various concentration regimes. They found out for dilute and semi-dilute regimes, two plateau regions at very low and high shear rates. One at low shear rates corresponded to the Newtonian plateau of randomly oriented particles and one at high shear rates related to the flow of oriented suspensions. There was a shear-thinning region between these two plateaus. The viscosity at the

high shear rate plateau was found to be linearly proportional to the concentration and much lower than that of the Newtonian low shear-rate plateau.

Shafiei-Sabet et al. [76] investigated the effect of ultrasonication on different CNC concentrations in aqueous suspensions (Figure 2.4). At high concentrations, for CNC suspensions before ultrasonication, a gel-like behavior was observed. It was noticeable that the viscosity of all samples was higher prior to sonication, and the difference became more significant for concentrated suspensions. The behavior of suspension containing 7 wt% CNCs changed from gel-like to liquid crystal behavior after sonication. This confirmed that ultrasound energy can break the gel structure and disperse the nanocrystals in the system, so that transition from isotropic to chiral nematic liquid crystal could occur in the system.

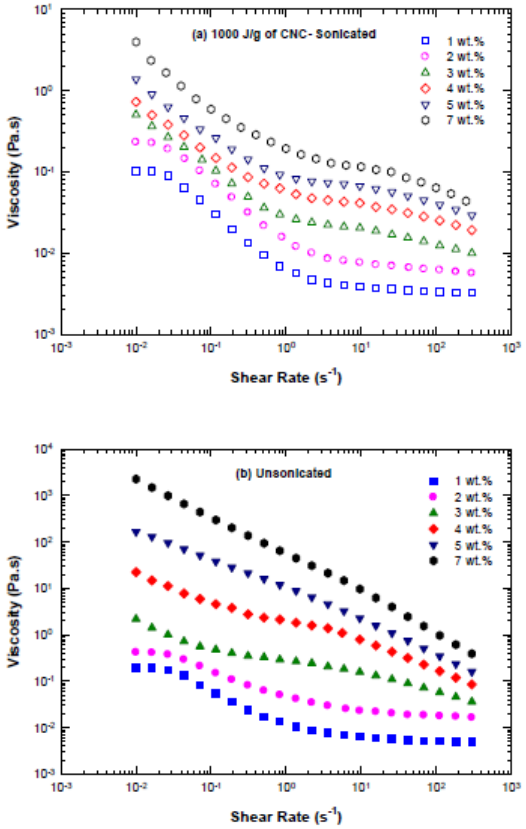

Figure 2.4 Steady-state viscosity versus shear rate for (a) CNC suspensions sonicated at 1000 J/g of CNCs, and (b) non-sonicated CNC suspensions with concentrations varying from 1 to 7 wt.% [76].

Hasani et al. [77] studied the properties of aqueous suspension of CNC particles modified through cationic modification with 2,3-epoxypropyltrimethylammonium chloride. Like HCl hydrolyzed-

CNC [73], the hydroxypropyltrimethylammonium chloride CNC (HPTMAC-CNC) suspensions exhibited a thixotropic behavior. They observed that the surface modification did not alter the dimension of particles. The gelation concentration for the modified CNCs was around 3.5 wt% where as for CNCs this behavior was observed at 7 wt% [76]. The gelation of the HPTMAC-CNC avoided chiral nematic phase formation [77].

As mentioned before the use of water as the dispersing medium for CNCs limits the preparation of CNC nanocomposites to water-soluble polymers like PEO. Using organic solvents like dimethylformamide (DMF) or dimethylsulfoxide (DMSO) in order to disperse CNCs has been proven successful [30, 78-80]. The negatively charged $O\text{-}SO_3^-$ groups on the surface of CNC particles are required to disperse freeze-dried nanoparticles in water or aprotic organic solvents like DMSO and DMF [30]. It has been observed that, since protic solvents like formic acid and *m*-cresol are well-known for their ability to break hydrogen bonds between particles, they are able to re-disperse CNCs that has been prepared via HCl hydrolysis and which do not have negative groups on their surface [30]. Viet et al. [79] observed that re-dispersing freeze-dried CNCs in DMSO and DMF containing a small amount of water (0.1%) was feasible. The apparent hydrodynamic radius of re-dispersed CNC in DMF and DMSO was 170 ± 153 nm and 160 ± 48 nm, respectively and it was concluded that DMSO was a better solvent than DMF for dispersing CNCs.

Fidale et al. [81] studied the swelling pattern of cellulose in protic and aprotic solvents. They observed that among all aprotic solvents, DMSO has superior swelling potential for cellulose of different sources. DMSO can form strong hydrogen bonds with mono and disaccharide oligomers and cellulose. Also they may form several hydrogen bonds with the same sugar moiety or several anhydroglucose units (AGU) of cellulose. Since the size of DMSO molecules is relatively small, they can penetrate between cellulose and form hydrogen bonds with one or several AGU on cellulose.

Toluene has also been used to disperse CNCs in an atactic polypropylene by solvent casting [82]. Since toluene was not able to break the agglomerates, the resulting mechanical properties and dispersion were not improved. This emphasises the importance of choosing the appropriate solvent for a given polymer, in which the CNC nanoparticles can be dispersed individually.

2.9 CNC nanocomposites

Since their discovery, cellulose whiskers have been used as reinforcing nanofillers in both synthetic and natural polymer matrices. The methods for preparing nanocomposites based on CNCs can be

divided into two general groups, which gave different mechanical and rheological properties to the resulting nanocomposites:

-Preparing films by cast/evaporated methods both with water and organic solvents

-Melt mixing

In cast/evaporating methods, water is the preferred processing medium because of the high stability of aqueous cellulose whisker dispersions and the expected high level of dispersion of the filler within the host matrix in the resulting composite film. On the other hand, this restricts the choice of the matrix to hydrosoluble polymers, and also this method is time consuming, which makes it inappropriate for industrial usage. A second alternative method of preparing is dispersing cellulose whiskers in an organic medium. This method is possible by coating whiskers surface with a surfactant or by chemically modifying their surface. The hydrophilic nature of CNCs favors their use in water soluble polymer matrices or water-based emulsions such as latex [8], starch [83], polyvinyl alcohol (PVOH) [9, 84] and polyethylene oxide (PEO) [10] to prepare composites, mainly using solvent casting. Other polymers used in recent investigations are: polylactic acid (PLA) [85, 86], polypropylene (PP) [20, 87-89], polyamide 6 [90], LDPE [91] and polyvinyl acetate [92].

Extrusion and melt processing of CNC composites has been the subject of a few investigations. This is the most economical and environment-friendly method of preparing polymer composites. However, in melt mixing, due to poor dispersion, a network formation among whiskers does not necessarily occur and, hence, the mechanical properties of these composites are generally inferior in comparison with solvent-casted composites [93]. Due to strong inter-particle hydrogen bonding, using solvent or high mechanical force is essential in order to disperse CNCs individually.

Alloin et al. [33] compared two methods of preparing polyethylene oxide (PEO)/ramie whiskers nanocomposite, cast/evaporating and extrusion. To extrude their samples, they prepared a solution of their sample and evaporated the solvent, and extruded the sample. Based on the viscoelastic behavior and mechanical performance, they observed at the same concentration of CNC, samples prepared via cast/evaporating showed the evidence of network formation whereas extruder prevented this network formation at low concentration. They suggested that using higher concentration of CNC in extruding process is key to have a network in nanocomposites. It has been also revealed that in extrusion processes, as a mechanical network formation among whiskers did not occur or at least the formed percolation network is weak, the mechanical properties of these

nanocomposites are poor in comparison with solvent casted nanocomposites [93]. The general decreases of the rheological and mechanical properties of the extruded nanocomposites compared to cast/evaporated ones are due to four combined effects:

-The rheological properties of the matrix decreased through chain scission induced by extrusion.

- The mechanical degradation of CNCs during extrusion, which reduces the ability of cellulosic fibers to connect each other.

-The whisker aggregation induced by the extrusion process, which decreases the amount of whiskers available for the formation of the percolating network, as reported from different SEM observations.

-The expected orientation effect of the extrusion process that prevents the formation of the network [33].

The general mechanical behavior of the nanocomposite can be divided into two distinguished region; the behavior of nanocomposite with network formation of filler in matrix, and the behavior without network formation. The concentration at which a network is formed has been defined as the percolation threshold. This concentration is a function of temperature and also method of preparing the nanocomposite [93].

When reinforced by a small quantity of whiskers and a network of filler is formed in the matrix, the composite films show increased mechanical properties; the increases are particularly striking when the film temperature is above the polymer T_g, but at lower temperatures, the increases are marginally [94].

Khoshkava and Kamal [95] used an innovative way to produce spray freeze dried CNCs (CNCSFD). In that method the particles formed a porous network during spray freeze drying and the network was partially preserved during melt mixing. The effect of incorporating 5 wt% of these particles in PP can be seen in Figure 2.5. There is high potential for PP melt infiltration into these porous agglomerates. Two different initial concentrations of 1 and 2 wt% in water have been used to prepare spray-freeze dried samples and they are named CNCSFD1 and CNCSFD2, respectively. It seems that a lower initial concentration, i.e. 1 wt%, by providing a more open structure, resulted in an easier polymer melt infiltration and, consequently, more dispersed CNCs into PP. Therefore, a uniform dispersion of the CNCs into PP was achieved.

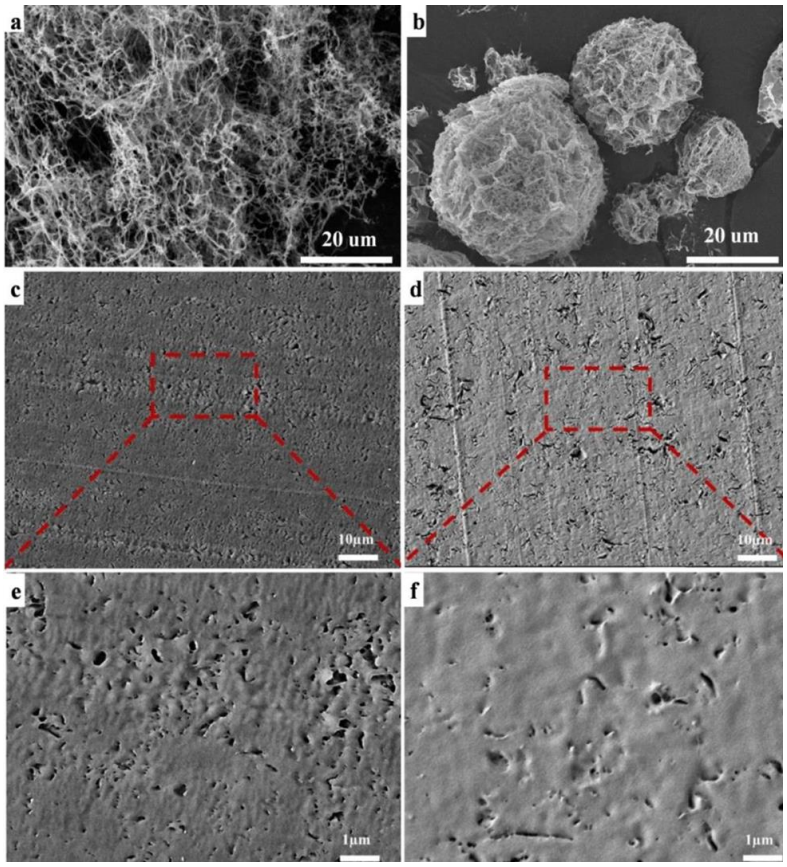

Figure 2.5 SEM images of (a) CNCSFD1 and (b) CNCSFD2 and of (c, e) PPCNCSFD1-5 and (d, f) PPCNCSFD2-5 at (c, d) low and (e, f) high magnification [95].

The particles were well dispersed in the matrix. The existence of an interconnected network was confirmed by rheological measurements.

To explain the mechanical properties of the neat PP and PP nanocomposites containing different CNCs, Figure 2.6 [95] reports the variations of storage modulus for a wide range of temperature. The addition of spray dried CNCs (CNCSD) did not change the storage modulus of PP for the whole range of temperature due to poor dispersion and existence of large agglomerates. The nanoparticles were less efficient to improve the properties when the initial concentration of CNCs was larger. However, by incorporating 5 wt% spray-freeze dried CNCs, the storage modulus was increased up to ca. 60% at room temperature.

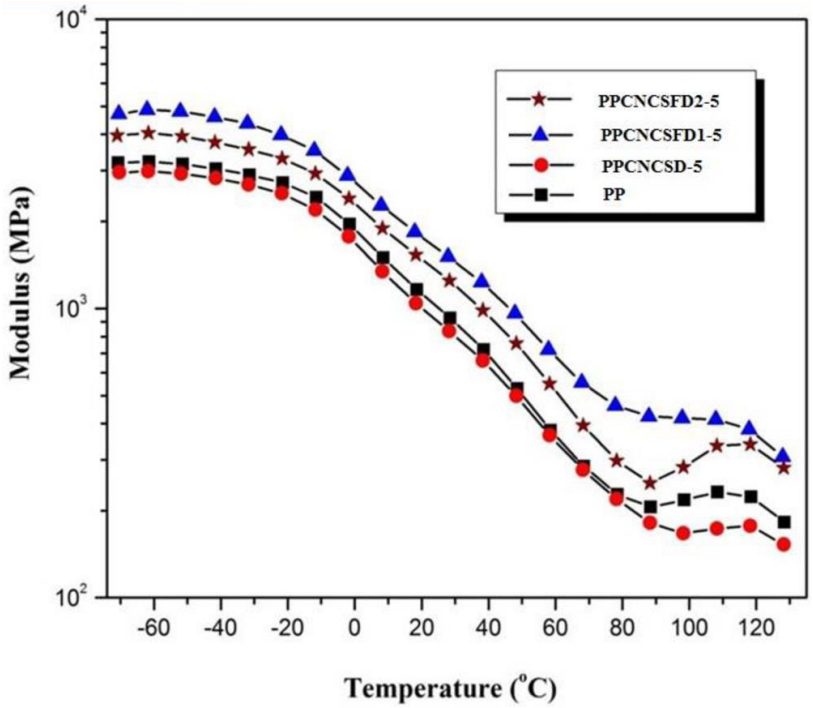

Figure 2.6 Storage modulus vs. temperature for PP, PPCNCSD-5, PPCNCSFD1-5, and PPCNCSFD2-5 [95].

Khoshkava and Kamal [89] studied the effect of surface energy on the dispersion and mechanical properties of PP and PLA composites reinforced with CNCs. The surface energy of CNCs was lowered as the temperature was increased. Also by decreasing the size of the nanoparticles, the required energy for the dispersion of CNCs increased drastically.

It was shown that cellulose whiskers could be dispersed in dimethylformamide, dimethyl sulfoxide or N-methyl pyrrolidine without additives or any surface modifications. Bagheriasl et al. [96] used an aprotic polar solvent, N,N-dimethyl formamide (DMF), to disperse CNCs in PLA. Figure 2.7 compares the SEM and TEM images of CNCs in an aqueous suspension with PLA/CNC nanocomposite containing 4 wt% CNC.

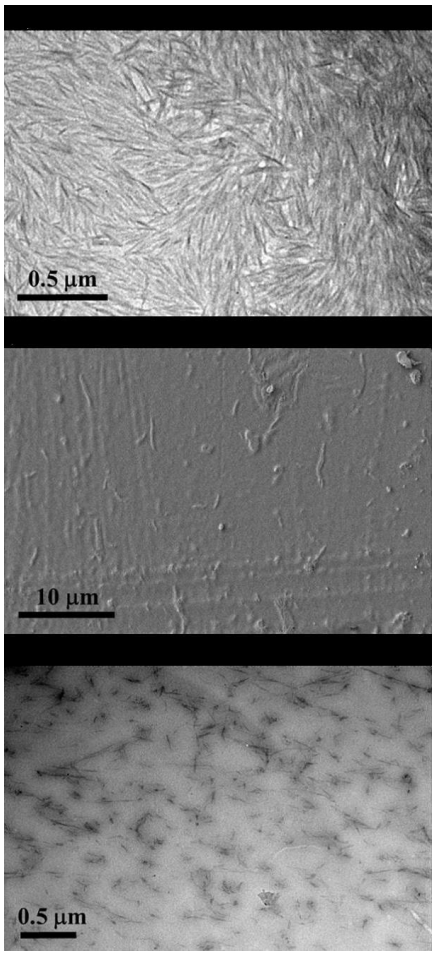

Figure 2.7 (a) TEM image of CNC aqueous suspension (0.5 wt%), (b) SEM micrograph and (c) TEM image of PLA4CNC [96].

According to the SEM and TEM images, a fine dispersion of CNCs was achieved by using DMF as the solvent and just a few aggregates in the range of 1-3 µm could be observed. The good dispersion without the use any compatibilizer led to a nanocomposite of individual CNC whiskers or small bundles of a few whiskers. The rheological properties of PLA/CNC nanocomposites prepared by solvent casting confirmed a strong network formation and good dispersion of CNCs in PLA, whereas samples prepared by melt mixing did not show significant improvements in rheological and mechanical properties. Figure 2.8 presents the tensile properties of PLA/CNC nanocomposites at different concentrations of CNCs. The number above each bar shows the deviation from the neat PLA.

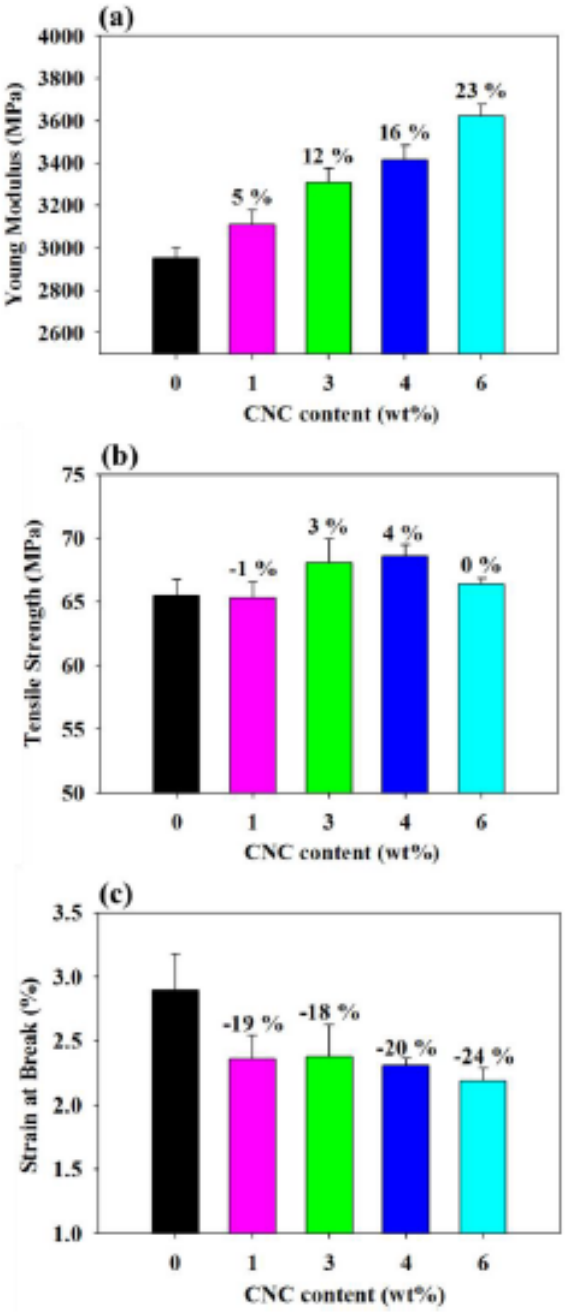

Figure 2.8 Comparison of the tensile properties of the samples: Young modulus (a), tensile strength (b) and strain at break (c) [96].

As expected the Young modulus of the nanocomposite increased significantly with content of CNCs. The tensile strength can be used as a measure for stress transfer and compatibility between the polymer and filler. Bagheriasl et al. [96] observed that the tensile strength was the same as the

neat PLA, which was attributed to the lack of stress transfer between PLA and CNC particles due to difference in their polarity [96].

Polyethylene oxide (PEO) has been used as a carrier polymer to compatibilize CNCs with LDPE [91] and PLA [86]. LDPE/CNC composites exhibited a brownish color whereas the samples modified with PEO had the same color as the unfilled matrix. Also, the presence of large CNC agglomerates has been reported for untreated composites [91]. Arias et al. [86] investigated the effect of high and low molecular weight PEOs and different PEO/CNC ratios on the crystallinity, rheological, mechanical, and morphological properties of PLA/PEO/CNC composites. The low molecular weight PEO was found to be more efficient for dispersing the nanoparticles, but, on the other hand, that PEO plasticized the composites and changed its behavior from brittle to ductile. No significant improvements in the tensile modulus and strength were reported.

PLA/CNC nanocomposites have also been prepared by Bondeson and Oksman [97] using two different methods of feeding polyvinyl alcohol (PVOH) as a coupling agent for CNC. They prepared an aqueous suspension of PVOH/CNC as a masterbatch. In the next step they freeze-dried the masterbatch to prepare samples for solid feeding in the extruder. To compare the effect of drying the masterbatch prior to process, they used a pump for feeding the suspension of PVOH/CNC directly to the extruder in liquid form. Analysis of microtomed and fractured samples in SEM showed that PLA and PVOH formed two immiscible phases with a continuous PLA phase and a discontinuous PVOH phase. TEM analysis showed that the whiskers were better dispersed in the nanocomposite produced with liquid feeding, PLA–PVOH/5CNC, and these whiskers were also partially dispersed in the PLA phase. The relative small improvements of the tensile modulus, tensile strength, and elongation to break for the nanocomposites, compared to the unreinforced counterparts, were also indications that it was primarily the PVOH phase that was reinforced, not the PLA phase [97].

Bagheriasl et al. [98] used poly (ethylene-co-vinyl alcohol) as a compatibilizer in nanocomposite of PP/CNC. They observed that even though the copolymer formed a separate phase from the matrix, it helped dispersing the CNCs in the matrix. In order to have the ideal dispersion of CNCs in masterbatch of copolymer/CNC they used dimethylformamide (DMF) as a solvent. Figure 2.9 reports the tensile properties of PP/CNC nanocomposites with and without copolymer prepared from different masterbatches.

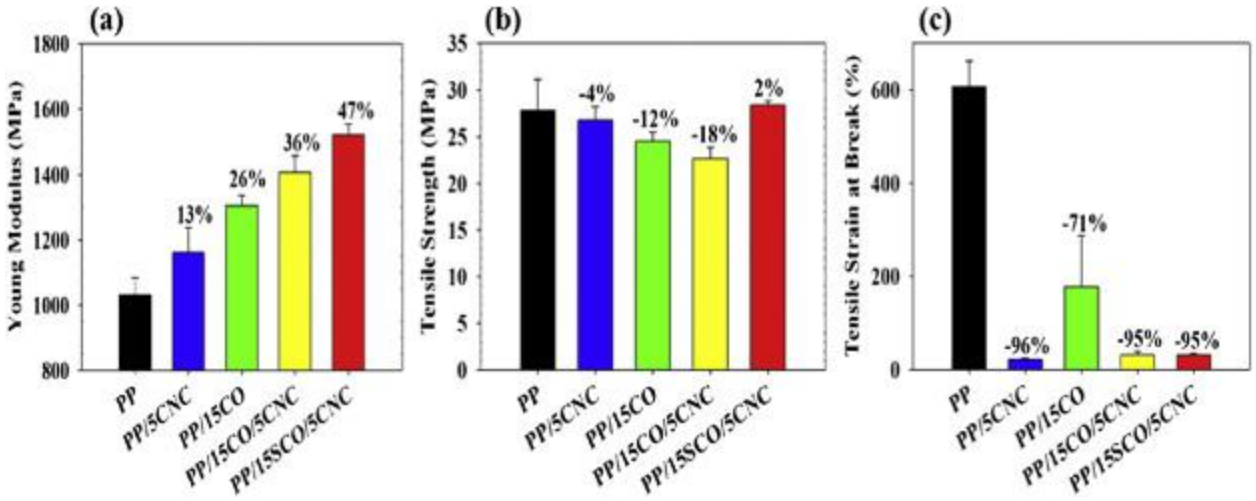

Figure 2.9 Comparison of the tensile properties: Young modulus (a), tensile strength (b) and tensile strain at break (c) of the samples.

PP/15SCO/5CNC refers to the sample from masterbatch prepared by solution mixing. As expected, by aid of DMF in the masterbatch preparation, the CNCs could be dispersed better and consequently the mechanical properties of PP/15SCO/5CNC were superior to PP/15CO/5CNC, the nanocomposite with the same contents of CNCs and copolymer produced by melt mixing. The increase in the Young modulus was partially due to increases in the crystallinity of the nanocomposite.

Ljungberg et al. [20, 87] compounded different types of modified cellulose whiskers in atactic (aPP) and isotactic polypropylenes. They observed that with incorporation of CNCs, the ductility was improved in comparison with the neat aPP by the use of PPMA or a surfactant (phosphoric ester of polyoxyethylene- 9-nonylphenyl ether) by 200 and 900 %, respectively [20].

Hassanabadi et al. [21] studied the effect of the acid value and molecular weight of PPMA on their efficiency as a compatibilizer between PP and CNCs. Table 2.3 presents the effect of different filler/coupler (*F/C*) on the tensile properties of the composites. Different grades of PPMA where named from A to E. The molecular weight has ascending order from 9 to 208.2 (kg/mol) and their acid values has descending order from 45 to 2 (mg KOH/g).

Table 2.3.Tensile properties of PP/CNC composites containing 1 wt% CNCs with different couplers at different (*F/C)* ratios. The letter at the end of the sample nomenclature refers different grades of PPMA [21].

	***F/C*=5/1**		***F/C*=7.5/1**		***F/C*=10/1**	
	Modulus (MPa)	Strength (MPa)	Modulus (MPa)	Strength (MPa)	Modulus (MPa)	Strength (MPa)
PP	450	33.2	450	33.2	450	33.2
PP/CNC	508	32.3	508	32.3	508	32.3
PP/CNC/A	584	39.1	599	40.2	565	36.5
PP/CNC/B	550	35.5	663	38.2	573	36.4
PP/CNC/C	495	35.7	556	38.1	519	36.2
PP/CNC/D	566	36.2	572	37.2	553	36.9
PP/CNC/E	509	33.8	574	37.3	528	36.1

They reported that for all the grades of PPMA, the optimum filler/coupler ratio for all compatibilizers was similar (7.5/1). The content of PPMA should be enough to cover the surface of CNCs and any excess amount of PPMA would remain in the matrix and act as a plasticizer, which may decrease the mechanical properties of the composite. The acid value (AV) of PPMA was the most crucial parameter since it defines the number of active sites on the chain to interact with the surface of the CNCs. With equal AV the higher molecular weight of PPMA favored better entanglement with the matrix chains and consequently better compatibilization between PP and CNCs [21].

2.10 Nanocomposites based on modified CNCs

Due to the acid that has been utilized to produce CNCs, negative charges from sulfuric acid are introduced on the surface of nanoparticles and stabilize their aqueous suspensions [26, 30, 71]. Different surface modifications of CNCs like acetylation [11], TEMPO-mediated oxidation [12], grafting [13-17] have been investigated. Common chemical surface modifications of CNC surfaces

include sulfuric acid treatment that provides sulfate half esters, using carboxylic acid halides that create ester linkages, and TEMPO mediated hypochlorite oxidation which creates carboxylic acids and using halogenated acetic acids which create carboxymethyl surfaces [99]. It is expected that surface modification of CNCs will improve the dispersion of the filler within a polymeric matrix or increase the mechanical properties of nanocomposite in comparison with pristine CNCs [100], but in most cases it includes some complicated and expensive chemical reactions that may also decrease the hydrogen bonds between the nanoparticles. These bonds were reported to be the basis of the reinforcing effect of cellulose whisker nanocomposites [93].

One of the interesting one-step methods to graft aliphatic carbon chains with different lengths on the surface of CNCs is esterification. In this method an organic acid chloride is added to the suspension of CNCs in the presence of a catalyst [15]. It has been reported that such surface modification can improve the dispersion of nanocomposites in LDPE [16]. However no significant improvement in terms of tensile strength or modulus could be observed in comparison to pristine CNC. Elongation at break was improved when longer chains were grafted to the surface of CNC. They believed this could be due to co-crystallization of these grafted chains with polymer chains of the matrix.

Junior De Menezes et al. [16] modified the surface of ramie cellulose whiskers chemically by grafting organic acid chlorides of different lengths of the aliphatic chain by an esterification reaction. They extruded both treated and untreated whiskers with polyethylene. They observed that a significant improvement in terms of elongation at break was observed when sufficiently long chains were grafted on the surface of the nanoparticles, as the esterification improved the interface interaction and consequently stress transfer between filler and matrix.

Poaty et al. [15] used a similar method to modify the surface of CNCs for a reinforcement of wood coating. The reaction aimed at grafting carbon chains with ionic bonds being created and replacing most of the surface O-H and O-SO_3- groups of the CNCs by hydrophobic moieties. 1,4-dioxane and 1-methylimidazole were used as a catalyst. The proposed reaction is presented in Figure 2.10. The less hydrophilic (or more hydrophobic) properties of the CNC particles were determined from water wettability measurements.

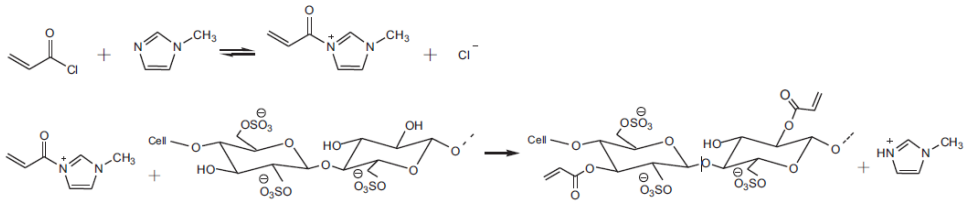

Figure 2.10 Reaction of 1 MIM catalyzed esterification. The acryloyl chloride reacts with 1 MIM to form a N-acryloyl-N-methylimidazolium ion, which then reacts irreversibly with the alcohol group from the CNCs. 1 MIM also reacts as proton scavenger during the reaction of the imidazolium ion with the CNC [15].

Gwon et al. [100] modified the surface of CNCs with toluene diisocyanate and used the modified CNCs in PLA-based nanocomposites. They used solvent casting method with chloroform as the solvent to prepare their samples. These modified particles could be dispersed in chloroform and PLA solutions; the tensile strength of the resulting PLA nanocomposites was improved up to about 13 % in comparison with unmodified CNCs, depending on particle concentration and the grade of PLA [100]. An optimum loading concentration was noted for different matrices. This concentration refers to the maximum loading capacity of the nanocomposite before the particles start re-aggregating. The optimum concentration was higher for semi-crystalline matrices in comparison to amorphous one.

2.11 Gel formation

In addition to forming equilibrium chiral nematic phases above some critical concentration, CNC suspensions tend to gel or aggregate due to different chemical and physical processes: change of surface charges via decreases of the half-ester sulfate groups at the surface of CNCs [101], modification of the ionic strength of the suspension medium [102] and charge reversal through surface functionalization of CNCs [21].

Lenfant et al. [103] investigated the effect of changing ionic strength of the suspension medium on gelation of CNCs and electrosterically stabilized nanocrystals of cellulose (ECNCs) . They observed that CNC aqueous suspension turn into a gel at 10 wt% CNC. The gelation concentration depends on different parameters like CNC aspect ratio and ultrasonication for sample preparation [76]. Adding salt could increase the viscosity of the suspension and cause gel formation at lower concentration of CNC. Gelation has been attributed to weakening electrostatic repulsion between CNC particles. $CaCl_2$ and NaCl have been used in CNC suspensions with different concentrations of CNC. They observed that adding different salts resulted in forming gels with different strength;

the effect of $CaCl_2$ is more pronounced than NaCl at a constant ionic strength. In order to explain different effects, they prop(d the mechanism presented in Figure 2.11. Based on the suggested mechanism, sodium only screens the charges on the surface of particles, whereas calcium ions can bridge the nanoparticles through their sulfate half-ester groups. This resulted in weaker agglomerates of CNCs in presence of Na^+ in comparison to Ca^{2+}. For ECNCs the formed network is weaker than that of CNCs with added $CaCl_2$. NaCl only screens the charges without bridging the nanoparticles.

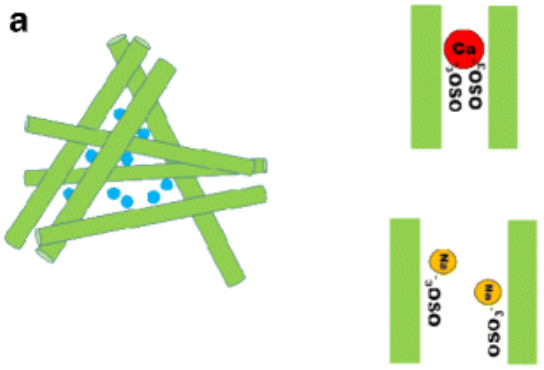

Figure 2.11 Schematic interaction mechanism of NA^+ and Ca^{2+} with CNC [103].

Dorris and Gray [101] observed that glycerol/CNCs alone did not produce a gel or even a stable suspension. However, by mixing an aqueous suspension of an acid form of CNCs with glycerol, and removing excess water by evaporation under controlled conditions, gels could be obtained. They also claimed that the reason behind this gel formation was desulfation, which was slow at room temperature, but a significant level of desulfation was observed for the CNC suspensions kept at 60 °C for 3 days [104]. Heat alone could cause desulfation, but presence of glycerol in the system accelerated the process. Table 2.4 reports gel formation for 1.3 wt% CNC suspensions prepared in water/glycerol mixture at different temperatures and rest times. By measuring the desulfation level, they suggested that a minimum of 20% desulfation was necessary to form a gel. For samples prepared at higher temperature, they could obtain higher levels of desulfation during evaporation, but for other samples prepared at 30 or 40 °C, the samples needed to be kept at room temperature for longer times to reach the acquired level of desulfation and form a gel.

Table 2.4 Effect of evaporation temperature and time on desulfation and gel formation for CNC suspensions in glycerol–water mixtures containing 1.3 wt% CNCs with initial water content of 35 wt% [101].

T_{evap} (°C)	**Duration of evaporation (h)**	**Resting time (week)**	**Desulfation level in glycerol (%)**	**Gel formed?**
30	16	0	18	No
30	16	2	22	Yes
40	16	0	20	No
40	16	2	30	Yes
50	16	0	26	Yes
60	8	0	34	Yes
70	8	0	31	Yes

This desulfation was also observed at temperatures above 50 °C for CNCs with half ester sulfate groups on their surface [105].

Lewis et al. [106] reported hydrothermally formed gels from aqueous suspensions when CNC concentration was about 4 wt% and the suspensions heated up to 110 °C for 20 h. Figure 2.12 reports the storage and loss modulus of 4 wt% CNC suspensions treated at different temperatures for 20 h. For samples prepared at temperatures higher than 80 °C, gel-like behavior could be observed; *G'* was larger than *G"* and they both were almost independent of angular frequency. This behavior can confirm the formation of a robust three-dimensional network for these samples. They attributed this gelation to desulfation or partial removal of sulfate half-ester groups on the surface of CNCs [105, 106].

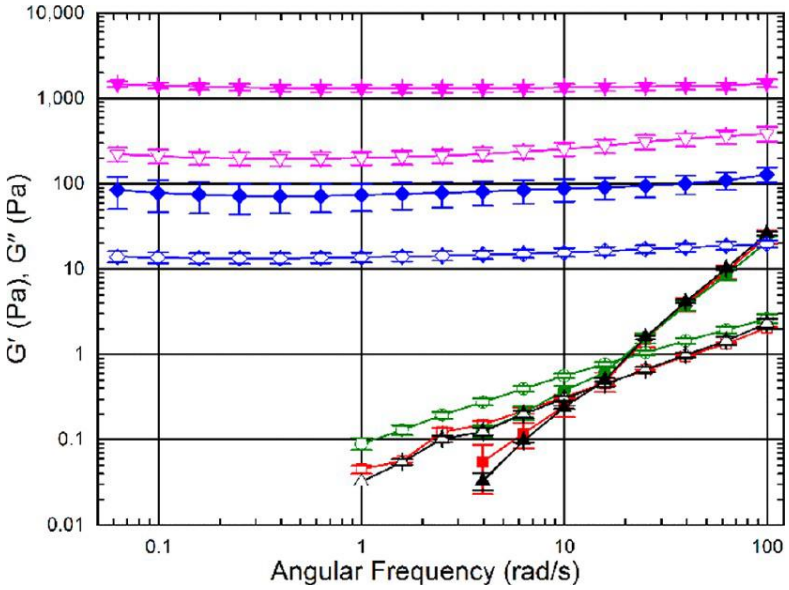

Figure 2.12 Frequency sweep of 4 wt % CNC aqueous suspensions treated at various temperatures for 20 h. CNC-not treated (black ▲), CNC-60 (red ■), CNC-70 (green ●), CNC-80 (blue ◆), and CNC-90 (magenta ▼). Storage modulus (*G′*, closed symbols) and loss modulus (*G″*, open symbols) as functions of angular frequency. The number after CNC refers to the temperature of preparation [106].

2.12 Summary

Cellulosic reinforcements have been the subject of various studies and a few methods of preparing their biocomposites with thermoplastic polymers like PP or PLA have been discussed here. Very few conclusive studies tried to correlate mechanical and morphological properties of lignocellulosic fiber composites with their rheological properties and fiber breakage by taking in to consideration all significant parameters simultaneously. Comparing composites prepared from cellulosic fibers in nano and micro scale was not carried out thoroughly. Since the production of CNC is a costly procedure, this comparison can help demonstrating the added value of using cellulosic nanoparticles as reinforcement in the composite industry. Using different CNC modifications or different coupling agents were the subject of several studies but the effect of important processing parameters like mixing temperature or molecular weight of the matrix has not been verified in the literature. The rheological behavior of nanoparticle suspensions can give information about the state of dispersion, stability, possible network formation and etc. CNC aqueous suspensions have been investigated extensively in different studies. In past few years some polar solvents like DMF and DMSO where introduced as good solvents for CNC, and DMF was

recently used to produce PLA/CNC nanocomposites. To prepare PLA/DMF solution increasing temperature to about 70 °C is essential. To the best of our knowledge the rheological behavior of suspensions of CNC in DMF and DMSO at different temperatures was never studied. Also the properties of PLA/CNC nanocomposites in DMSO or DMF as a media were not investigated.

CHAPTER 3 OBJECTIVES

As mentioned earlier, the quality of the particle dispersion and the reinforcement of polymers is strongly associated with the compatibility of the matrix and reinforcing agent and the compounding method. The main goal of this project is **to develop biocomposites with enhanced mechanical properties based on cellulosic reinforcement via common preparation methods**. In order to meet this objective, the following specific objectives are:

1- To investigate the effect of different compatibilizers on the rheological, mechanical and morphological properties of flax fiber reinforced PPs. Key parameters are: concentration of fibers, melt flow index (MFI) of the compatibilizer, type and content of the grafted groups in the compatibilizers.

2- To develop a composite of PP/CNC via melt mixing. PPMA is used as the compatibilizer for these composites. The effects of changing the process temperature and using two different molecular weight PPs are studied in this part. Moreover, the mechanical properties of the PP/CNC composites are compared to the PP/flax composites.

3- To develop partially hydrophobic CNC particles via grafting chains of carbon on the surface of CNCs.

4- To examine the possibility of using dimethyl sulfoxide (DMSO), a polar solvent to prepare polylactide (PLA)/CNC nanocomposites. As a preliminary step the rheological behavior of suspensions of CNCs and modified CNCs (mCNCs) in DMSO is investigated. The effects of increased temperature and adding a biopolymer (PLA) are examined.

CHAPTER 4 ORGANIZATION OF THE ARTICLES

Chapters 5 to 7 present the main results of this study in the form of three articles. In chapter 5 the efficiency of different coupling agents for compatibilizing flax fiber reinforced PP composites is presented. This work on flax fibers was initiated because of the major delay in obtaining the CNCs from FPInnovations at the beginning of this doctoral study. All the composites were prepared via melt mixing. The effect of compatibilizers on mechanical and rheological properties is reported and morphology is used to discuss structure-property correlation. This chapter was published as a scientific article in 2014 in Cellulose (2016 impact factor: 3.195).

In Chapter 6 PP/CNC composites compatibilized by PPMA were prepared by melt mixing. The effects of two different molecular weight PPs and different processing temperature on the dispersion and mechanical properties of PP/CNC composites were investigated. This chapter was published as a scientific article in Polymer Composites (2016 impact factor: 2.004) in April 2017.

In chapter 7 rheological properties of CNC and hydrophobic CNC suspended in an organic solvent are compared. The detail of surface modification is also reported in this chapter. This chapter was accepted with minor revision in April 2017 as a scientific article to be published in Rheologica Acta (2016 impact factor: 2.184).

CHAPTER 5 ARTICLE 1: RHEOLOGICAL, MORPHOLOGICAL AND MECHANICAL PROPERTIES OF FLAX FIBER POLYPROPYLENE COMPOSITES: INFLUENCE OF COMPATIBILIZERS [1]

Helia Sojoudiasli, Marie-Claude Heuzey, Pierre J. Carreau*
Department of Chemical Engineering and Research Center for High Performance Polymer and Composite Systems (CREPEC), Polytechnique Montreal, C.P. 6079, succ. Centre-Ville, Montreal, QC, Canada, H3C 3A7
* Corresponding author. Email address: pcarreau@polymtl.ca

Abstract

In this work, the rheological, mechanical and morphological properties of flax fiber polypropylene composites were investigated. The effect of incorporating a polypropylene grafted acrylic acid (PPAA) or a polypropylene grafted maleic anhydride (PPMA) on these properties has been studied as well. According to scanning electron microscopic observations and tensile tests, the addition of a compatibilizer improved the interfacial adhesion between the flax fibers and the polymer matrix. The tensile modulus of composite containing 30 wt% flax fibers was improved by 200% and the tensile strength improved by 60% in comparison with the neat PP. Plasticizing effect of the compatibilizers as a result of their lower melt flow index was also shown to decrease the rheological properties of the composites, even though the effect was not pronounced on the mechanical properties.

.

Keywords:

Flax fiber composites, PPMA compatibilizer, PPAA compatibilizer, rheology, tensile properties, morphology

---

[1] Published in Cellulose 2014; 21(5):3797-3812.

5.1 Introduction

Short conventional fibers (glass, carbon, etc.) have been extensively used over the last decades as reinforcements for thermoplastics in order to improve the mechanical properties of polymers and reduce the cost of the final products [1]. Recently the use of short natural fibers such as sisal, jute, hemp, coir and flax in reinforced thermoplastics has triggered new investigations in a number of industrial sectors, notably the automotive industry, construction, textiles, etc. [2]. Natural fibers, depending upon the source, are classified into three types, namely: seed hair (cotton), bast fibers (ramie, jute and flax) and leaf fibers (sisal and abaca). Jute, ramie, flax and sisal are the most commonly used fibers in polymer composites [3]. They offer numerous advantages compared to "man-made" ones: low density, low cost, availability, biodegradability, absence of health hazard, high filling potential, high stiffness and good specific mechanical and acoustic insulation properties [4, 5]. Also the abrasive action of natural fibers to equipments is less severe compared to that of glass and carbon fibers [3].

Flax fibers are widely used in Europe and North-America. They possess a specific elastic modulus between 20 and 50 m^2/s^2 [6] and a very high tensile strength (up to 1500 MPa for elementary fibers and around 800 MPa for bundles) [7]. However, the key issue for natural fiber-reinforced polymers is the incompatibility between the hydrophilic fibers and non-polar polyolefin matrices such as polyprolylene (PP) [7]. This incompatibility generally results in poor fiber wetting [8], presence of bundles [1], and weak fiber-matrix adhesion. Furthermore, the hydrophilic character of cellulosic fibers leads to a high moisture absorption tendency [9]. Another important limitation of lignocellulosic materials is their relatively low degradation temperature, limiting the processing temperature to about 200 °C. This restrains the choice of polymers that can be used with natural fibers to thermoplastics with relatively low processing temperatures such as polyethylene (PE), polypropylene (PP) and polyvinyl chloride (PVC) [4]. Beside the incompatibility between natural fibers and hydrophobic polymers, the cause of the lower strength of natural fiber composites is the presence of bundles. These fibers consist of bundles of two to twenty elementary fibers bonded together by a pectic cement [10]. The presence of these bundles results in overestimation of the stiffness and strength value in the modeling of the composite [11]. Another noticeable drawback of these fibers lies in their intrinsic variability. The behavior and the properties of natural fibers depend on many factors, such as harvest period, weather variability, and quality of soil and climate of the specific geographic location as well as preconditioning [1, 12]. In addition, the fiber diameter

distribution is much wider and the surface roughness of natural fibers is sensitive to the preparation technique [1, 12, 13], in comparison with synthetic ones.

Because of its low price, good mechanical properties, processability, relatively low melting temperature and widespread use in technical applications [7], polypropylene (PP) is one of the best candidates as a matrix for natural fiber composites. Even though its hydrophobic nature can protect the cellulosic fibers [14], this characteristic nature of PP makes it highly incompatible with these fibers [15].

The most important factor for good fiber reinforcement in a composite is the strength of adhesion between the matrix polymer and the fibers [16]. In order to overcome the problem of their incompatibility with polyolefins, two methods have been proposed in the literature: impregnation and chemical modification. The former does not result in covalent bonding between the cellulosic material and the coupling agent. The latter, depending on the chemical reaction that occurs, can lead to different types of chemical bonds between the fibers and the matrix [17]. Two possible routes for chemical modifications are the grafting of molecules with functional groups compatible with the matrix, and the matrix modification by a surfactant or compatibilizer [2, 13, 18]. It has been reported by Van de Velde and Kiekens [19] that a matrix modification resulted in higher improvements in mechanical and sorption characteristics (except for flexural modulus) than a fiber modification. Maleic anhydride modification of polypropylene has often been used to make PP less hydrophobic and thus more compatible with polar fibers. Another advantages of matrix modification with compatibilizers over fiber surface modification is the easier and more economical solvent-free processing, which is more environmental-friendly and less energy consuming.

Most effective chemical modifications involve coupling agents containing chemical groups that are able to react with the fibers and the polymeric matrix [14]. Copolymers, such as maleic anhydride grafted polypropylene (PPMA), have proven to be suitable additives for cellulosic fiber-reinforced PPs. The maleic anhydride polar groups form covalent and hydrogen bonds with the surface of the fibers, which improve the fiber–matrix adhesion. On the other hand, the PP segments of PPMA, through co-crystallization, form compatible blends with the bulk PP matrix [18]. Besides co-crystallization in the solid state, PP chains of PPMA may entangle with the chains of PP in the molten state, resulting in a better compatibility [16, 20]. Paunikallio et al. [20] investigated the reactions between PPMA and viscose fibers via Fourier transform infrared (FT-IR) spectroscopy

and proposed a two-step mechanism: 1) the activation of the copolymer by changing the carboxyl groups present in the PPMA to more reactive anhydride groups, which react more easily with hydroxyl groups at 150 – 160 °C and, 2) the esterification of cellulose. The authors observed that the esterification, besides the creation of hydrogen bonding between PPMA and the surface of cellulosic fibers, led to a better adhesion of the fibers to the polymer chains. Unlike acrylic or methacrylic acid, maleic anhydride do not react with itself under typical industrial grafting conditions [21]. The decreased tendency to participate in side reactions makes maleic anhydride an appropriate moiety when grafting polar groups on PP [22].

According to Gauthier et al. [23] important parameters for the treatment using PPMA are the degree of grafting and the length of the grafted alkyl chains. When the hydrophilic group content is larger, the interactions between these groups and the surface of the fibers increase but, on the other hand, the possibility of the existence of free MA in the material is higher. MA has been reported to react with the surface of cellulosic fibers and decreases their active sites ([22]). Another key parameter is the length of the PP chains in PPMA compatibilizers. Long chains of PP will entangle with the matrix chains and cannot penetrate the fiber bundles. It has been also reported that the improved adhesion between the fibers and the matrix also prevented to some extent the flax fibers from absorbing water [19].

Rheological characterization provides knowledge essential both for process development and for fundamental flow characterization of filled plastics. Generally, the rheological behavior of filled systems is quite complex, and the relationships between the fibers at the micro structural level and the macroscopic properties are still not fully understood [24]. Because of the great interest in cellulose and natural fiber composites, the rheological behavior of suspensions of these fillers in different polymer matrices has been examined by different investigators to some extent. The flow properties depend on fiber length, stiffness, and strength, volume fraction of the filler, and nature of fiber-matrix adhesion [13, 25-27]. The effect of a coupling agent on the flow properties of composites has also been studied by Hristov and Vlachopoulos [28]. They investigated different coupling agents (maleated polyethylenes, Polybond 3009, Polybond 3109 and Coesive F30) on maple wood flour composites based on high density polyethylenes (HDPEs) of different molecular weights (MW) and molecular weight distributions (MWD). Using rotational and capillary rheometers combined with scanning electron microscopy (SEM) for morphological analysis, they found that low MW and narrow MWD HDPEs led to larger viscosity increases with wood flour

addition. They also showed that the presence of coupling agents led to significant interfacial adhesion improvements, as confirmed by scanning electron microscopy (SEM) analysis and increased pressure drops. Nevertheless, their investigation did not account for possible plasticizing effects of the coupling agents. Disregarding the plasticizing effect of the coupling agent, the viscosity of compatibilized composites may increase as a result of better wettability and high interfacial adhesion [8]. It also improved the mechanical properties of natural fiber-reinforced composites [29]. Moreover, PPMA resulted in a better dispersion of flax bundles [30].

PP/flax composites have been investigated by quite a few authors [18, 19, 30-33]. In most of the studies the effect of surface modification or using compatibilizers on the mechanical properties has been investigated. Arbelaiz et al. [18, 30] and Cantero et al. [31] compared the effect of different surface modifications like silanation and alkalization and they observed that adding a maleated polypropylene (PPMA) was a more effective way to improve the tensile and flexural properties of PP/flax composites. They also found out that there is an optimum content for each PPMA, based on its MFI and MA content. Van de Velde and Baetens (2001) investigated the thermal degradation of flax fibers and compared the mechanical properties of glass fiber with flax fiber composites. They showed that matrix modification with PPMA was more effective than fiber modification (boiling and retting) to improve mechanical properties. Le Moigne et al. [33] investigated the rheological behavior of flax and sisal-reinforced PP composites compatibilized with a PPMA. Even though they did not compare the properties of non-compatibilized samples with compatibilized ones, they observed a drastic decrease in the viscosity of the PP/PPMA blend in comparison with the neat PP, but this plasticization effect could have been counterbalanced by the effect of fibers to increase the viscosity. In general the studies on PP/flax composites focused on either mechanical or rheological properties of the composites. As far as we are aware, the combined effects of different parameters including fiber content, compatibizer type and content and efficiency of the compatibilizers on rheological, mechanical and morphological properties have not been so far reported.

The aim of the present work is to investigate the efficiency of different coupling agents for compatibilizing flax fiber PP composites. The addition of compatibilizers with different characteristics is expected to improve the polymer-flax fiber interactions to various degrees and alter the flow behavior of the composites in the molten state. The rheological and mechanical

properties of the composites, with and without compatibilizers, are compared and the structure-property relationships are discussed in light of the morphology.

5.2 Experimental

5.2.1 Materials

The polypropylene (PP) used in this work was Profax 6523 from Basell with a melt flow rate (MFR) of 4 (g/10 min- @ 230 °C/ 2.16 kg). Flax fibers, with a nominal length of 1 mm, were kindly supplied by LIMATB (France). Three different compatibilizers have been used: 1) Epolene E43 (EP) that is a maleic anhydride grafted polypropylene (PPMA), a wax with 3.8 wt% MA (Perrin-Sarazin et al. 2005), 2) Orevac 18729 (OR), which is a PPMA with a melt flow index MFI of 4.5 (g/10 min- @ 230 °C/ 2.16 kg) and MA content lower than 1 wt%, and 3) Polybond 1002 (AA), an acrylic acid grafted polypropylene (PPAA) with a MFI of 20 (g/10 min- @ 230 °C/ 2.16 kg) and AA content of 6 wt%.

The composites were prepared by melt mixing using an internal mixer (C.W. Brabender Plasticorder) with a volumetric capacity of 30 mL under a nitrogen atmosphere. For all composites, the mixing time was 10 min at 60 rpm and 200 °C. The compatibilizers and flax fibers were dried at 80 °C for 24 h under vacuum prior to mixing. To apply the same thermo-mechanical cycle to all samples, the neat PP was also processed with the same procedure. The PP was dry mixed with the compatibilizers prior to feeding into the Brabender. The mix was melted in the internal mixer for 3 min before adding the fibers. Four different weight fractions of the filler have been investigated: 10 wt% (PP/10), 20 wt% (PP/20), 26 wt% (PP/26) and 30 wt% (PP/30). The corresponding volume fractions for PP/10 and PP/30 are 5.3 and 17.8 vol% in the molten state, respectively. Using the criteria established for concentration regimes (Sepehr et al. 2004; Tucker III and Advani 1994) ($\varphi \leq 1/r^2$ for dilute suspensions, $1/r^2 \leq \varphi \leq 1/r$ for semi-concentrated suspensions, and $\varphi > 1/r$ for concentrated suspensions), PP/10 corresponds to a semi-concentrated suspension and PP/30 to a concentrated one.

The compatibilizers were used at 5, 10 and 50 wt% of the fiber content in the composites, for example PP/10/0.1 EP means a composite containing 10 wt% fibers with respect to PP and 10 wt% of Epolene based on the fiber content). The reproducibility of sample preparation was verified by investigating at least two batches for each formulation. The samples were compression molded at 200 °C for 11 min under a nitrogen atmosphere while the pressure was increased slowly from 0 to 14 MPa, followed by quenching in a water-cooled press for 3 min.

5.2.2 Characterization

Thermogravimetry (TGA)

Thermogravimetric analyses were carried out using a TGA Q500 from TA Instruments. The measurements were done at a heating rate of 2 °C/min in high resolution mode in an air atmosphere with a flow rate of 60 mL/min. Temperature ranged from 45 to 700 °C. The sample weights were 12-17 mg.

Optical microscopy

As received fibers and the PP/30 composite with a thickness of 100 µm were observed using a Zeiss Axioskop 40 optical microscope in transmission mode. The size and state of dispersion of the flax fibers before and after blending were quantified. The diameter and length averages were calculated based on a population of 250 fibers.

Scanning electron microscopy (SEM)

In order to investigate the efficiency of the compatibilizers and the nature of the adhesion between the fibers and the matrix, scanning electron microscopy (SEM) has been performed on cryo-fractured surfaces, which were gold-coated. The microscope was a JEOL JSM 7600TFE Scanning Electron Microscope (SEM) operated at a voltage of 2 kV.

Rheological measurements

The rheological measurements were carried out using an Anton Paar rotational rheometer (MCR 301) equipped with a 25 mm parallel plate flow geometry at 190 °C and under a nitrogen atmosphere. The gap between the plates was 1.2 mm. It was verified that the rheological results were independent of the gap used to carry out the experiments. Prior to the frequency sweeps, the region of linear viscoelasticity was first determined by performing stress-sweep tests. The thermal stability of the various composites was verified from dynamic time sweeps at 0.628 rad/s under nitrogen for 45 min. All samples were stable during the rheological tests and the changes in the complex viscosity during time sweeps were less than 5% over 45 min. Steady-shear tests have been carried out on the samples as well. To investigate the effect of preconditioning, samples were pre-sheared for 5 and 10 min at 0.1 s^{-1} prior to frequency sweeps. All the curves were reproducible and the deviations were less than 8% and 4% at low and at high frequencies, respectively.

Tensile properties

Tensile testing was carried out using an Instron universal testing machine according to ASTM D638. Measurements were performed on standard type V dog-bone shaped samples at room

temperature with a crosshead speed of 10 mm/min, and using a load cell of 5 kN. A minimum of six specimens were tested for each formulation.

5-3 Results and discussion

5.3.1 Thermal stability

The thermal stability of the flax fibers and sample PP/30/0.1 EP was verified using the TGA technique. Fig. 5.1 shows the relative weight (left ordinate) and the weight drop first derivative (right ordinate) as functions of temperature in air. For the as-received fibers, three different rapid weight loss regions can be identified. As the fibers were not dried in the oven prior to the test, the first weight loss is associated to the residual moisture loss that occurred between room temperature and about 100 °C. The second important weight loss, accounting for more than 50 % of the total loss, takes place between 240 and 380 °C. This weight loss region is shown as a peak with a shoulder in the weight drop first derivative curve. The shoulder in the second peak can be related to the degradation of hemicelluloses followed by the first step of cellulose depolymerisation [37]. A third region also can be distinguished from the second one above 400 °C, which can be associated to the final stage of degradation of cellulose and hemicelluloses [38]. This weight loss has also been reported as the non-cellulosic thermal degradation, which consists of degradation of residues and aromatics [39]. Considering these results, the processing temperature of 200 °C under nitrogen should not cause any thermal degradation of the flax fibers. Also the thermal stability of the composite at the highest content of flax fibers has been investigated. As it is shown in Fig. 5.1, this composite at the testing temperature in rheometry of 190 °C and mixing temperature of 200 °C is quite stable.

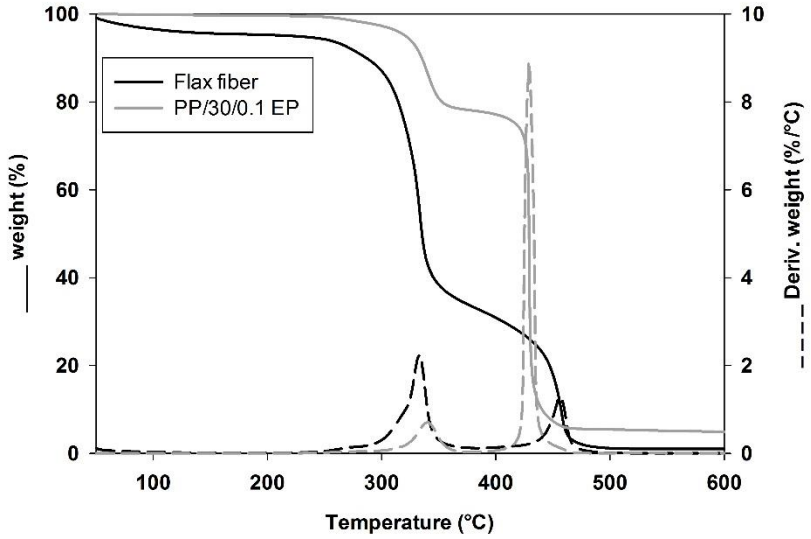

Fig. 5.1 Thermogravimetry results of the as-received flax fibers and the PP/30/0.1 EP composite in air.

5.3.2 Fiber morphology

Melt processing affects the final fiber aspect ratio and thus the mechanical properties of the composite. If the energy transferred to the fiber during the melt mixing surpasses the cohesive bonds energy, the bundles can break into individual fibers and also the fibers might break through their weak points, which can be seen as kinks on their surface [18]. As fiber dimensions and aspect ratio are determining parameters for rheological and mechanical properties, it is important to verify changes after compounding as a result of breakage.

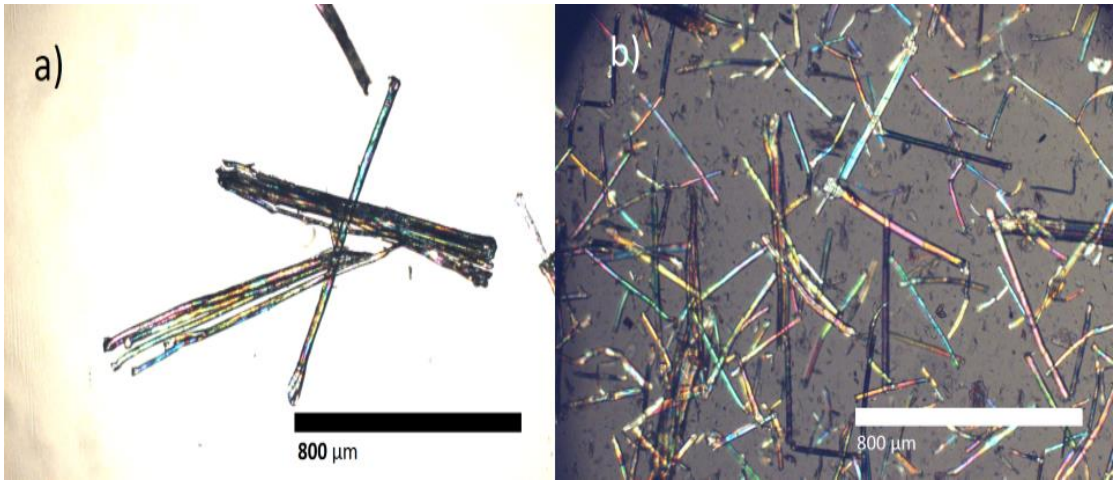

Fig. 5.2 Optical micrographs of a) as-received flax fibers; and b) PP/30/0.1 EP composite from a 100 µm film.

Fig. 5.2 shows the optical micrographs of as-received flax fibers (a), and a PP composite film containing 30 wt% flax fibers and compatibilized with Epolene E43 (b) without fiber extraction from the composite. The as-received flax fibers are in the form of bundles and single fibers, with an approximate nominal length of 1 mm. In the case of the PP/30/0.1 EP composite, the presence of shorter fibers and more frequent single fibers in comparison with the as-received flax is obvious. Table 5.1 reports the values for average length, diameter and aspect ratio of the as-received fibers and after compounding.

Table 5.1 Fiber length, diameter and aspect ratio before and after melt blending

	As-received fibers	**After compounding PP/30/0.1 EP**
Average length, *L* (μm)	**976 ± 87**	**308 ± 104**
Average diameter, *D* (μm)	**70 ± 34**	**30 ± 12**
Average aspect ratio (*L/D*)	**28 ± 12**	**12 ± 4**

The mean length of the as-received flax fibers was 976 μm and it varied from 800 to 1245 μm. After compounding, as a result of fiber breakage, the mean of fiber length decreased by about 70%, to reach 308 μm. It has been observed that before mixing, the diameter distribution of the fibers was large and the average diameter was about 70 μm. After compounding, the diameter had a narrow distribution, where more than 85% of the fibers had a diameter smaller than 50 μm and the aspect ratio was reduced from 28 to 12 following compoundingBoth breakage of fibers and delamination of fiber bundles occurred during compounding, but breakage appears to be dominant and explain the large drop of the aspect ratio. Flax fiber breakage has been reported before by Barkoula et al. [7] in polypropylene composites and Arias et al. [13] in polylactide composites, using the same flax fibers in the latter case

5.3.3 Rheological properties

Small amplitude oscillatory shear (SAOS)

The small amplitude oscillatory shear (SAOS) frequency data are presented in Fig. 5.3 for the neat PP and Epolene-based composites. As expected, the higher the fiber content in the composite, the larger the complex shear viscosity, η*, (Fig. 5.3a) and the storage modulus, G', (Fig. 5.3b). Note

that the η* and *G*' data for the neat PP and PP10 are nearly superposed, while there is no low frequency plateau for the η* data of PP30 (Fig. 5.3a). As well, a low frequency slope smaller than 2 for the G' data of PP30 (Fig. 5.3b) suggests that this sample exhibits an apparent yield stress, as observed by other authors for suspensions of an anisotropic filler [40, 41]. Here it can be seen that the slope has been decrease to 0.66 for low frequencies.

Fig. 5.3 also shows that the presence of the Epolene compatibilizer reduces considerably the complex viscosity and storage modulus of the composites. Epolene is expected to reinforce the matrix/fiber interface, but at the same time it might plasticize the polymer matrix since it has such a lower molecular weight (wax-type material, supposedly very high MFI but not measureable). Therefore, a competition between both effects occurs as reported before [42, 43]. To stress the possible plasticizing effect of Epolene, a blend of PP and EP without fibers (PP/0/4.2 EP) was prepared, at the same EP contain with respect to PP as PP/30/0.1 EP. The η* and *G*' data of Fig. 5.3 illustrate the strong plasticizing effect with respect to the neat PP for sample PP/0/4.2 EP. For the composite containing 10 wt% of fibers, the plasticizing effect of EP is dominant and the rheological properties are decreased with respect to those of the neat PP, as reported in the work of Twite-Kabamba [42]. The large plasticizing effect of Epolene E43 for the composite containing 30 wt% of flax fibers is also striking when compared to the data of PP/30. The plasticizing effect remains dominant compared to the improvement of the interface and, consequently, η* and *G*' decrease. The decrease in viscosity has been reported elsewhere, and it was attributed to the fact that only part of PPMA played the role of improving the adhesion of PP and fibers, while the rest remained in the matrix as a plasticizer [44].

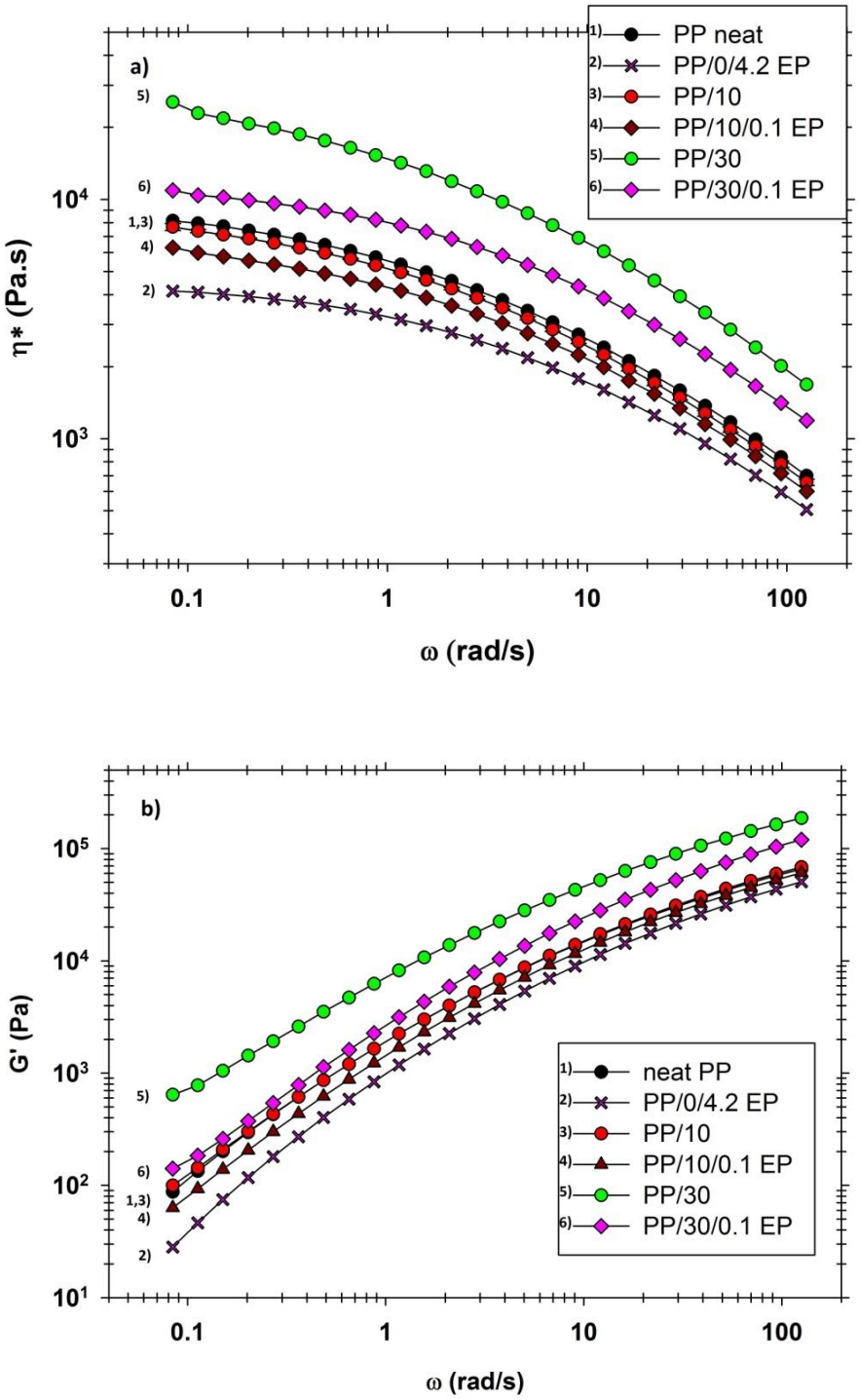

Fig. 5.3 Effect of Epolene E43 (EP) on a) complex viscosity and b) storage modulus of PP composites with different fiber contents.

Figs. 5.4 and 5.5 present the effects of three different compatibilizers (EP, OR and AA, 10 wt% based on fiber content) on composites containing 30 wt% fibers for low and high compatibilizer

contents, respectively. Also the effect of lower content Epolene on rheological properties of the composite has been revealed. The drop in rheological properties for Epolene containing samples is proportional to its content, and even at low content (5 wt%) a slight decrease in complex viscosity can be observed in comparison with PP/30. Orevac 18729 (OR) has an MFI of 4.5 g/10 min, similar to the PP matrix used, and little plasticizing effect on the matrix was observed, even at the largest content (PP/0/22 OR, data not shown). For the composite containing 30 wt% of flax fibers, the content of OR is apparently not sufficient since for PP/30/0.1 OR there is no effect when compared with PP30 and the η* and *G*' data are superposed, as illustrated in Fig 5.4. This may be attributed to the low content of MA in Orevac 18729. For PPAA a slight plasticizing effect can be seen for sample PP/0/4.2 AA, which resulted into a slight decreases in η* and *G*' when compared to the neat PP. We note that the properties of the compatibilized composites containing 30 wt% flax fibers are the largest when with OR, followed closely by AA and then EP.

Fig. 5.5 shows that by increasing the content of Epolene E43 by 5 times (50 wt% based on fiber content), η* and *G*' decrease drastically as a result of the plasticizing effect of this compatibilizer. And in this case, η* and *G*' of the composite are even lower than those of the neat polymer but still higher than the plasticized matrix. Surprisingly, the viscosity of PP/30/0.5 OR is decreased as well, even though this compatibilizer had no plasticizing effect. Increasing the weight ratio of the compatibilizers, while keeping the ratio of the fibers to the matrix constant, results in the dilution of the fibers in the composites. In the case of the compatibilized systems in this graph, the overall content of the fibers in the composite is only 26 wt%. As shown in Fig. 5.5, by decreasing the content of the fibers from 30 to 26 wt%, the decreases in η* and *G*' are significant with respect to PP30. We also observe that the η* and *G*' of PP/30/0.5 OR and PP/30/0.5 AA are larger than that of the PP/26 composite, which can be attributed to the improvement of the interactions between the fibers and the matrix.

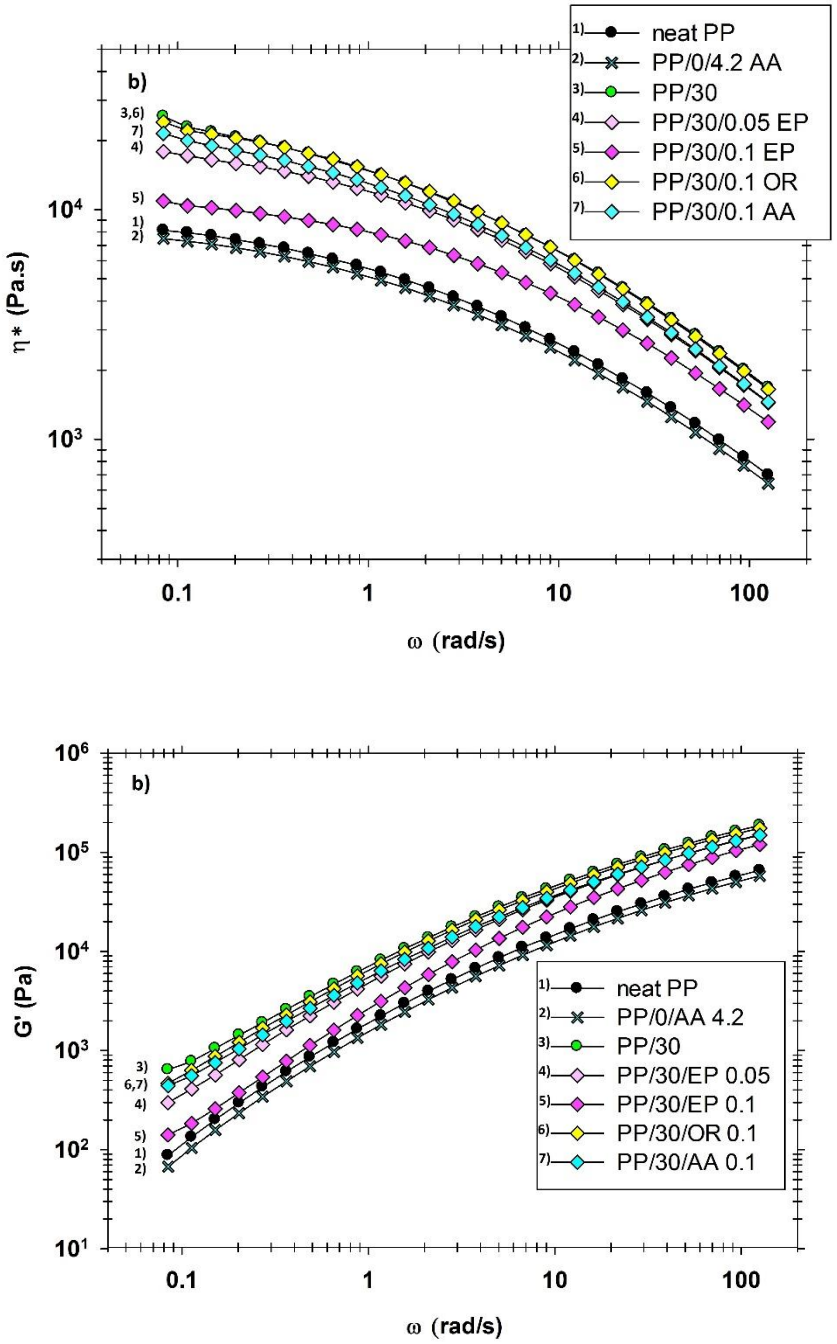

Fig. 5.4 Effect of three different compatibilizers at low content (10 wt% based on the fiber content) on a) complex viscosity and b) storage modulus of PP and PP-based composites with 30 wt% of flax fibers.

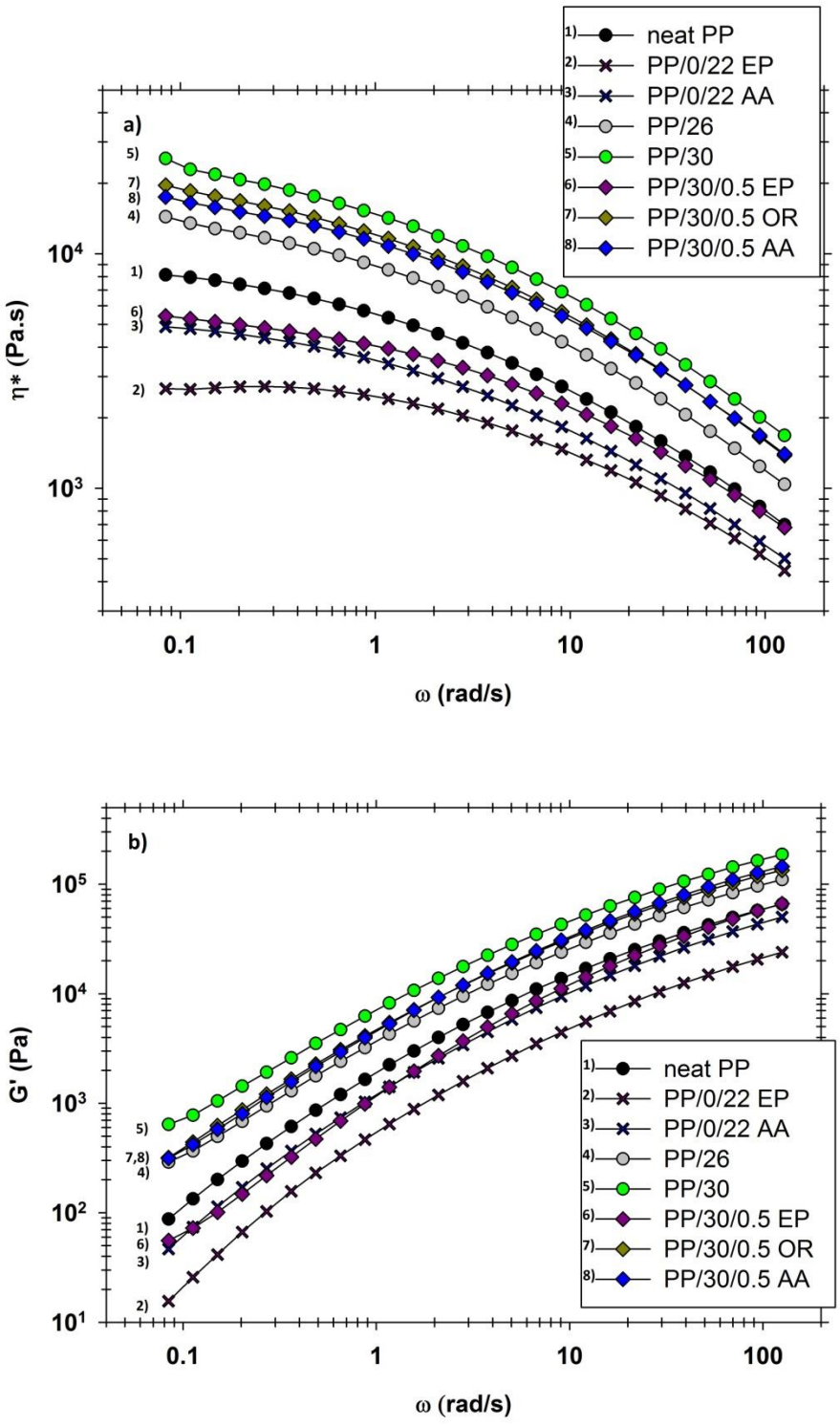

Fig. 5.5 Effect of three different compatibilizers at high content (50 wt% based on the fiber content) on a) complex viscosity and b) storage modulus of PP and PP-based composites with 30 wt% of flax fibers.

Fig. 5.6 illustrates the effect of pre-shearing on the complex viscosity of the PP/30/0.1 EP composite. Under shear the fibers will orient in the flow direction, which will result in lower rheological properties. The decrease in complex viscosity is marginal after shearing for 5 min at a shear rate of 0.1 s^{-1}; however, the decrease becomes significant after shearing for 10 min. Similar results have been reported for short sisal fibers [45].

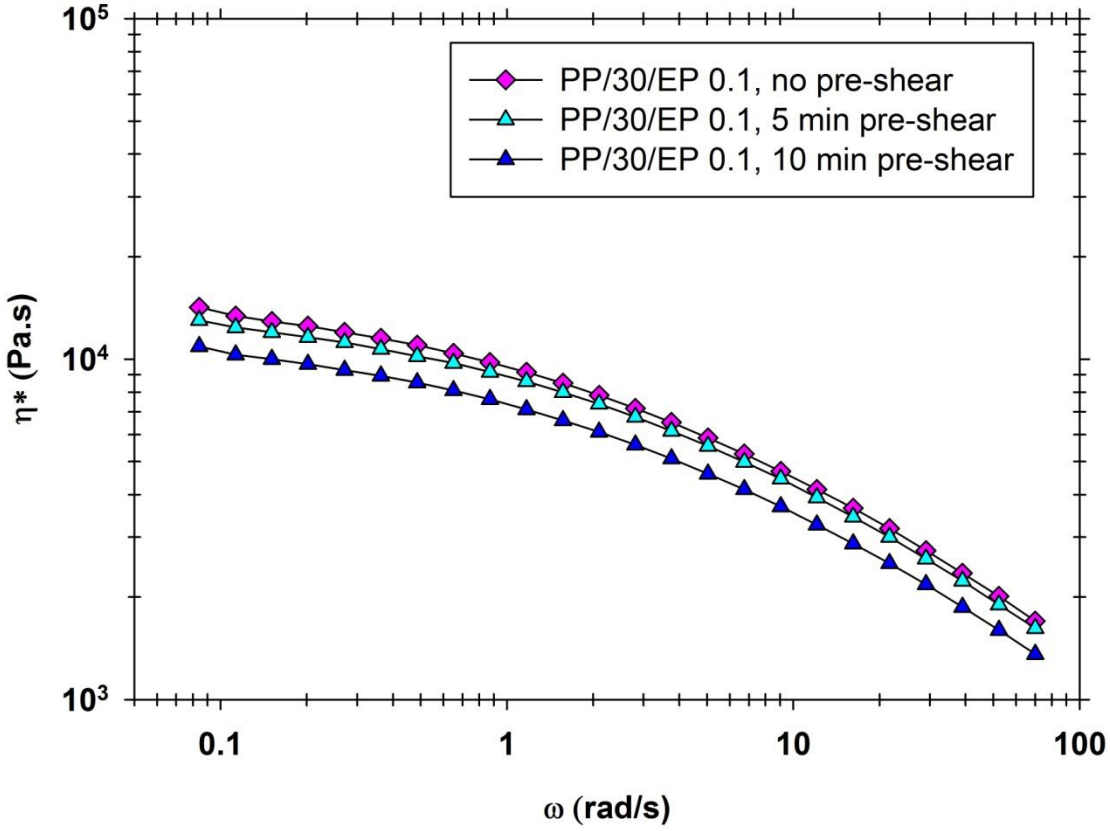

Fig. 5.6 Effect of pre-shearing on the complex viscosity of composite PP/30/0.1 EP.

Steady-shear viscosity

Fig. 5.7 compares the steady-shear viscosities (η) of compatibilized and uncompatibilized composites containing 10 and 30 wt% flax fibers. While no effect at 10 wt% of fibers was seen on the complex viscosity, the shear viscosity is larger than for neat PP at low shear rates. It can also be seen that the viscosity of the composites increases markedly with the fiber content and the composites are considerably more shear-thinning than the neat PP. The power-law index (n) related to the slope of η vs. $\dot{\gamma}$ on log-log plots at high shear rates (i.e. $\eta = m\left|\dot{\gamma}\right|^{n-1}$) changes from 0.86 for

the neat PP to 0.67 and 0.33 for PP/10 and PP/30, respectively. The power-law parameters have been determined in the range of 0.1- 0.5 s^{-1}. The alignment of fibers in simple shear in the flow direction has been reported in other investigations [42, 46] and this is known to enhance the shear-thinning behavior. As can also be seen in Fig. 5.7, the plasticizing effect of Epolene E43 decreases again the rheological properties of the compatibilized composites, even to a lower value than the neat matrix in the case of PP/10/0.1 EP. These results confirm the plasticizing effect observed for the linear viscoelastic data reported in Fig. 5.3. The power-law index for PP/10/ 0.1 EP is the same as for PP/10, but in the case of the compatibilized PP/30 it is 0.42 compared to 0.33 for the non compatibilized sample.

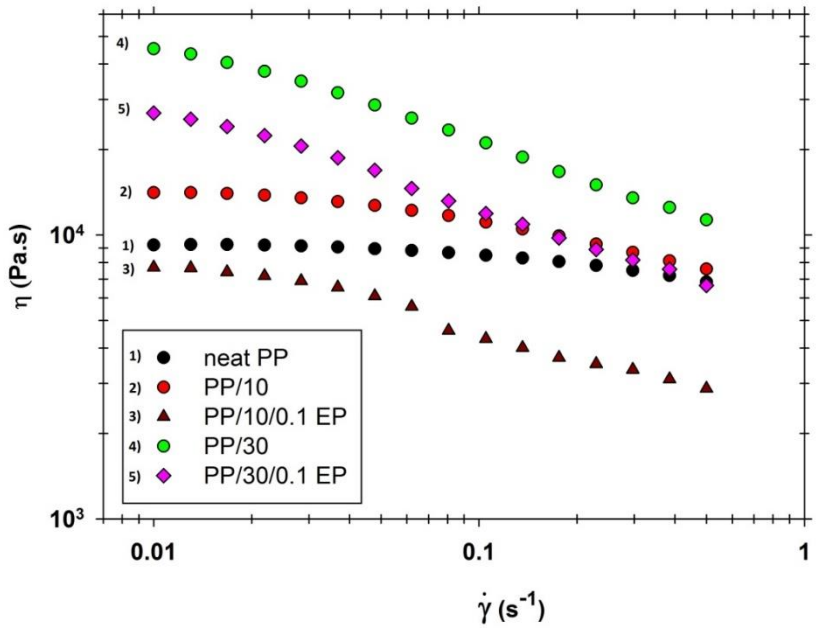

Fig. 5.7 Steady-shear viscosity of the neat PP and PP composites containing 10 and 30 wt% of flax fibers.

The shear and complex viscosity data are compared in Fig. 5.8 for the neat PP and the composites containing 30 wt% flax fibers with and without Epolene E43. The Cox-Merz rule is well verified for the neat PP, but is not valid for the composites containing 30 wt% flax fibers. It has been reported before [26, 47] that the Cox-Merz rule may not be valid for composites and complex systems. This can be the result of interactions in filled polymers and/or the orientation of the particles in the flow direction under simple shear [48]. Finally, when comparing the reduced steady-shear viscosity of PP suspensions of our flax fibers and glass fibers using the data of [26] at 14

vol% concentration of fibers (data not shown), the reduced viscosity for the flax fiber suspension was considerably larger and more shear-thinning than that of the glass fiber case. These effects were attributed to the flexibility of the flax fibers, as confirmed by the results of Keshtkar et al. [49].

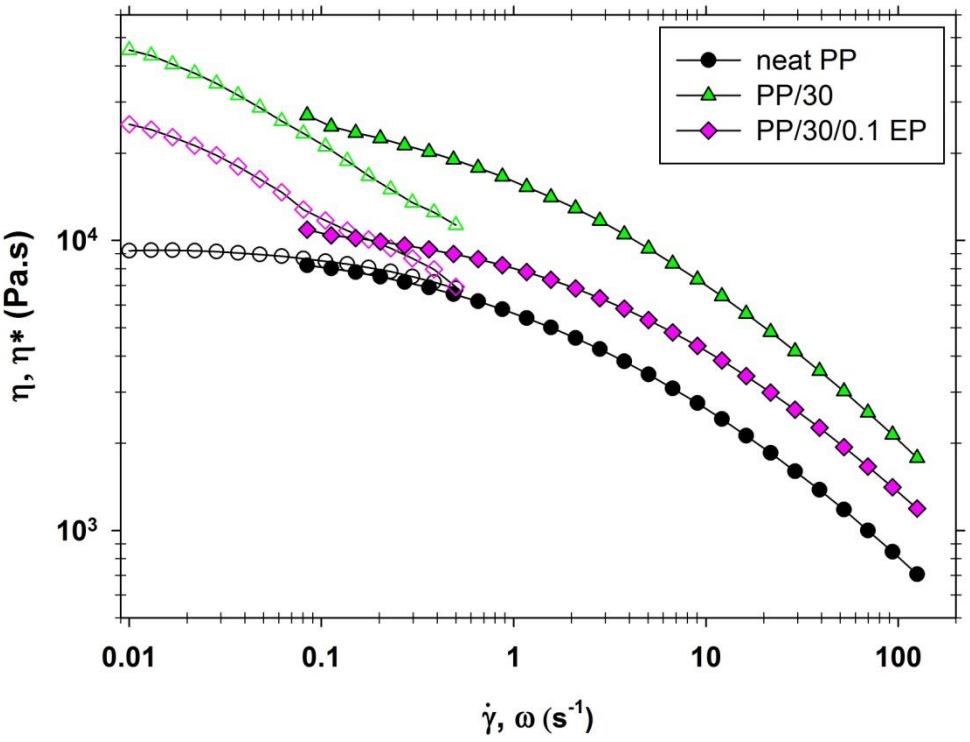

Fig. 5.8 Shear viscosity (open symbols) and complex viscosity (filled symbols) data for the neat PP and 30 wt% flax fiber reinforced PP, with and without Epolene E43. The lines are drawn to help the reading of the figure.

5.3.4 Mechanical properties

The mechanical properties of compatibilized and non-compatibilized PP-flax fiber composites in tensile testing were characterized and compared with those of the matrix. It should be mentioned that the orientation of fibers may change during material processing, from the molten to the solid state. It should also be mentioned that compression molding generally leads to an isotropic fiber orientation in the plane perpendicular to the disk axis (orthotropic orientation) [26], while

maximum reinforcement can be obtained only when the fibers are oriented in the drawing direction [27].

As revealed in Fig. 8 and 9, all composites show remarkably higher tensile modulus values than the neat PP. This can be attributed to the fact that the Young modulus of the fibers is around 28 GPa [50], hence much larger than that of the matrix (around 1 GPa). In addition, fibers may restrict the mobility of the PP chains [30]. Even though the modulus is increased as a result of the fiber contribution, the tensile strength of the composites in the absence of a compatibilizer decreases slightly with respect to the neat PP (see Figs. 5.9-b). This suggests a lack of stress transfer from the matrix to the fibers [4, 30], and the decrease is irrespective of the fiber content.

As shown in Fig. 5.9, the effect of Epolene E43 at 10 wt% with respect to the fiber content is important, especially for the composite containing 30 wt% flax fibers. The modulus and maximum tensile strength of the composite compatibilized with 10 wt% Epolene E43 increase by 200% and 30%, respectively, in comparison with the neat PP. By adding PPMA, the surface energy of the fibers is lowered to a level much closer to that of the matrix, and thus a better wetting is obtained. The improvement may also be related to a better dispersion of the fibers in the PP matrix [18].

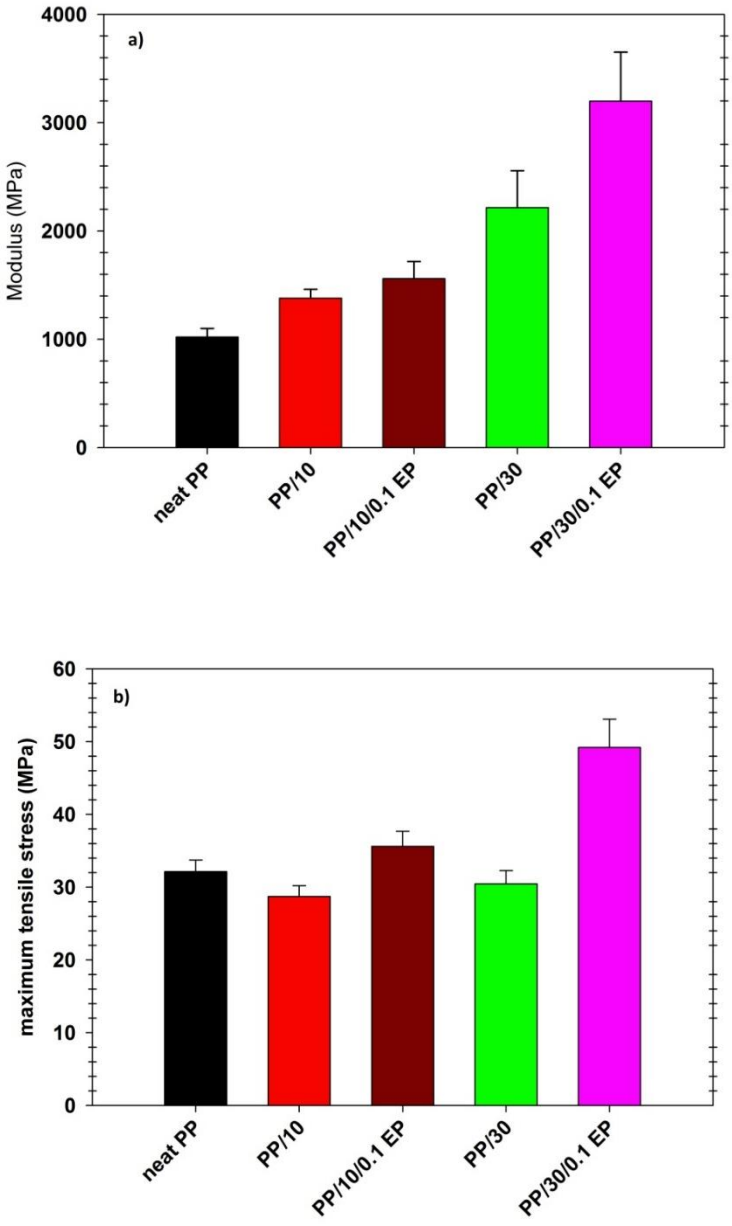

Fig. 5.9 Effect of Epolene E43 on the mechanical properties of composites: a) Young modulus, b) maximum tensile strength.

Yuan et al. [44] have reported that for different PPMA coupling agents there is an optimum concentration, which results in the best improvement of the mechanical behavior of systems such as flax fiber/PP composites. Arbelaiz et al. [18] investigated the effect of two different coupling agents with different molecular weights and acid numbers (Epolene E43 and Epolene G3003) and they observed that the optimum content for Epolene E43 and G3003 was 5 wt% and 10 wt%,

respectively and at higher contents slight increases in the strength and modulus could be observed. As a matter of fact, improvements of composites are significantly dependent on the MA content and on the MFI of the coupling agents. The MA content indicates the functionalities present in a coupling agent, whereas the melt flow index is somehow related to its miscibility with the neat PP and to the ability of the maleated PP chains to create entanglements with the PP chains. Fig. 5.10 compares the mechanical properties of the various compatibilized composites with those of the neat PP. OR (Orevac 18729) has a lower amount of maleic groups per chain length than EP, so at low modifier content it does not have enough maleic groups to cover the surface of the fibers. This results in a partial interface improvement and, consequently, less improvement of the tensile strength. EP (E43) is a wax of a lower molecular weight and contains 3.8 wt% MA. As a consequence, EP shows a better compatibilizing effect yielding enhanced mechanical properties. This is attributed to the stronger interactions with the hydrophilic fibers, fewer entanglements of the PPMA chains with the PP chains and facility to penetrate deeper inside the fiber bundles. Also it should be mentioned that sample PP/30/0.1 EP showed better mechanical properties in terms of tensile modulus and strength in comparison with PP/30/0.05 EP. This can be due to insufficient MA when using 5 wt% of Epolene to compatibilize this composite.

Fig. 5.10 also shows the effect of PPAA on the tensile properties. The tensile modulus of PP/30/0.1 AA is about 2.8 times that of the neat PP. The marginal decrease of the modulus for PP/30/0.5 AA can be the result of a dilution in the composite containing a large quantity of compatibilizer. However, the tensile strength of the 30 wt% fiber composites rises from 37 to 47 MPa as the content of PPAA is increased to 50% with respect to the fibers. With more acrylic acid groups to interact with the flax fibers the stress transfer at the interface is improved. Finally, as expected, the elongation at break of all composites decreased drastically from 144% for the neat PP to 21 and 5% for composites containing 10 and 30 wt% of fibers, respectively (data not shown). The compatibilization improved these values marginally.

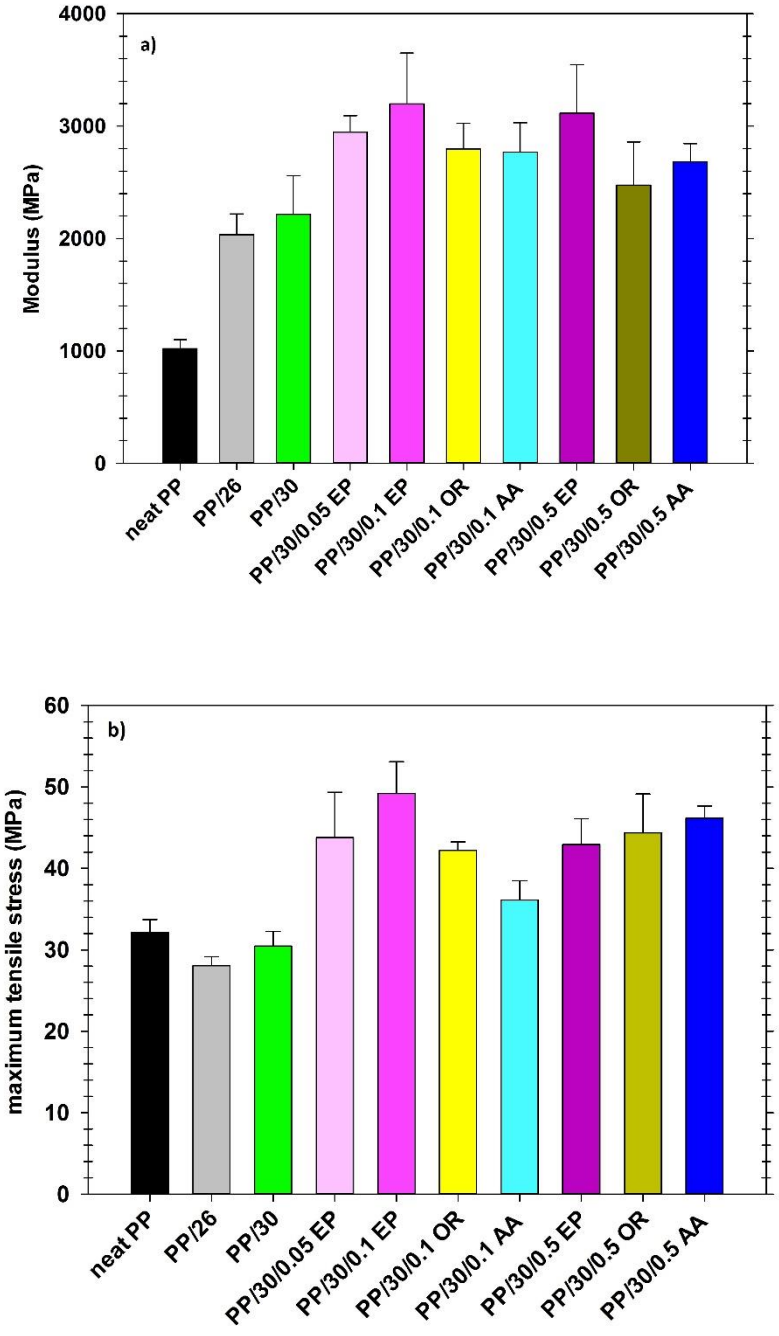

Fig. 5.10 Effect of different compatibilizers on the mechanical properties of composites containing 30 wt% fibers: a) Young modulus, b) maximum tensile strength.

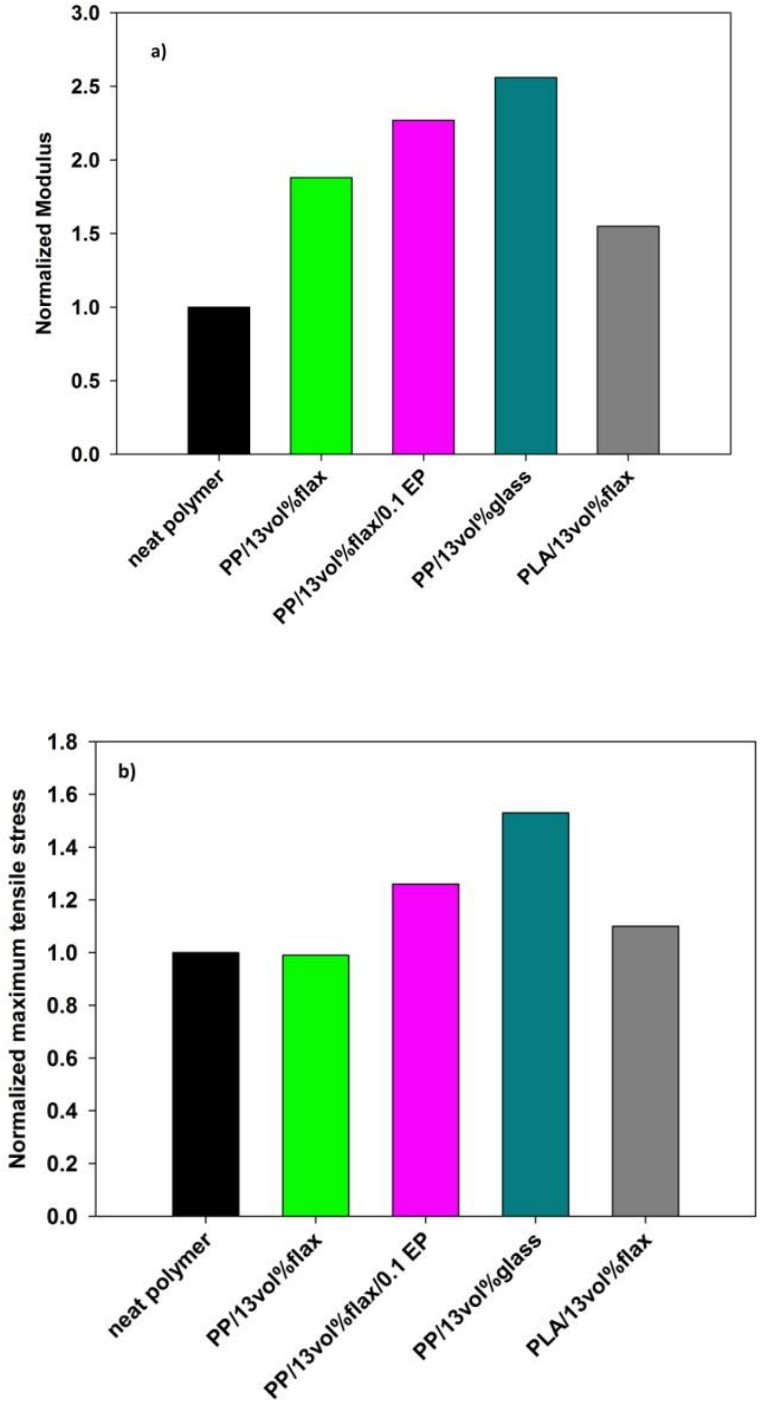

Fig. 5.11 Comparison between flax and glass fiber based composites containing 13 vol% of fibers: a) normalized modulus, b) normalized maximum tensile stress. The data for PP/13 vol% glass and PLA/13 vol % flax has been extracted from Arbelaiz et al. [30] and Arias et al. [13], respectively.

Fig. 5.11 compares the mechanical properties of different composites containing 13 vol % flax or glass fibers using our own data and some from the literature ([30]; [13]). The normalized values have been obtained by dividing the modulus and tensile strength by the values for the neat matrix. The normalized moduli of the PP non-compatibilized and EP-compatibilized flax composites are 1.8 and 2.2 times that of the matrix, whereas for the PP/glass and PLA/flax composites the corresponding values are 2.6 and 1.5, respectively. The tensile strength of the PP/flax composite is slightly lower than that of the matrix. For the compatibilized PP/flax and PLA/flax composite, the strength is respectively 1.2 and 1.1 times that of the matrix, while the tensile strength of the PP/glass composite is 1.6 times that of the matrix. The higher mechanical properties of the PP/glass composite in comparison with the PP/flax composites are due to the superior modulus and stiffness of glass fibers in comparison with natural fibers [3]. It should be mentioned that normalized specific modulus (modulus divided by density) of non-compatibilized and EP-compatibilized flax composites of PP and PP/glass are 1.76, 2.15 and 1.88, respectively. The tensile strength of compatibilized PP/flax and PP/glass composites are 1.17 and 1.16. The superior specific mechanical properties of the compatiblized PP/flax composite in comparison with PP/glass are attributed to its lower density, which results in lighter composites with acceptable mechanical properties.

5.3.5 SEM

Examination of the fracture surfaces of the composites by scanning electron microscopy provides information about the nature of adhesion between the matrix and the reinforcement and how different compatibilizers affect the morphology and mechanical properties of the composites [51]. Damage in composites is typically associated to matrix cracks, failed interfacial bonds between the fibers and the matrix and fiber breakage [15]. Fig. 5.12 compares SEM images of compatibilized and non-compatibilized PP/30 composites.

In Fig. 5.12a for the non-compatibilized composite, a gap is observed at the interface between the fibers and the PP matrix. The clean surface of the fibers with almost no remaining matrix on their surfaces and many pulled-out holes on the fractured surface of the composite indicate poor interactions between the flax fibers and the PP matrix [30]. This can explain the drop in the tensile strength of the unmodified composites in comparison with the neat PP.

When a composite is compatibilized with a coupling agent, it is difficult to differentiate the flax fibers from the PP matrix, as illustrated in the work of Arbelaiz et al. [30]. Generally, when the

content of the compatibilizer is sufficient and, consequently, the interface between the fibers and the matrix has been improved, no gaps between the fibers and the matrix can be seen; and a large quantity of the matrix adheres to the flax fibers, indicating better fiber/matrix adhesion resulting in improved mechanical properties [30].

When EP (Epolene E43) is used as the coupling agent, even at 10 wt% of compatibilizer to the fibers, as shown in Fig. 5.12-b the surface of the fibers is thoroughly covered with the matrix and we are in the presence of fiber failure. It was also observed that layers of the matrix material were pulled out together with the fibers during fracture. So in this case, as revealed by Fig. 5.12-e, increasing the compatibilizer content does not result in any further gain. In the case of OR (Orevac 18729), it is obvious in Fig. 5.12-c that there are areas where the adhesion between the PP and the flax fibers is promoted, as broken fibers can be seen with no gap between the PP matrix and flax fiber surfaces, but on the other hand some fiber pull-out can also be observed. This is an indication of poor interfacial adhesion and insufficient wetting of the flax fibers, which can be attributed to the low content of maleic anhydride. As seen in Fig. 5.12-f, the adhesion at the interface of the flax fibers and PP can be improved by increasing the content of OR. These observations indicate that OR modifies the interface adhesion between PP and flax fibers to some extent and improves the tensile strength of the composites, but its efficiency is inferior to EP. As illustrated by Fig. 5.12-d for PP/30/0.1 AA the matrix covering of the fibers is only partial and some fiber pullout can be observed on the fractured surface. As for the case of OR, increasing the content of PPAA improves the PP/fiber interface and more fiber breakage and less fiber pullouts are observed (Fig. 5.12-g).

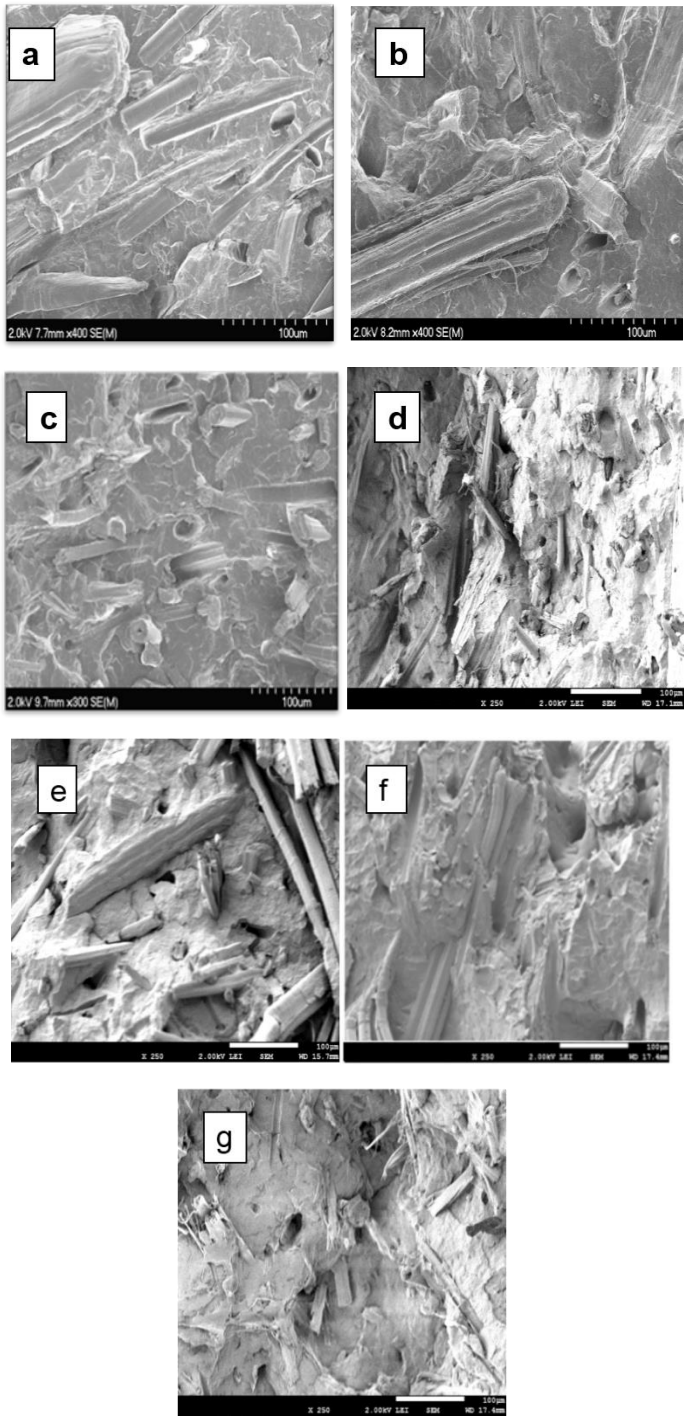

Fig. 5.12 SEM images of PP/flax composite: a) PP/30, b) PP/30/0.1 EP, c) PP/30/0.1 OR, d) PP/30/0.1 AA, e) PP/30/0.5 EP, f) PP/30/0.5 OR, g) PP/30/0.5 AA.

5.4 Conclusions

In this study the effect of different compatibilizers on the rheological and mechanical properties of flax fiber polypropylene composites has been investigated. The mean flax fiber length was decreased after compounding by 70% from its initial nominal length of 1 mm. Rheological characterization showed that the fiber content has the most significant effect on the complex viscosity of the filled systems. It has been observed that compatibilizing with PPMA and PPAA, besides enhancing fiber/polymer interaction, can lead to plasticization and the balance between these competing effects determines the overall rheological behavior of the composite. The increase in tensile properties demonstrated that PPMA and PPAA were effective compatibilizers for PP/flax fiber composites, but their efficiency depended on their MFI and grafted group content. The PPMA with the highest content of MA (Epolene E43) was found to be the most efficient in improving the interface between the PP matrix and the flax fibers. However, because of its low molecular weight Epolene E43 was found to decrease the rheological properties of the PP composite, favoring their processability.

5.5 Acknowledgments

The authors gratefully acknowledge the Natural Sciences and Engineering Research Council of Canada (NSERC) for funding. They also thank Gilles Ausias from Laboratoire d'Ingénierie des Matériaux de Bretagne (LIMATB) for providing the flax fibers.

5.6 References

1. Biagiotti, J., S. Fiori, L. Torre, M.A. López-Manchado, and J.M. Kenny, Mechanical properties of polypropylene matrix composites reinforced with natural fibers: A statistical approach. Polymer Composites, 2004. 25(1): p. 26-36.
2. Oksman, K., A.P. Mathew, R. Långström, B. Nyström, and K. Joseph, The influence of fibre microstructure on fibre breakage and mechanical properties of natural fibre reinforced polypropylene. Composites Science and Technology, 2009. 69(11-12): p. 1847-1853.
3. Bledzki, A.K. and J. Gassan, Composites reinforced with cellulose based fibres. Progress in Polymer Science, 1999. 24: p. 221–274.

4. Soleimani, M., L. Tabil, S. Panigrahi, and A. Opoku, The Effect of Fiber Pretreatment and Compatibilizer on Mechanical and Physical Properties of Flax Fiber-Polypropylene Composites. Journal of Polymers and the Environment, 2008. 16(1): p. 74-82.

5. Wielage, B., T. Lampke, H. Utschick, and F. Soergel, Processing of natural-fibre reinforced polymers and the resulting dynamic–mechanical properties. Journal of Materials Processing Technology, 2003. 139(1-3): p. 140-146.

6. Bismarck, A., S. Mishra, and T. Lampke, Plant Fibers as Reinforcement for Green Composites, in Natural Fibers, Biopolymers, and Biocomposites. 2005, CRC Press Taylor & Francis Group. p. 37-108.

7. Barkoula, N.M., S.K. Garkhail, and T. Peijs, Effect of Compounding and Injection Molding on the Mechanical Properties of Flax Fiber Polypropylene Composites. Journal of Reinforced Plastics and Composites, 2009. 29(9): p. 1366-1385.

8. Mingzhu, P., S.Y. Zhang, and Z. Dingguo, Preparation and Properties of Wheat Straw Fiber-polypropylene Composites. Part II. Investigation of Surface Treatments on the Thermo-mechanical and Rheological Properties of the Composites. Journal of Composite Materials, 2009. 44(9): p. 1061-1073.

9. Nayak, S.K., S. Mohanty, and S.K. Samal, Influence of short bamboo/glass fiber on the thermal, dynamic mechanical and rheological properties of polypropylene hybrid composites. Materials Science and Engineering: A, 2009. 523(1-2): p. 32-38.

10. Charlet, K. and A. Béakou, Mechanical properties of interfaces within a flax bundle – Part I: Experimental analysis. International Journal of Adhesion and Adhesives, 2011. 31(8): p. 875-881.

11. El-Sabbagh, A., L. Steuernagel, and G. Ziegmann, Processing and modeling of the mechanical behavior of natural fiber thermoplastic composite: Flax/polypropylene. Polymer Composites, 2009. 30(4): p. 510-519.

12. Barkakaty, B.C., Some structural aspects of sisal fibers. Journal of Applied Polymer Science, 1976. 20(11): p. 2921-2940.

13. Arias, A., M.-C. Heuzey, and M.A. Huneault, Thermomechanical and crystallization behavior of polylactide-based flax fiber biocomposites. Cellulose, 2012. 20(1): p. 439-452.

14. Garkhail, S., R. Heijenrath, and T. Peijs, Mechanical properties of natural-fibre-mat-reinforced thermoplastics based on flax fibres and polypropylene. Applied Composite Materials, 2000. 7(5): p. 351-372.

15. Luz, S.M., A.R. Gonçalves, and A.P. Del'Arco, Mechanical behavior and microstructural analysis of sugarcane bagasse fibers reinforced polypropylene composites. Composites Part A: Applied Science and Manufacturing, 2007. 38(6): p. 1455-1461.

16. Khalid, M., A. Salmiaton, T. Chuah, C. Ratnam, and S.T. Choong, Effect of MAPP and TMPTA as compatibilizer on the mechanical properties of cellulose and oil palm fiber empty fruit bunch–polypropylene biocomposites. Composite Interfaces, 2008. 15: p. 251–262.

17. Rensch, H.P. and B. Riedl, Characterization of chemically modified chemithermomechanical pulp by thermal analysis. Part 1. Treatment with anhydrides. Thermochimica Acta, 1992. 205: p. 39-49.

18. Arbelaiz, A., B. Fernández, J.A. Ramos, A. Retegi, R. Llano-Ponte, and I. Mondragon, Mechanical properties of short flax fibre bundle/polypropylene composites: Influence of matrix/fibre modification, fibre content, water uptake and recycling. Composites science and technology, 2005. 65(10): p. 1582-1592.

19. Velde, K.V.d. and P. Kiekens, Influence of Fibre and Matrix Modifications on Mechanical and Physical Properties of Flax Fibre Reinforced Poly(propylene). Macromolecular Materials and Engineering, 2001. 4(286): p. 237-242.

20. Paunikallio, T., J. Kasanen, M. Suvanto, and T.T. Pakkanen, Influence of Maleated Polypropylene on Mechanical Properties of Composite Made of Viscose Fiber and Polypropylene. Journal of Applied Polymer Science, 2003. 87: p. 1895–1900.

21. Keener, T.J., R.K. Stuart, and T.K. Brown, Maleated coupling agents for natural fibre composites. Composites Part A: Applied Science and Manufacturing, 2004. 35(3): p. 357-362.

22. Qiu, W., T. Endo, and T. Hirotsu, Interfacial interaction, morphology, and tensile properties of a composite of highly crystalline cellulose and maleated polypropylene. Journal of Applied Polymer Science, 2006. 102(4): p. 3830-3841.

23. Gauthier, R., C. Joly, A.C. Coupas, H. Gauthier, and M. Escoubes, Interfaces in polyolefin/cellulosic fiber composites: Chemical coupling, morphology, correlation with adhesion and aging in moisture. Polymer Composites, 1998. 19(3): p. 287-300.

24. Puglia, D., A. Terenzi, S.E. Barbosa, and J.M. Kenny, Polypropylene-natural fibre composites. Analysis of fibre structure modification during compounding and its influence on the final properties. Composite Interfaces, 2008. 15: p. 111-129.

25. Kalaprasad, G., G. Mathew, C. Pavithran, and S. Thomas, Melt Rheological Behavior of Intimately Mixed Short Sisal–Glass Hybrid Fiber-Reinforced Low-Density Polyethylene Composites. I. Untreated Fibers. Journal of Applied Polymer Science, 2003. 89: p. 432-442.

26. Mobuchon, C., P.J. Carreau, M.-C. Heuzey, M. Sepehr, and G. Ausias, Shear and extensional properties of short glass fiber reinforced polypropylene. Polymer Composites, 2005. 26(3): p. 247-264.

27. Kim, J.K. and J.H. Song, Rheological properties and fiber orientations of short fiber-reinforced plastics. Journal of Rheology, 1997. 41(5): p. 1069-1078.

28. Hristov, V. and J. Vlachopoulos, Influence of Coupling Agents on Melt Flow Behavior of Natural Fiber Composites. Macromolecular Materials and Engineering, 2007. 292(5): p. 608-619.

29. Hwang, B.S., B.S. Kim, J.H. Lee, J.H. Byun, and J.M. Park, Physical parameters and mechanical properties improvement for Jute fiber/polypropylene composites by maleic anhydride coupler., in 16th international conference on composite materials 2007: Kyoto, Japan.

30. Arbelaiz, A., B. Fernández, G. Cantero, R. Llano-Ponte, A. Valea, and I. Mondragon, Mechanical properties of flax fibre/polypropylene composites. Influence of fibre/matrix modification and glass fibre hybridization. Composites Part A: Applied Science and Manufacturing, 2005. 36(12): p. 1637-1644.

31. Cantero, G., A. Arbelaiz, R. Llano-Ponte, and I. Mondragon, Effects of fibre treatment on wettability and mechanical behaviour of flax/polypropylene composites. Composites Science and Technology, 2003. 63(9): p. 1247-1254.

32. Van de Velde, K. and P. Kiekens, Effect of material and process parameters on the mechanical properties of unidirectional and multidirectional flax/polypropylene composites. Composite Structures, 2003. 62(3–4): p. 443-448.

33. Le Moigne, N., M. van den Oever, and T. Budtova, Dynamic and capillary shear rheology of natural fiber-reinforced composites. Polymer Engineering & Science, 2013. 53(12): p. 2582-2593.

34. Perrin-Sarazin, F., M.T. Ton-That, M.N. Bureau, and J. Denault, Micro- and nano-structure in polypropylene/clay nanocomposites. Polymer, 2005. 46(25): p. 11624-11634.

35. Tucker III, C.L. and S.G. Advani, eds. Flow and Rheology in Polymer Composites Manufacturing. Ed. S.G. Advani. 1994, Elsevier Science: New York.

36. Sepehr, M., G. Ausias, and P.J. Carreau, Rheological properties of short fiber filled polypropylene in transient shear flow. Journal of Non-Newtonian Fluid Mechanics, 2004. 123(1): p. 19-32.

37. George, J., E. Klompen, and T. Peijs, Thermal degradation of green and upgraded flax fibres. Advanced Composites Letters (UK), 2001. 10(2): p. 81-88.

38. Shafizadeh, F. and A.G.W. Bradbury, Thermal degradation of cellulose in air and nitrogen at low temperatures. Journal of Applied Polymer Science, 1979. 23(5): p. 1431-1442.

39. Van de Velde, K. and E. Baetens, Thermal and Mechanical Properties of Flax Fibres as Potential Composite Reinforcement. Macromolecular Materials and Engineering, 2001. 286: p. 342-349.

40. Wu, D., Y. Sun, L. Wu, and M. Zhang, Linear viscoelastic properties and crystallization behavior of multi-walled carbon nanotube/polypropylene composites. Journal of Applied Polymer Science, 2008. 108(3): p. 1506-1513.

41. Utracki, L.A., Flow and flow orientation of composites containing anisometric particles. Polymer Composites, 1986. 7(5): p. 274-282.

42. Twite-Kabamba, E., A. Mechraoui, and D. Rodrigue, Rheological properties of polypropylene/hemp fiber composites. Polymer Composites, 2009. 30(10): p. 1401-1407.

43. Li, T.Q. and M.P. Wolcott, Rheology of wood plastics melt. Part 1. Capillary rheometry of HDPE filled with maple. Polymer Engineering & Science, 2005. 45(4): p. 549-559.

44. Yuan, X., Y. Zhang, and X. Zhang, Maleated polypropylene as a coupling agent polypropylene-waste Newspaper Flour Composites. Journal of Applied Polymer Science, 1999. 77: p. 333-337.

45. Nair, K.C.M., R.P. Kumar, S. Thomas, S.C. Schit, and K. Ramamurthy, Rheological behavior of short sisal fiber-reinforced polystyrene composites. Composites Part A: Applied Science and Manufacturing, 2000. 31(11): p. 1231-1240.

46. González-Sánchez, C., C. Fonseca-Valero, A. Ochoa-Mendoza, A. Garriga-Meco, and E. Rodríguez-Hurtado, Rheological behavior of original and recycled cellulose–polyolefin composite materials. Composites Part A: Applied Science and Manufacturing, 2011. 42(9): p. 1075-1083.

47. Pötschke, P., T.D. Fornes, and D.R. Paul, Rheological behavior of multiwalled carbon nanotube/polycarbonate composites. Polymer 2002. 43(11): p. 3247-3255.

48. Barbosa, S.E. and J.M. Kenny, Processing of short-fiber reinforced polypropylene. I. Influence of processing conditions on the morphology of extruded filaments. Polymer Engineering & Science, 2000. 40(1): p. 11-22.

49. Keshtkar, M., M.C. Heuzey, and P.J. Carreau, Rheological behavior of fiber-filled model suspensions: Effect of fiber flexibility. Journal of Rheology, 2009. 53(3): p. 631-650.

50. Malkapuram, R., V. Kumar, and Y.S. Negi, Recent Development in Natural Fiber Reinforced Polypropylene Composites. Journal of reinforced plastics and composites, 2008. 28(10): p. 1169-1189.

51. Oksman, K. and C. Clemons, Mechanical Properties and Morphology of Impact Modified Polypropylene-Wood Flour Composites. Journal of Applied Polymer Science, 1998. 67: p. 1503-1513.

CHAPTER 6 ARTICLE 2: MECHANICAL AND MORPHOLOGICAL PROPERTIES OF CELLULOSE NANOCRYSTAL (CNC)-POLYPROPYLENE COMPOSITES [2]

*Helia Sojoudiasli, Marie-Claude Heuzey, Pierre J. Carreau**

Research Center for High Performance Polymer and Composite Systems (CREPEC), Department of Chemical Engineering, Polytechnique Montreal, C.P. 6079, succ. Centre-Ville, Montreal, QC, Canada, H3C 3A7

* Corresponding author. Email address: pcarreau@polymtl.ca

Abstract

In this work, the rheological, mechanical, morphological and thermal properties of cellulose nanocrystal (CNC)-polypropylene (PP) composites prepared in the molten state were investigated. All samples contained a maleated polypropylene used as combatibilizer. Degradation of the PP in the presence of CNCs at high processing temperature was shown to have a significant effect on the rheological behavior. For PPs with two different molecular weights and prepared at different temperatures, the tensile modulus of composites containing 2 wt% CNC was improved by about 30% and the tensile strength was increased up to 16%, in comparison with the unfilled matrices. The tensile strain at break of composites decreased by 17% up to 75% with respect to the matrix, depending on the processing conditions and PP used. Preparing the low molecular weight PP composites via twin-screw extrusion was shown to be more efficient than using an internal batch mixer. The tensile modulus of the PP/CNC composites could be fairly well described by a model proposed by Nielsen based on the Halpin-Tsai equation. Finally, properties of the PP/CNC composites have been compared to those of a PP reinforced with flax fibers and a PP filled with nanoclay.

Keywords Cellulose nanocrystals (CNCs), polypropylene, maleated polypropylene (PPMA), melt compounding, composite, tensile properties.

---

[2] Published in Polymer Composites 2017; 10.1002/pc.24383.

6.1 Introduction

Cellulose is renewable, biodegradable, non-toxic and the most abundant natural biopolymer on earth. In the last decades, the use of cellulose-based fillers in reinforced thermoplastics has triggered new investigations. Aqueous suspensions of cellulose nanocrystals (CNCs) can be prepared by acid hydrolysis of the biomass such as bacteria, cotton, and wood pulp [1]. The number of sulfate groups on the surface and crystallinity content of CNC depends on duration of acid hydrolysis [2]. The nanoparticles are stabilized in aqueous suspension by negative charges of sulfuric acid on the surface, which are introduced during the hydrolysis process [3,4]. The resulting nanocrystals are rod-like particles or whiskers [5], and depending on the source, these nanocrystals offer a wide range of aspect ratios (L/d, L being the length and d the diameter), from 1 to about 100 [6]. Different terms are used to refer to CNCs in literature: nanocrystalline cellulose (NCC), cellulose whiskers and cellulose nanowhiskers (CNWs). As these nanowhiskers generated from cellulose fibers contain only a small number of defects in the crystalline structure, they have much higher mechanical properties than those of the initial fibers. It was reported that the cellulose crystal regions exhibit a Young modulus of up to 143 GPa [7], whereas the Young modulus of flax fibers has been reported to be about 28 GPa [8]. These nanoparticles have been used as reinforcements in different polymer matrices. The hydrophilic nature of CNCs favors their use in water soluble polymer matrices or water-based emulsions such as latex [9], starch [10], polyvinyl alcohol (PVOH) [11,12] and polyethylene oxide (PEO) [13] to prepare composites, mainly using solvent casting. Other common polymers used are: polylactic acid (PLA) [14,15], polypropylene (PP) [16-19], polyamide 6 [20], LDPE [21] and polyvinyl acetate [22]. Ljungberg et al. [16,19] compounded different types of modified cellulose whiskers in atactic (aPP) and isotactic polypropylenes. They observed that the incorporation of CNCs improved the tensile strength in comparison with the neat aPP; the use of a maleated PP (PPMA) or a surfactant (phosphoric ester of polyoxyethylene- 9-nonylphenyl ether) improved the ductility of the composites in comparison with the non-modified composite by 200 and 900 %, respectively [19]. Hassanabadi et al. [23] studied the effect of the acid value and molecular weight of PPMA on their efficiency as a compatibilizer between PP and CNCs. The acid value (AV) of PPMA was the most crucial parameter since it defines the number of active sites on the chain to interact with the surface of the CNCs. With equal AV the higher molecular weight of PPMA favored better entanglement with the matrix chains and consequently better compatibilization between PP and CNCs [23]. PPMA has been also used for compatibilizing

cellulosic fibers such as hemp and flax with PP in composites [24-26]. The best compatibilization would occur at an optimum content of PPMA to fibers, depending on the melt flow index (MFI) and MA content of the PPMA [26].

It is expected that surface modification of CNCs improve the dispersion of the filler within a polymeric matrix or increase the mechanical properties of nanocomposite in comparison with pristine CNC [27], but in most cases it includes some complicated and expensive chemical reactions that may also decrease the hydrogen bonds between the nanoparticles. These bonds were reported to be the basis of the reinforcing effect of cellulose whisker nanocomposites [28].

Khoshkava and Kamal [18] studied the effect of surface energy on the dispersion and mechanical properties of PP and PLA composites reinforced with CNCs. The surface energy of CNCs was lowered as the temperature was increased. Also by decreasing the size of the nanoparticles, the required energy for the dispersion of CNCs increased drastically.

Polyethylene oxide (PEO) has been used as a carrier polymer in LDPE [21] and PLA [15] composites reinforced with CNCs. LDPE/CNC composites exhibited a brownish color whereas the samples modified with PEO had the same color as the unfilled matrix. Also, the presence of large CNC agglomerates has been reported for untreated composites [21]. Arias et al. [15] investigated the effect of high and low molecular weight PEOs and different PEO/CNC ratios on the crystallinity, rheological, mechanical, and morphological properties of PLA/PEO/CNC composites. The low molecular weight PEO was found to be more efficient for dispersing the nanoparticles, but, on the other hand, this PEO plasticized the composites and changed its behavior from brittle to ductile. No significant improvement in the tensile modulus and strength was reported.

The effect of CNC particles on crystallinity of their composites with PP has been investigated [29, 30]. Gray [29] observed that CNCs in PP composites act as a nucleating agent and a transcrystalline layer forms around CNCs. Khoshkava et al. [30] used their spray freeze-dried CNCs to prepare PP/CNC composites. By incorporating 1 wt% CNCs, DSC results showed that the composites had a higher crystallization rate and higher crystallization temperature in comparison to the neat PP [30].

Extrusion and melt processing of CNC composites has been the subject of a few investigations. This is the most economical and environment friendly method of preparing polymer composites. However, in melt mixing, due to poor dispersion, a network formation among whiskers does not

necessarily occur and, hence, the mechanical properties of these composites are generally inferior in comparison with solvent-casted composites [28]. This behavior has been explained by a possible degradation at high temperature in the extruder and also the existence of CNC agglomerates [31]. Also the required energy to break CNC agglomerates increases drastically as the particle size decreases [18] and in order to disperse the particles individually the use of a solvent and/or high mechanical force is essential.

The aim of the present work is to investigate the effect of two different molecular weight PPs on the dispersion and mechanical properties of PP/CNC composites, which to the best of our knowledge has not been reported in the literature. A maleated PP (PPMA) is used as a compatibilizer between the PPs and CNCs. The mechanical properties of the composites, processed at two different temperatures, are compared and the structure-property relationships are discussed in light of the morphology. To investigate the effect of higher shear stresses, the properties of a composite processed via twin-screw extrusion are also compared with samples processed using an internal batch mixer.

6.2 Experimental

6.2.1 Materials

The two polypropylenes (PPs) used as matrices were Profax 6823 (PP1) and Profax 6323 (PP2) from Basell Polyolefins, with melt flow rates (MFR) of 0.4 and 12 (g/10 min- @ 230 °C/ 2.16 kg) and molecular weights of about 812 and 300 kg/mol, respectively. The cellulose nanocrystals (CNCs) used in this work were spray-dried in the form of powder and provided by FPInnovations (Pointe-Claire, Canada) prepared from fully bleached commercial softwood pulp [32]. Based on the information from the supplier, the average length and diameter of individual CNC is about 100 and 15 nm, respectively. Based on the XPS results the number of sulfate half-ester groups per 100 bulk anhydroglucose is 4.18. Orevac 18729 (OR), which is a PPMA from Arkema with a melt flow index MFI of 4.5 (g/10 min- @ 230 °C/ 2.16 kg) and MA content lower than 1 wt%, has been used as a compatibilizer between the PPs and CNCs; 10 wt% of OR based on the content of PP has been used in all composites.

6.2.2 Melt compounding

The composites were prepared by melt mixing using an internal batch mixer (C.W. Brabender Plasticorder) with a volumetric capacity of 30 mL under a nitrogen atmosphere. The mixing was carried out at 100 rpm. The compatibilizer and CNCs were dried at 80 °C for 24 h under vacuum prior to mixing. To apply the same thermo-mechanical cycle to all samples, the unfilled PPs with compatibilizer were also processed using the same procedure. The PPs were dry-mixed with the compatibilizer prior to feeding into the internal batch mixer or extruder. Two different processing conditions were used with the internal batch mixer. In the first, the pellets of PP and OR were fed to the internal mixer initially operating at 190 °C to ensure their melting. After 2 min of mixing at 190 °C the temperature was lowered gradually to 175 °C and the CNCs were added. The mixing continued at 175 °C for 12 min. For the second procedure, PP and OR were mixed at 210 °C for 2 min and the CNCs were added afterwards. The mixing continued for 10 more min at 210 °C. For both mixing temperatures the highest available rotational speed of the internal mixer (100 rpm) was used to prepare the composites.

All the samples were molded using compression molding at 185 °C with the same procedure for 11 min (5 min preheating + 6 min under pressure) and the pressure increased gradually from 0 to 14 MPa under a nitrogen atmosphere, followed by quenching in a cold press for 3 min. The nomenclature and composition of samples are presented in Table 6.1.

Table 6.1 Formulations prepared in the internal mixer. "T" indicates the mixing temperature. "PPx" stands for either PP1 or PP2.

SAMPLE	PP (wt %)	OR (wt %)	CNC (wt %)
PPx/0-T	90	10	0
PPx/2-T	88.2	9.8	2
PPx/5-T	85.5	9.5	5

The composite defined by PP1/5-175 refers to the PP1 (Profax 6823) based matrix containing 5 wt% of CNCs and processed under the lower temperature conditions. Also to compare the effect of the mixing method, a co-rotating 18 mm diameter twin-screw extruder (Leistritz Model ZSE18HP) was used to prepare a PP2-based composite containing 2 wt% CNCs, followed by water cooling of the extrudate in a bath and pelletizing. The temperature profile along the barrel (from hopper to die) was set to 170/180/190/200/210/210/210 °C. The extrusion was carried out at 100 rpm. PP2/2-ext refers to the PP2 (Profax 6323) based sample containing 2 wt% CNCs processed in the twin-screw extruder.

6.2.3 Characterization

TGA

Thermogravimetric analyses were carried out using a TGA Q500 from TA Instruments. The measurements were performed at a heating rate of 2 °C /min in high resolution mode. Since in the internal mixer and in compression molding the procedures were carried out under nitrogen, N_2 at a flow rate of 60 mL/min was also used for the TGA tests. Temperature ranged from 350 to 600 °C. The samples weights were 10-15 mg.

Rheometry

An Anton Paar rotational rheometer (MCR 301) equipped with a 25 mm parallel plate flow geometry was used to carry out the rheological measurements at 175 and 210 °C under a nitrogen atmosphere. A 1.2 mm gap between the plates was set and it was verified that the rheological results were independent of the gap used to carry out the experiments. The region of linear viscoelasticity was first determined by performing stress-sweep tests. The thermal stability of the various composites was verified from dynamic time sweeps at 0.628 rad/s for 20 min. All measurements were reproducible with deviations less than 6%.

Tensile properties

Tensile properties were investigated using an Instron universal testing machine according to ASTM D638. Measurements were performed on standard type V dog-bone shaped samples prepared by compression molding, at room temperature with a crosshead speed of 10 mm/min and using a load cell of 5 kN. The reported results are the average of at least 6 tests for each composite sample.

Differential scanning calorimetry (DSC)

The crystallization behavior of PP/CNC composites was evaluated using a DSC882 from Mettler-Toledo under a helium atmosphere. Samples were sealed in aluminum pans. The first heating, from room temperature to 200 °C at 10 °C/min, was used to compare the crystallinity of different samples and correlate with mechanical properties. The non-isothermal crystallization temperature was examined by cooling the samples from 200 down to 30 °C at a cooling rate of 10 °C/min. A minimum of 3 specimens were tested for each formulation.

Scanning electron microscopy (SEM)

To evaluate the degree of dispersion of the nanoparticles, scanning electron microscopy (SEM) has been performed on cryo-microtomed cross-section surfaces prepared with a Leica RM2165 microtome equipped with liquid nitrogen cooling; the sample surfaces were coated with platinum. The microscope was a JEOL JSM 7600TFE instrument operated at a voltage of 2 kV.

6.3 Results and discussion

6.3.1 Thermal stability

The thermal stability of spray-dried CNCs was compared with that of flax fibers using the TGA technique. Fig. 6.1 shows the relative weight (left ordinate) and the weight drop first derivative (right ordinate) as functions of temperature. For flax fibers three different rapid weight loss regions can be identified, whereas for CNCs two regions can be seen. As CNCs and flax were not dried in the oven prior to the test, the first weight loss is associated to the evaporation of residual moisture that occurred between room temperature and about 100 °C. The second important weight loss, accounting for more than 50 % of the total loss, takes place between 270 and 280 °C for CNCs and between 240 and 380 °C for flax fibers. This weight loss region is shown as a peak with a shoulder in the weight drop first derivative curve for flax fibers, but for CNCs it is described as a sharp peak. The shoulder in the second peak of the flax fibers can be related to the degradation of hemicellulose, followed by the first step of cellulose depolymerization [26]. The content of hemicellulose for flax is reported between 18.6 to 20.6 wt% [7]. The shift of the peak to lower temperature for CNCs, in

comparison with flax, can be related to the existence of a small amount of sulfate groups on the surface of CNCs. It has been reported [3] that these groups, resulting from the acid hydrolysis during CNC production, induce a considerable decrease in the degradation temperature. A third region can also be distinguished from the second one above 400 °C, which can be associated to the final stage of cellulose degradation [27]. Considering these results, the processing temperature of 210 °C or 175 °C under nitrogen should not cause any thermal degradation of the CNCs. Isothermal TGA has been also carried out for 20 min at 210 °C for the CNC powder and it did not show any noticeable degradation (data not reported).

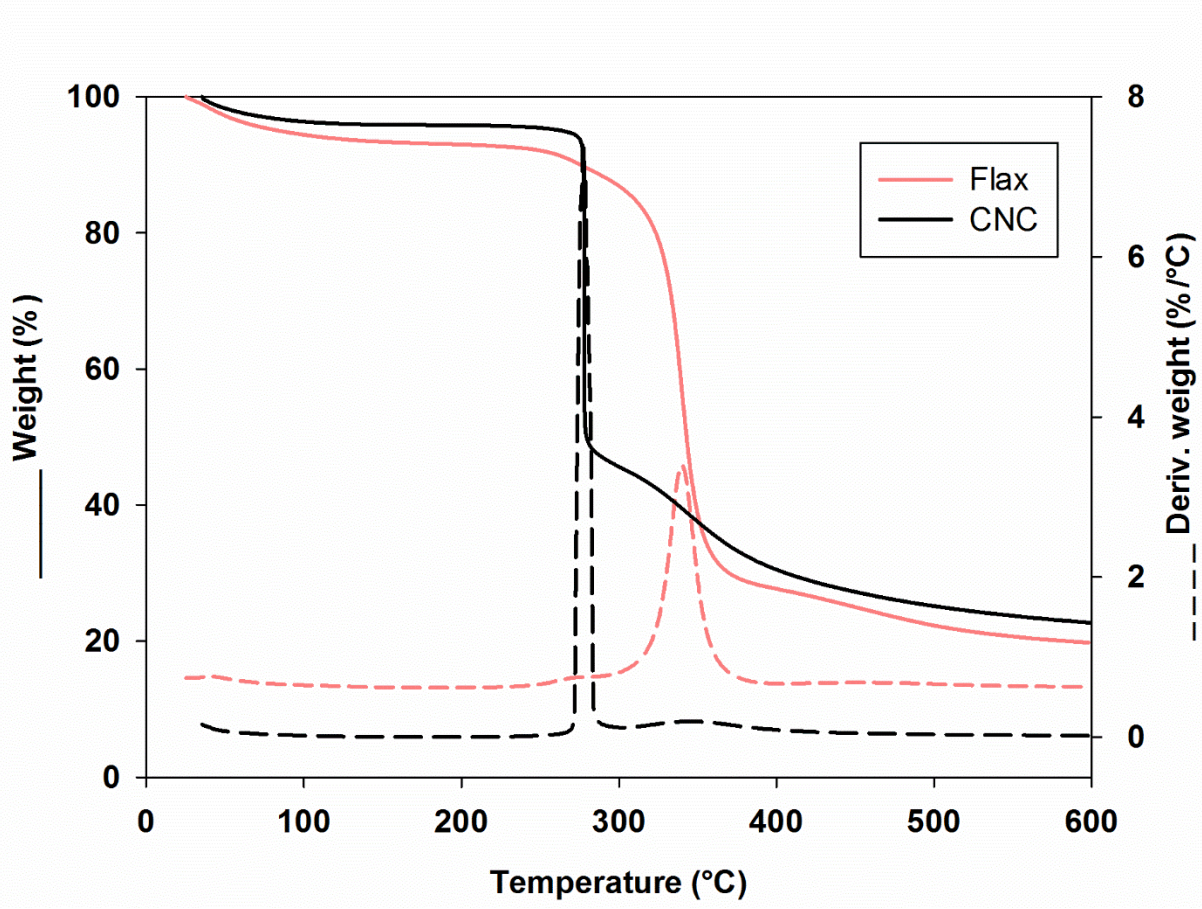

Fig. 6.1 Thermogravimetry results of as-received flax fibers [23] and CNCs in nitrogen.

6.3.2 Scanning electron microscopy (SEM)

Examination of the samples by scanning electron microscopy provides information on how the use of different molecular weights for the PPs and different processing temperatures affect the morphology and, ultimately, the mechanical properties of the composites. All the composites prepared in this work are hybrids of micro and nanoparticles, with the aspect ratio and size of

particles varying with composition and processing conditions and, hence, are not considered as nanocomposites. Fig. 6.2e reveals the pristine spray-dried CNCs prior to processing. Spray-dried CNCs are highly agglomerated and of micron size. The average diameter of the agglomerates is around 15±7 μm. In order to break the intra-particle hydrogen bonds and disperse the particles individually the use of a solvent and/or high mechanical force is the key factor. As studied by Khoshkava et al. [18] the required energy to break the CNC agglomerates of flakes drastically increases as their size decreases. Figures 6.2a-d compare SEM images of the high molecular weight PP composites containing 2 and 5 wt% CNCs, processed at two different temperatures. For PP1/2-175 (Fig. 6.2a), most of the large agglomerates have been broken in flake stacks of CNCs. It should be mentioned that for this composite large agglomerates in the size range of 1-2 μm have also been observed, but their number was negligible in comparison with the smaller flake particles. The average length and diameter of some 70 particles have been measured to be 1.0 and 0.16 μm, respectively. Each particle represents in average a bundle of over 100 single CNCs, but this remains highly qualitative as the particles are not necessarily aligned in the plane of the microtomed surface. Note that some of the dots, mainly seen in Figs. 6.2b and d, could be flakes aligned perpendicularly to the microtomed surface. Increasing the content of CNCs from 2 to 5 wt% (Fig. 6.2c) results in the presence of less flake particles and more agglomerates. The average diameter of the agglomerates increases to 1.5 - 3 μm. This coarser morphology may be attributed to an insufficient content of compatibilizer, since the latter is based on the PP content. Increasing the temperature from 175 to 210 °C in preparing the composites should improve the affinity of PP with CNCs as the hydrogen bonds of CNCs become weaker at higher temperatures. Consequently, smaller particles can be observed in Figs. 6.2b and 2d, but at the same time, more agglomerates are seen due to the lower viscosity of the matrix resulting in smaller stresses to break down the agglomerates. The size distribution of the particles in the composites processed at 210 °C varied from a few nm to almost 4.5 μm. The average lengths of the flake particles in PP1/2-210 and PP1/5-210 are 0.6 and 0.7 μm, respectively. The average diameters of agglomerates are 2 - 3.5 and 3 - 4.5 μm for PP1/2-210 and PP1/5-210, respectively.

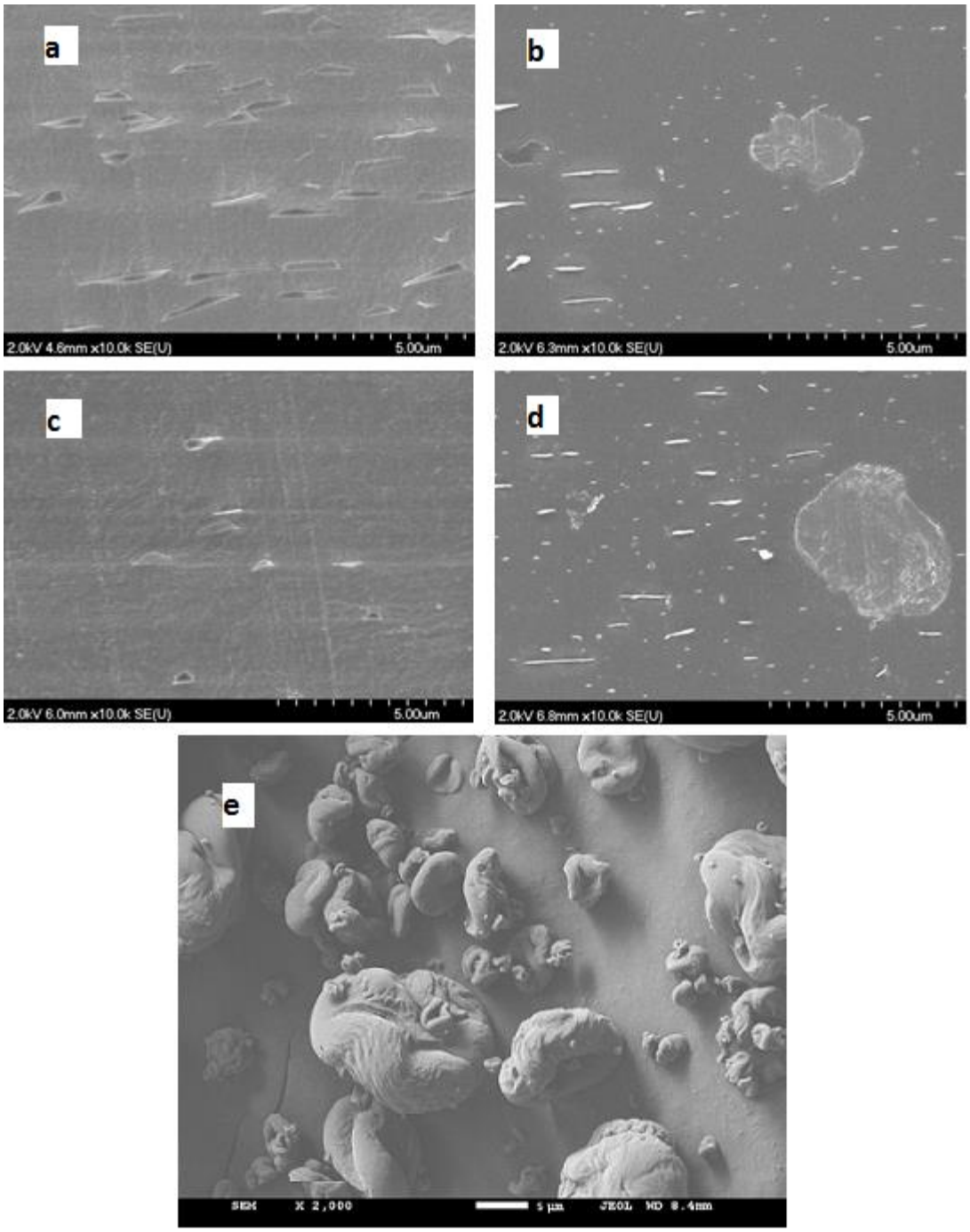

Fig. 6.2 SEM images of PP1/CNC composites: a) PP1/2-175, b) PP1/2-210, c) PP1/5-175, d) PP1/5-210, e) spray-dried CNCs.

Fig. 6.3 compares SEM images of low molecular weight PP composites containing 2 and 5 wt% processed under different conditions. We observe for PP2/2-175 (Fig. 6.3a) that the number of flake particles is less in comparison with PP1/2-175 (Fig. 6.2a). The average length and diameter measured for some 40 particles of PP2/2-175 are 1.5 and 0.3 µm, respectively. For PP2/5-175, we

observe very few flake particles and large agglomerates (Fig. 6.3c) with an average diameter of 2 - 5 μm. However, as seen in Figs.6.3b and d, the dispersion of the particles is improved at higher temperature, suggesting more affinity between CNCs and the matrix and increased diffusion. Also the diameter of the particles decreases to about 90 nm for these samples (bundles of some 20 single CNCs). The large agglomerates shown in Figure 6.3d are also more porous, which can facilitate the polymer diffusion into the structure. The average diameter of the few agglomerates for PP2/-210 is 1 - 3.5 μm. The SEM micrograph of the PP2/2-ext sample prepared via twin-screw extrusion is presented in Fig. 6.3e. As expected, the size of the particles is decreased in comparison with PP2/2-175 and PP2/2-210 processed by the internal mixer. The homogeneity of the sample has also been improved. The average length and diameter of the flake particles are 0.9 and 0.08 μm, respectively.

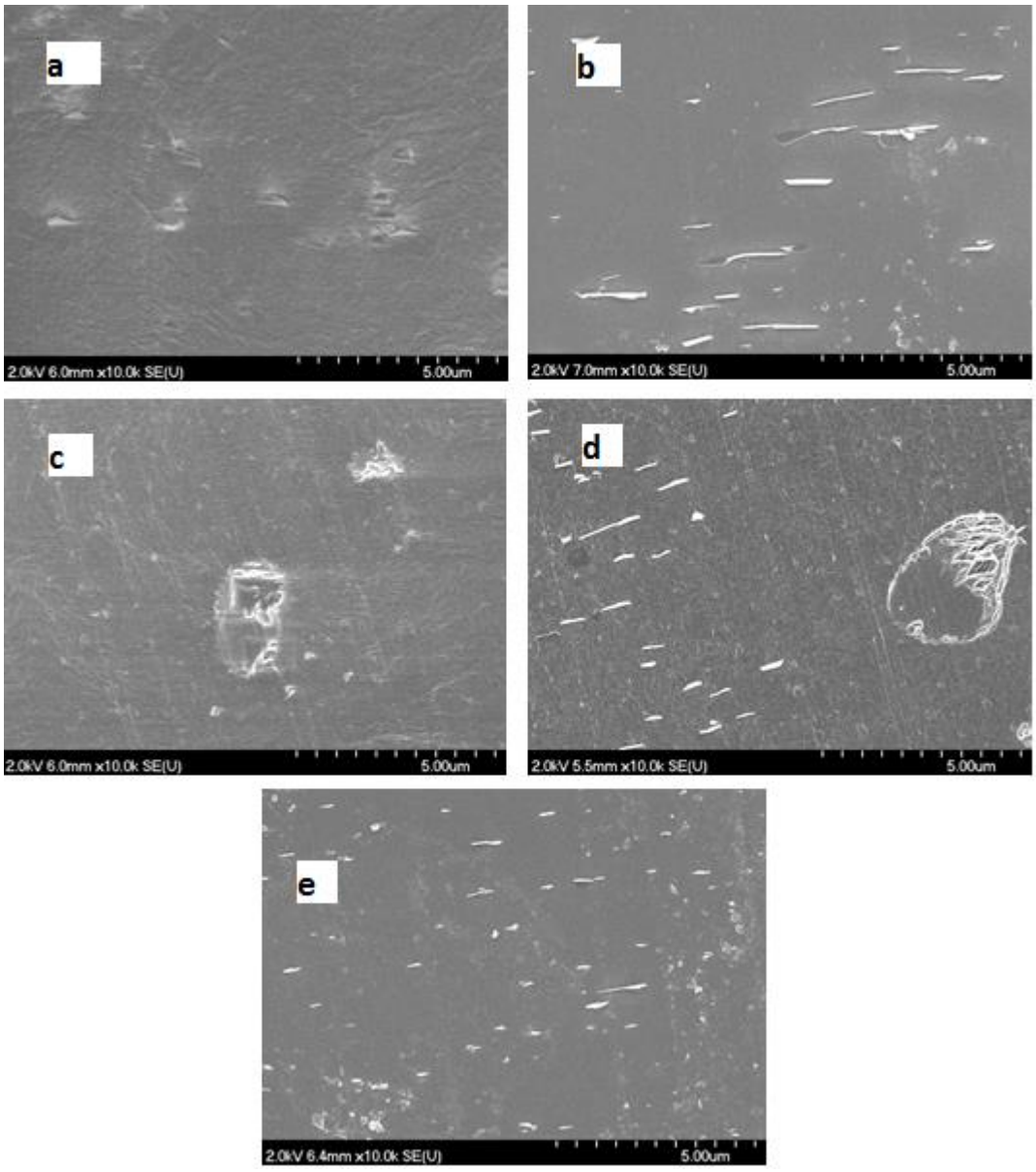

Fig. 6.3 SEM images of PP2/CNC: a) PP2/2-175, b) PP2/2-210, c) PP2/5-175, d) PP2/5-210, e) PP2/2-ext.

6.3.3 Rheological measurements

At 175 °C, the PPs with and without CNCs did not show any reduction of their complex viscosity with time (data not shown). The dynamic time sweeps at 0.628 rad/s under nitrogen for 20 min are reported in Fig. 6.4 for samples prepared and measured at the higher temperature, i.e. 210 °C. The unfilled PP1 (Fig. 6.4a) and PP2 (Fig. 6.4b) modified with OR are quite stable during the test. However, adding 2 and 5 wt% CNCs causes around 36 and 56% reductions, respectively, of the initial complex viscosity, η^*, in comparison with the unfilled PP1-based matrix (PP1/0-210). Also

η^* is further reduced by 17 and 30 % over the 20 min test for PP1/2-210 and PP1/5-210, respectively, suggesting that the polymer matrix is seriously degraded by the presence of the CNCs. The thermal degradation of PP in presence of fillers, especially when processed at high temperature, has been observed previously [28]. Adding CNCs also causes degradation of the low molecular weight PP (PP2) as illustrated in Fig. 6.4b. The initial values of η^* of PP2/2-210 and PP2/5-210 decrease by about 5 and 30 %, respectively, in comparison with the unfilled matrix (PP2/0-210). During the 20 min dynamic time sweep test, η* drops by 20 and 30% for PP/2-210 and PP/5-210, respectively. The initial decreases in the viscosity of the composites based on PP2 are less pronounced than for the PP1 composites. This can be explained by the higher viscous dissipation during processing of the high molecular weight PP1, which can result in more local temperature increase and, consequently, more degradation. Also according to the mechanical degradation theory of Bueche [36] the probability of chain scission is higher for higher molecular weight polymers.

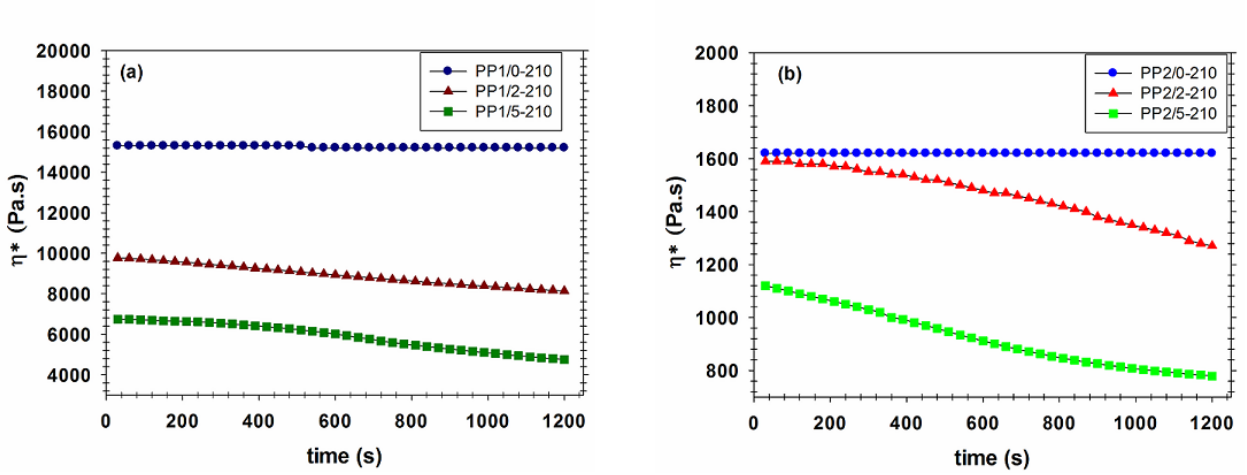

Fig. 6.4- Complex viscosity as a function of time for the matrix and its composites; a) based on PP1, b) based on PP2; ω = 0.628 rad/s and T = 210 °C.

6.3.4 Crystallization

The addition of nanoparticles can influence the crystallization behavior of polymer composites [17,37,38]. Nanoparticles can act as effective nucleating agents [39] and the heterogeneous nucleation process can accelerate the crystallization of the polymer matrix. On the other hand, the restrained polymer chain mobility can delay the crystallization growth. The nucleating ability of CNCs on the crystallization of PP1 and PP2 composites has been examined by differential scanning calorimetry (DSC) and the results are presented in Table 6.2. The crystallinity was calculated based

on a value of 209 J/g [40] for the enthalpy of fusion of 100% crystalline PP. The value of X_m extracted from the first heating can provide an indication of the possible effect of crystallinity on mechanical properties. As seen in Table 6.2, the melting temperature does not change significantly for the composites in comparison with the unfilled matrices. Lower crystallinity of PP1 in comparison with PP2 can be explained in terms of its lower chain mobility. Adding the nanoparticles increases the crystallization temperature (T_c) of the composites in the first cooling cycle, suggesting a nucleating effect [38]. The table shows that X_m of PP1/2-175 is increased by 15% in comparison with PP1/0-175, but the increase is somewhat less for the other PP1-based composites. Based on the morphology of PP1/2-175 (Fig. 6.2a) this effect can be attributed to the presence of more flake particles or single CNCs acting as nucleation agents. The effect of nanoparticles is less pronounced for the PP2-based composites. In this case the larger chain mobility of the matrix is already beneficial to crystallinity. It is believed that for both PPs the degradation for the samples processed at 210 °C was not important enough to explain the increase in crystallinity compared to the nucleation effect of CNCs.

Table 6.2 Transition temperatures and initial crystallinity for the various PP/CNC composites.

SAMPLE	T_c (°C)	T_m (°C)	X_m (%)
PP1/0-175	118.3	162.4	38.5±0.7
PP1/2-175	121.0	162.8	44.2±0.8
PP1/5-175	120.8	162.5	42.0±0.9
PP1/2 -210	120.8	161.4	42.0±0.7
PP1/5 -210	119.8	162.2	42.9±1.0
PP2/0-175	119.0	163.3	43.5±0.6
PP2/2-175	122.0	162.9	45.0±1.2
PP2/5-175	121.7	162.4	45.3±1.4
PP2/2 -210	120.4	163.8	45.8±0.8
PP2/5 -210	120.4	163.9	44.9±1.1
PP2/2 -ext	122.0	163.6	45.3±0.8

6.3.5 Tensile properties

The mechanical properties of PP/CNC composites processed in different conditions are compared with those of the neat matrices in Figs. 6.5 and 6.6 for the PP1- and PP2-based systems,

respectively. There are two main parameters that can affect the dispersion of the CNC particles: mechanical force or stresses applied during processing and affinity between the particles and the matrix. To improve the affinity between hydrophilic CNCs and hydrophobic PP, PPMA has been used as a compatibilizer for all composites. It should be mentioned that the tensile properties of the neat PPs, with and without 10 wt% of the compatibilizer, were almost the same (data not shown). As revealed by Figs. 6.5a and 6.6a, all composites show larger tensile modulus values than their respective matrices. This can be attributed to the much larger Young modulus of CNCs (around 143 GPa for a cellulose whisker [7]) than that of the matrices (around 1 GPa). Also the tensile strength of some composites increases with respect to the matrix (see Figs. 6.5b and 6.6b).

For the PP1-based composites, the Young modulus and maximum tensile strength of the composite containing 2 wt % CNCs processed at 175 °C (Figs. 6.5a and b) increase by 35% and 7%, respectively, in comparison with the PP1 matrix. Further increases in the content of CNCs do not affect the modulus significantly and the difference in the tensile strength in comparison with the matrix is insignificant. This can be attributed to the insufficient content of PPMA for compatibilizing the CNCs at the 5 wt% level. There is an optimum ratio of compatibilizer to filler content depending on the MA content and MFI of the compatibilizer [26]. Here, to retain the viscosity of the matrices constant, the content of the compatibilizer has been kept at 10 wt% with respect to the PP. In order to assess the efficiency of PPMA in compatibilizing CNCs with PP1, a composite containing 2 wt% CNCs without OR has been prepared at 175 °C. The Young modulus of this composite was the same as that of the matrix, but the tensile strength and strain at break decreased by 11.5 and 42 %, respectively, in comparison with the neat PP1 (data not shown). The decrease in tensile strength may be attributed to the lack of stress transfer from the matrix to the filler in absence of compatibilizer. The lower modulus and tensile strength for the composites processed at 210 °C could possibly be due to the presence of more agglomerates (see Figure 6.2b), as lower stresses were applied in the internal mixer to break down the CNC agglomerates. The surface energy thermal coefficient of CNCs (- 0.2 $mJ/m^2 \bullet K$) is lower than that of polymers like PP (- 0.03 to - 0.05 $mJ/m^2 \bullet K$) [18,41]. Consequently as the processing temperature increases, the surface energy of CNCs decreases to a level much closer to that of the matrix and, thus, a better wetting is expected [18]. This should lead to an improved dispersion of the CNCs. However, as seen here, the effect of the lower stresses applied to the agglomerates at 210 °C is probably dominating. Fig. 6.5c reports the tensile strain at break of the PP1-based composites. As expected,

by increasing the content of CNCs the tensile strain at break decreases. However the effect is much less dramatic than in the case of flax fibers [26], as illustrated in the next section. Also the samples processed at 175 °C have lower strain at break in comparison with composites processed at 210 °C, probably because of the poorer dispersion of the particles when mixed at lower temperature (see Fig. 6.2).

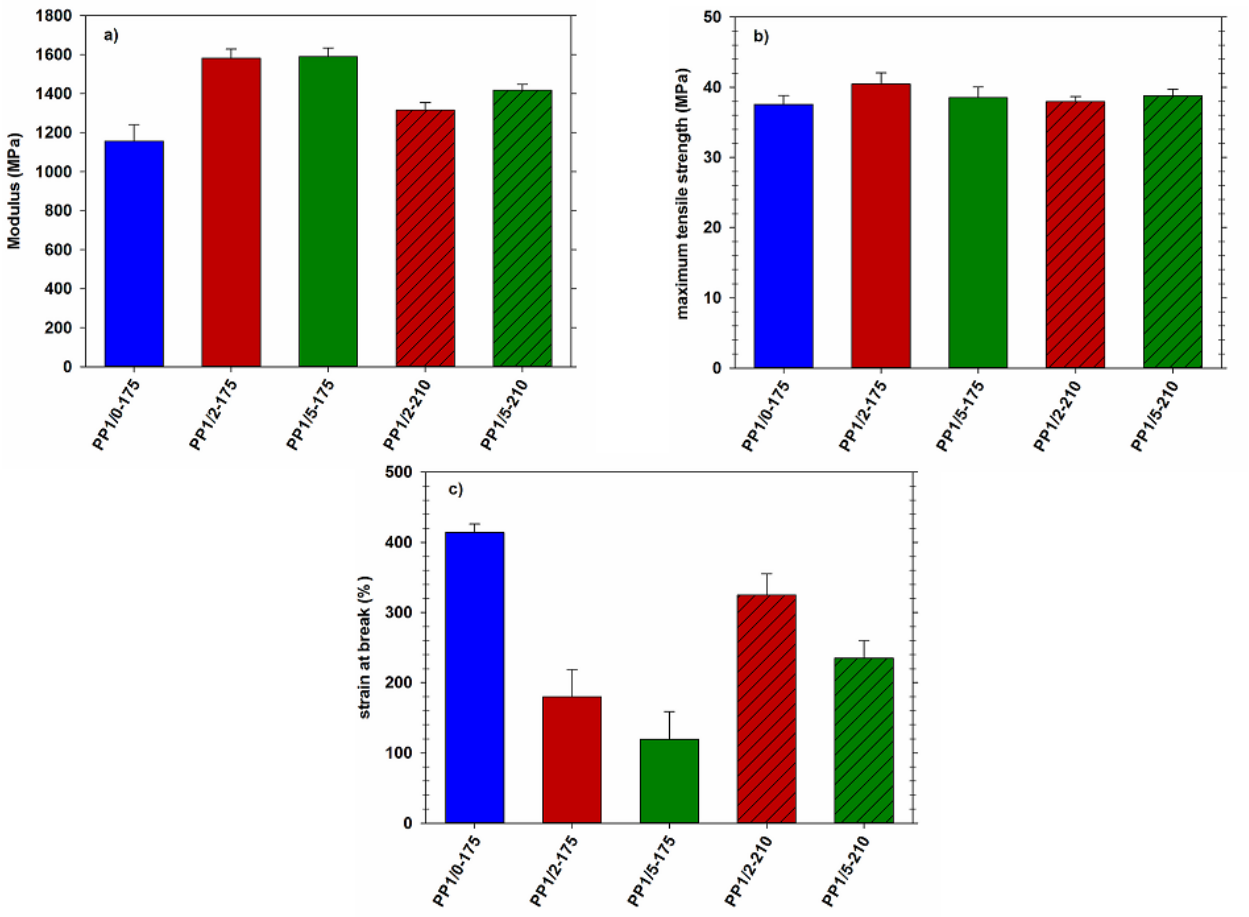

Fig. 6.5 Mechanical properties of PP1-based matrix and its composites: a) Young modulus, b) maximum tensile stress and c) tensile strain at break.

Tensile properties of the low molecular weight PP composites are reported in Fig. 6.6. As reported in Table. 6.2, the PP2-based composites are more crystalline than the PP1-based composites which can compensate for their lower molecular weight and result in comparable mechanical properties for the two different grades of PP. As done for PP1, a PP2 composite containing 2 wt% CNCs without PPMA has been prepared at 210 °C. The Young modulus of this composite was the same as that of the matrix, but the tensile strength and strain at break decreased by 7.2 and 32%, respectively, in comparison with the neat PP2 (data not shown). The effect of changing the

processing temperature on the low molecular weight PP2-based composites is different than that reported for the PP1-based systems. For the PP2 composites processed at 175 °C, adding 2 wt% nanoparticles increases the modulus by 15 %. The tensile strength and modulus of the composites reinforced with 5 wt% CNCs do not change significantly in comparison with the composites containing 2 wt% CNCs. As explained earlier, this can be the result of the low content of PPMA for the 5 wt% CNC composite. By increasing the process temperature from 175 to 210 °C the tensile modulus is improved by 23% and 30% for PP2/2-210 and PP2/5-210, respectively, whereas the tensile strength is increased by about 10% for both composites. The improved mechanical properties are attributed to the better dispersion of the nanoparticles when processed at higher temperature (see Figure 6.3). The decrease of the surface energy of CNCs (improved affinity with the matrix) and the more rapid diffusion of the lower molecular weight PP chains overcome the effect of the lower applied stresses when mixing at high temperature. The strain at break of the PP2-based composites is nearly independent of the process temperature and decreases with increasing CNC content (Fig. 6.6c).

To compare the effect of the mixing method on the mechanical properties, the PP2/2 composite has been also processed with the twin-screw extruder (PP2/2-ext), as mentioned earlier. The results presented in Fig. 6a show that the tensile modulus is slightly decreased in comparison with PP2/2-210 processed in the Brabender (but still within the error bar). The tensile strength of PP2/2-ext is somewhat improved with respect to PP2/2-210 (~5%) and it represents a 16 % enhancement in comparison with the unfilled PP2. The tensile strain at break is considerably improved in comparison with the other composites containing 2 wt% CNC prepared in the internal mixer. Processing via the twin-screw extruder should lead to a better dispersion of the CNCs (Figure 6.3e), due to a more efficient breakage of the agglomerates under the high stresses and more complex flow situation (appreciated in the section on SEM results, Fig. 6.3); also the high process temperature in the mixing zones near the die entrance should improve the affinity between the CNCs and the matrix. Overall, the mechanical properties presented in Figs. 6.5 and 6.6 are consistent with the results of the morphologies illustrated in Figs. 6.2 and 6.3.

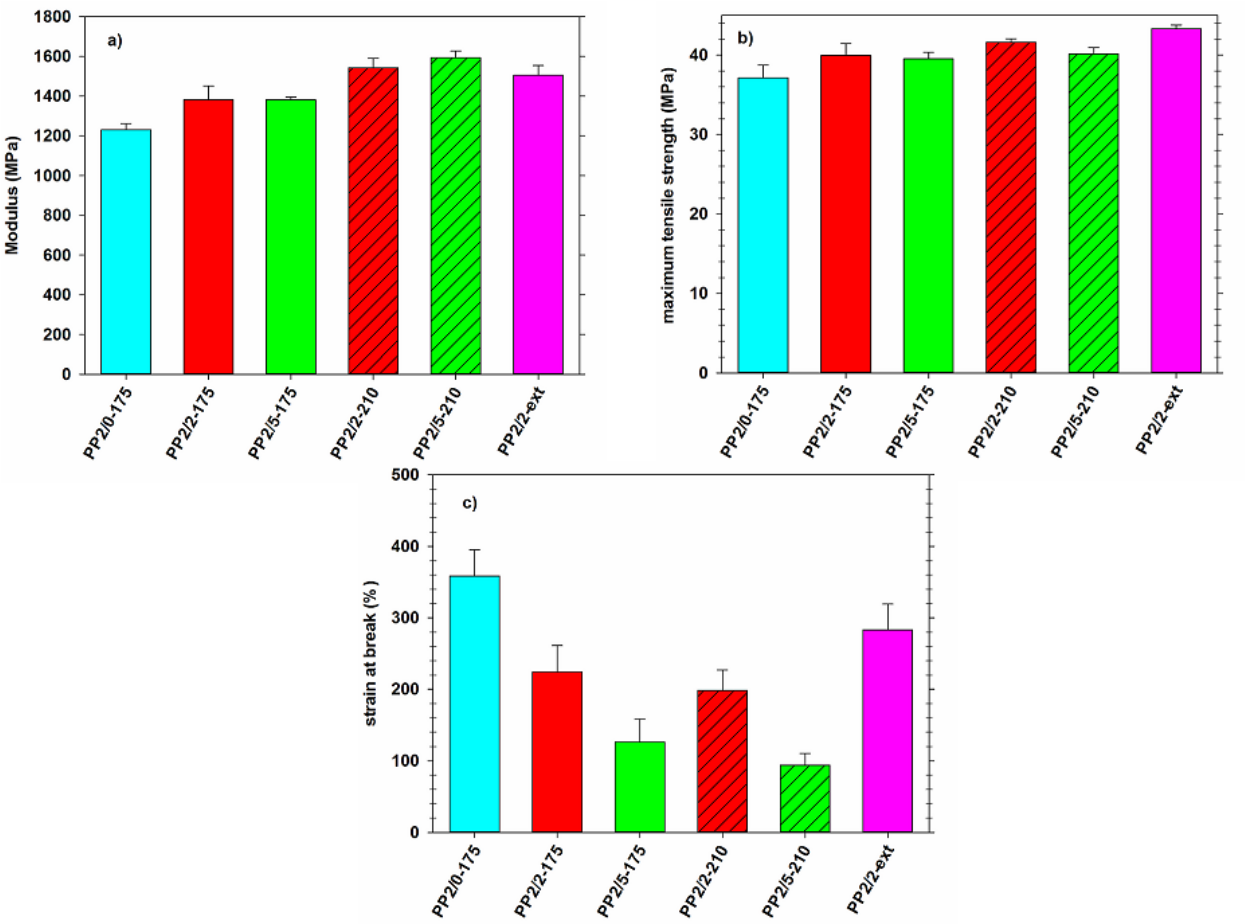

Fig. 6.6 Mechanical properties of PP2-based matrix and its composites: a) Young modulus, b) maximum tensile stress and c) tensile strain at break.

In order to assess the performance of the PP-CNC composites, a comparison is made for the properties of polypropylene filled with other particles. Fig. 6.7 compares the mechanical properties of different composites containing CNCs with composites containing flax fibers from our previous work [26] and nanoclay Cloisite 20A from the literature [42]. The normalized values have been obtained by dividing the modulus, tensile strength and tensile strain at break by the respective values for the unfilled matrices. PP3 is a different PP grade that has been used in our previous work to prepare flax fiber composites [26]. The composites of PP3/10 Flax and PP3/20 flax contain 10 wt% (based on the fiber content) of Epolen E43 (a PPMA with high MA content and low molecular weight). The CNC composites with superior mechanical properties based on the two different molecular weight PPs have been chosen for the comparison. The normalized modulus of the PP3/10 flax and PP3/20 flax composites is respectively 1.40 and 1.95 times that of the matrix, whereas for the PP2/2-210 and PP2/2-ext samples the corresponding values are 1.25 and 1.22, respectively,

while this value for PP1 composites processed at 175 °C is 1.37. The normalized tensile strength of the PP2/2-ext is 1.17, and is between 1.09 for PP3/10 flax and 1.23 for PP3/20 flax. The strain at break of the CNC composites is considerably superior to that of the composites based on the flax fibers. The normalized strain at break of the PP/flax fiber composites is less than 0.06, which makes these composites quite brittle, whereas the CNC composites retain largely the good ductility of PP with a strain at break varying between 43 to 73% of that the matrices. This illustrates one advantage of using a small amount of CNCs in comparison with larger contents of flax fibers as reinforcement for PP to have comparable tensile strength and modulus without the loss of ductility. In order to compare CNCs with another nanoparticle, the mechanical properties of PP4/2C20A has been taken from the literature [42]. This sample has also been compatibilized with a PPMA (Polybond 3200) and since a different grade of PP has been used here it has been mentioned as PP4. It can be seen that the normalized modulus, maximum strength and tensile strain at break of PP4/2C20A are very close to those of PP2/2-ext. This can show that CNCs, which have the advantage of being bio-based nanoparticles, can be as efficient in improving the mechanical properties of a composite as clay nanoparticles.

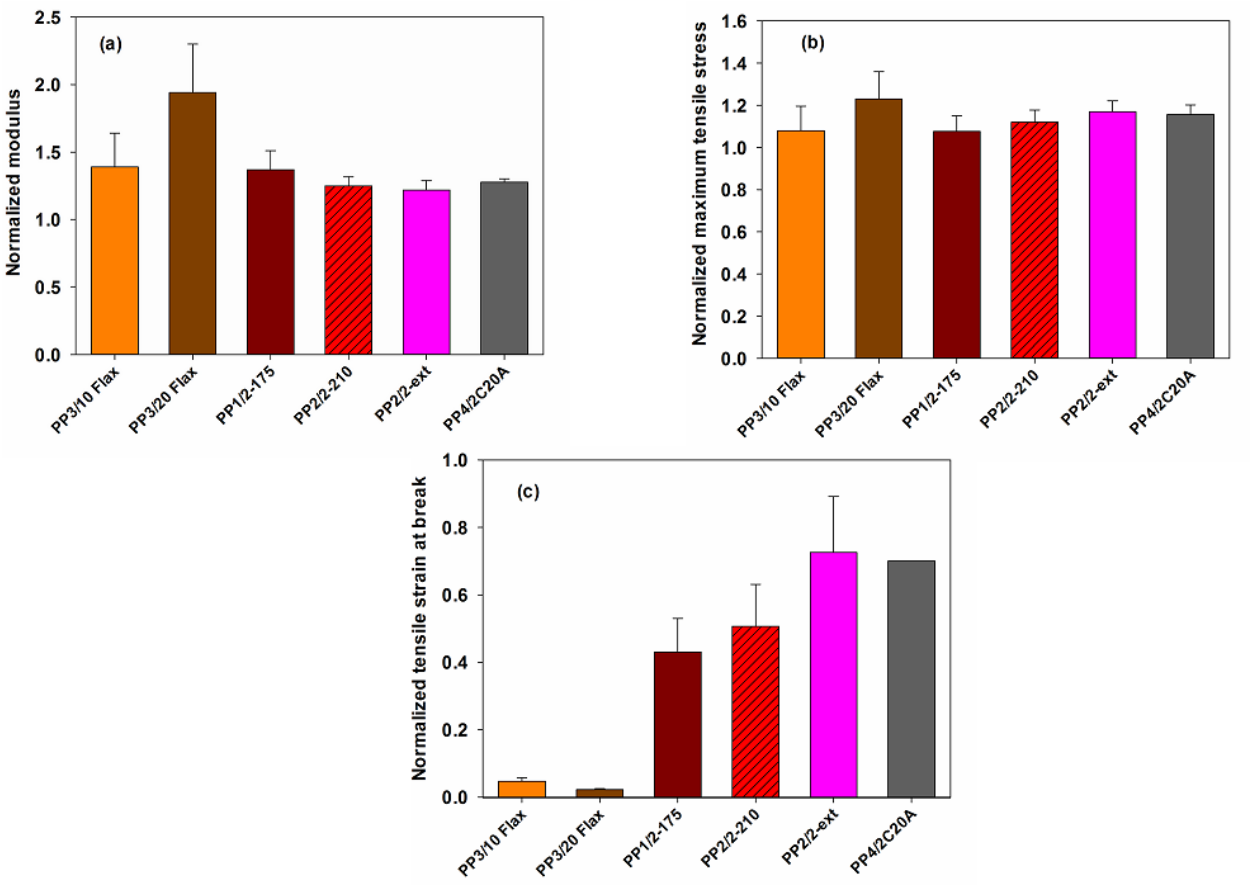

Fig. 6.7 Comparison of the mechanical properties of flax fiber and CNC-based composites: a) normalized modulus, b) normalized maximum tensile stress, c) normalized tensile strain at break. The data for PP3/10 flax and PP3/20 flax has been extracted from Sojoudiasli et al. [26] and the data for PP4/2C20A has been extracted from Lopez-Quintanilla et al. [42] .

6.3.6 Modeling of the tensile modulus

It is of interest to verify if classical models proposed to describe the modulus of composites made of short discontinuous fibers can be used to predict the behavior of composites made of CNCs. As the CNC composites were prepared by compression molding, they are considered to consist of 2D randomly oriented discontinuous fibers. Eq. 6.1 suggested by Nielsen [43] can be used in order to predict the modulus of these composites:

$$E_c = \frac{3}{8}E_L + \frac{5}{8}E_T \tag{6.1}$$

where E_L and E_T refer to the longitudinal and transverse modulus, respectively. To calculate E_L and E_T the Halpin-Tsai model has been used, as done for fiber-filled composites in different studies [44-47].

In this model the filler volume fraction, matrix modulus and aspect ratio are taken into consideration. The model can be written as:

$$E = E_m \left(\frac{1 + \xi \Psi \phi_f}{1 - \Psi \phi_f} \right) \tag{6.2}$$

$$\Psi = \frac{E_f / E_m - 1}{E_f / E_m + \xi} \tag{6.3}$$

where E_f, ϕ_f and ξ are, respectively, the Young modulus, volume fraction and the aspect ratio of the fibers (diameter d and length l) given by:

$$\xi = 2\frac{l}{d} \tag{6.4}$$

The subscripts m, f and c represent the matrix, filler and composite, respectively. The filler volume fraction is obtained from:

$$\phi_f = \frac{w_f \rho_m}{\rho_f - w_f (\rho_f - \rho_m)} \tag{6.5}$$

where w_f is the weight fraction of the CNCs, ρ_f and ρ_m are the density of CNCs and of the matrix, assumed to be 1.5 and 0.9 g/mL, respectively. The longitudinal modulus, E_L, is calculated via Eqs. 6.2, 6.3 and 6.4 and the transverse Young modulus, E_T, is also obtained from Eqs. 6.2 and 6.3, but for a value of ξ equal to 0.5 [43]. The aspect ratio of the flake particles was measured from SEM images and it has been assumed that all the CNC agglomerates are broken into flake particles.

Table 6.3 Experimental tensile modulus vs. model predictions for the CNC composites

	PP1/2-175	**PP1/5-175**	**PP1/2-210**	**PP1/5-210**	**PP2/2-175**	**PP2/5-175**	**PP2/2-210**	**PP2/5-210**	**PP2/2-ext**
Average ξ	13.6±2.6	12.2±3.0	11.0±2.4	3.8±1.8	10.0±2.0	8.0±2.4	24.6±4.6	10.6±2.6	20.0±3.2
Model (GPa)	1.23	1.35	1.22	1.34	1.29	1.38	1.35	1.41	1.33
Exp. (GPa)	1.58±0.02	1.59±0.03	1.32±0.02	1.42±0.02	1.38±0.03	1.38±0.02	1.54±0.02	1.59±0.03	1.50±0.02
Deviation (%)	-22	-15	-7.0	-5.0	-6.0	0.0	-12	-11	-11

Parameters used are:
E_m = 1150 and 1220 MPa for PP1 and PP2, respectively, based on tensile results.
E_f (assumed to be that of single CNCs) = 143 GPa [7]

Predicted modulus and average experimental Young modulus of the composites are compared in Table 6.3. The average aspect ratio reported in this table is based on SEM images. Overall the agreement of the model prediction with the data is good, but in most cases the model under-predicts the modulus of the composites. This could be largely due to the fact that in the estimation of the aspect ratio we took into consideration only the larger particles in the range of SEM resolution. As observed in SEM images of Fig. 6.2, the composites contain many smaller particles, which have not been considered when calculating the aspect ratio. Also the fibers might have been cut during microtoming of the sample, which would decrease the measured aspect ratio. Another reason for the under-predictions of the model for composites based on PP1 could be due to the effect of CNCs on the crystallinity of the composites, which has not been considered in the enhancement of the mechanical properties. As seen in the previous section, the CNCs increase the crystallinity of PP1-based composites and part of the increase in the tensile modulus can also be due to the higher crystallinity in the presence of the nanoparticles.

6.3.7 Transparency and appearance

Fig. 6.8 shows the appearance and transparency/opacity of PP/CNC and PP/flax fiber samples. As mentioned earlier, PP3/10, PP3/20 and PP3/30 flax are based on a different commercial grade PP and contain 10 wt% of Epolene E43 with respect to the flax fibers. The thickness of the samples varied between 0.35-0.45 and 0.25-0.35 mm for PP/flax and PP/CNC composites, respectively. All the PP/flax composites exhibit a brownish color getting darker with increasing flax fiber content. Based on the TGA and rheological studies, the PP/flax composites were thermally stable at the

processing temperature [26]. This brownish color is the result of the natural brown color of flax fibers and their relatively high content in the composites, since the PP3 film without flax is transparent. For the PP/CNC composites the color does not change significantly in comparison with the unfilled matrices, and all the samples have acceptable transparency and appearance, which is another advantage of using the nanocrystalline cellulose as opposed to a micro-sized cellulosic reinforcement. Only PP1/5-210 shows a light tan color, which can be attributed to the degradation of the composite during processing.

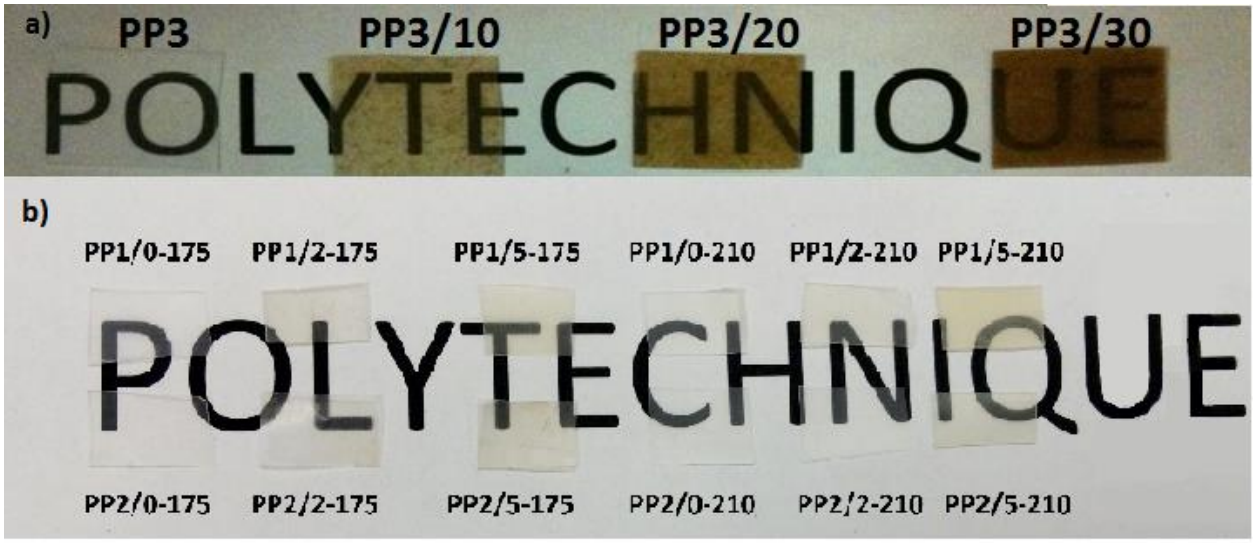

Fig. 6.8 Transparency and appearance of a) PP/flax fiber and b) PP/CNC samples.

6.4 Conclusion

Cellulose nanocrystal composites based on two different molecular weight polypropylenes were prepared using an internal batch mixer or via twin-screw extrusion. Maleic anhydride-PP has been used as a compatibilizer between the CNCs and PPs. The effect of two different processing temperatures on the rheology, dispersion of CNCs and mechanical properties of composites has been investigated. Rheological characterization showed that processing at high temperature can cause the degradation of the matrix in the presence of nanocellulose. For high molecular weight PP-based composites, a lower processing temperature resulted in larger stresses that favored the dispersion of CNCs and improved the mechanical properties of the composites. On the other hand, for low molecular weight PP the composites processed at higher temperature showed better mechanical properties. In addition, the composite based on the low molecular weight PP and prepared via twin-screw extrusion exhibited an improved dispersion and enhanced mechanical properties. From the lack of improvement in mechanical properties of the composites in absence

of compatibilizer it can be concluded that Orevac 18729 was an efficient compatibilizer for PP/CNC composites. The nanoparticles could also act as heterogeneous nucleating agents during crystallization, accounting partly for the improved mechanical properties of the composites. The tensile properties of the PP/CNC composites could be fairly well described by the model proposed by Nielsen [43] based on the Halpin-Tsai equation.

Finally, properties of the PP/CNC composites have been compared to those of a PP reinforced with flax fibers (micro cellulosic fibers) and a PP filled with nanoclay. The modulus of the composites containing 2 wt% CNCs was equivalent to the composite reinforced with 10 wt% flax fibers. If the PP/ flax composites were brittle and their strain at break was less than 0.06% of the matrix, the PP/CNC composites exhibited a good ductility, with their strain at break varying between 43 and 73 % of the matrix. For a PP/Cloisite20A composite containing 2 wt% clay and compatibilized with PPMA, the normalized mechanical properties were similar to those of the PP/CNC composites containing 2 wt% CNCs. The change in the color and transparency of the PP/CNC composites in comparison with the neat PPs was negligible, whereas the larger content of fibers in the PP/flax composites affected drastically their color and transparency, confirming the interest of using CNCs to reinforce thermoplastics.

6.5 Acknowledgments

The authors gratefully acknowledge the Natural Sciences and Engineering Research Council of Canada (NSERC) for funding. We are thankful to Dr. Jean Bouchard of FPInnovations who provided the CNCs used in this project.

6.6 References

[1] D. Liu, X. Chen, Y. Yue, M. Chen, Q. Wu, *Carbohydr Polym* **84** 316(2011).

[2] M.-C. Li, Q. Wu, K. Song, S. Lee, Y. Qing, Y. Wu, *ACS Sustainable Chemistry & Engineering* **3** 821(2015).

[3] B.L. Peng, N. Dhar, H.L. Liu, K.C. Tam, *The Canadian Journal of Chemical Engineering* **89** 1191(2011).

[4] M. Roman, W.T. Winter, *Biomacromolecules* **5** 1671(2004).

[5] V. Favier, J.Y. Cavaille, G.R. Canova, S.C. Shrivastava, *Polymer Engineering & Science* **37** 1732(1997).

[6] M.A.S. Azizi Samir, F. Alloin, A. Dufresne, *Biomacromolecules* **6** 612(2005).

[7] A. Šturcová, G.R. Davies, S.J. Eichhorn, *Biomacromolecules* **6** 1055(2005).

[8] R. Malkapuram, V. Kumar, Y.S. Negi, *Journal of Reinforced Plastics and Composites* **28** 1169(2008).

[9] P. Hajji, J.Y. Cavaillé, V. Favier, C. Gauthier, G. Vigier, *Polymer Composites* **17** 612(1996).

[10] M.N. Anglès, A. Dufresne, *Macromolecules* **33** 8344(2000).

[11] M. Roohani, Y. Habibi, N.M. Belgacem, G. Ebrahim, A.N. Karimi, A. Dufresne, *European Polymer Journal* **44** 2489(2008).

[12] L. Zhou, H. He, M.-C. Li, K. Song, H.N. Cheng, Q. Wu, *Carbohydrate Polymers* **153** 445(2016).

[13] M.A.S. Azizi Samir, F. Alloin, J.-Y. Sanchez, A. Dufresne, *Polymer* **45** 4149(2004).

[14] I. Kvien, B.S. Tanem, K. Oksman, *Biomacromolecules* **6** 3160(2005).

[15] A. Arias, M.-C. Heuzey, M.A. Huneault, G. Ausias, A. Bendahou, *Cellulose* **22** 483(2014).

[16] N. Ljungberg, J. Cavaille, L. Heux, *Polymer* **47** 6285(2006).

[17] M.R. Kamal, V. Khoshkava, *Carbohydr Polym* **123** 105(2015).

[18] V. Khoshkava, M.R. Kamal, *Biomacromolecules* **14** 3155(2013).

[19] N. Ljungberg, C. Bonini, F. Bortolussi, C. Boisson, L. Heux, J.Y. Cavaille, *Biomacromolecules* **6** 2732(2005).

[20] A.C. Corrêa, E. de Morais Teixeira, V.B. Carmona, K.B.R. Teodoro, C. Ribeiro, L.H.C. Mattoso, J.M. Marconcini, *Cellulose* **21** 311(2013).

[21] K. Ben Azouz, E.C. Ramires, W. Van den Fonteyne, N. El Kissi, A. Dufresne, *ACS Macro Letters* **1** 236(2011).

[22] N.L. Garcia de Rodriguez, W. Thielemans, A. Dufresne, *Cellulose* **13** 261(2006).

[23] H.M. Hassanabadi, A. Alemdar, D. Rodrigue, *Journal of Applied Polymer Science* **132** 2438(2015).

[24] E. Twite-Kabamba, A. Mechraoui, D. Rodrigue, *Polymer Composites* **30** 1401(2009).

[25] N. Le Moigne, M. van den Oever, T. Budtova, *Polymer Engineering & Science* **53** 2582(2013).

[26] H. Sojoudiasli, M.-C. Heuzey, P.J. Carreau, *Cellulose* **21** 3797(2014).

[27] J.-G. Gwon, H.-J. Cho, S.-J. Chun, S. Lee, Q. Wu, M.-C. Li, S.-Y. Lee, *RSC Advances* **6** 73879(2016).

[28] A. Junior de Menezes, G. Siqueira, A.A.S. Curvelo, A. Dufresne, *Polymer* **50** 4552(2009).

[29] D.G. Gray, *Cellulose* **15** 297(2008).

[30] V. Khoshkava, H. Ghasemi, M.R. Kamal, *Thermochimica Acta* **608** 30(2015).

[31] F. Alloin, A. D'Aprea, A. Dufresne, N. Kissi, F. Bossard, *Cellulose* **18** 957(2011).

[32] W.Y. Hamad, T.Q. Hu, *The Canadian Journal of Chemical Engineering* **88** 392(2010).

[33] J. George, E. Klompen, T. Peijs, *Advanced Composites Letters(UK)* **10** 81(2001).

[34] F. Shafizadeh, A.G.W. Bradbury, *Journal of Applied Polymer Science* **23** 1431(1979).

[35] M. Sepehr, G. Ausias, P.J. Carreau, *Journal of Non-Newtonian Fluid Mechanics* **123** 19(2004).

[36] F. Bueche, *Journal of Applied Polymer Science* **4** 101(1960).

[37] X. Liu, Q. Wu, *European Polymer Journal* **38** 1383(2002).

[38] H. Ghasemi, P.J. Carreau, M.R. Kamal, *Polymer Engineering & Science* **52** 372(2012).

[39] S. Reyes-de Vaaben, A. Aguilar, F. Avalos, L.F. Ramos-de Valle, *Journal of Thermal Analysis and Calorimetry* **93** 947(2008).

[40] J. Karger-Kocsis, Polypropylene: an A-Z reference., Springer, 1999.

[41] S. Wu, Polymer Interface and Adhesion, CRC Press, 1982.

[42] M.L. López-Quintanilla, S. Sánchez-Valdés, L.F. Ramos de Valle, F.J. Medellín-Rodríguez, *Journal of Applied Polymer Science* **100** 4748(2006).

[43] L.E. Nielsen, Mechanical properties of polymers and composites., Marcel Dekker, Inc., New York, 1974.

[44] T. Gómez-del Río, P. Poza, J. Rodríguez, M.C. García-Gutiérrez, J.J. Hernández, T.A. Ezquerra, *Composites Science and Technology* **70** 284(2010).

[45] G. Kalaprasad, K. Joseph, S. Thomas, C. Pavithran, *Journal of Materials Science* **32** 4261(1997).

[46] M.A. Rafiee, J. Rafiee, Z. Wang, H. Song, Z.-Z. Yu, N. Koratkar, *ACS Nano* **3** 3884(2009).

[47] M. Jonoobi, J. Harun, A.P. Mathew, K. Oksman, *Composites Science and Technology* **70** 1742(2010).

CHAPTER 7 ARTICLE 3: RHEOLOGICAL BEHAVIOR OF SUSPENSIONS OF MODIFIED AND UNMODIFIED CELLULOSE NANOCRYSTALS IN DIMETHYL SULFOXIDE [3]

Helia Sojoudiasli[a], Marie-Claude Heuzey[a], Pierre J. Carreau[a]*, Bernard Riedl[b]

a Research Center for High Performance Polymer and Composite Systems (CREPEC), Department of Chemical Engineering, Polytechnique Montreal, C.P. 6079, succ. Centre-Ville, Montreal, QC, Canada, H3C 3A7

b Département des Sciences du bois et de la forêt, Faculté de foresterie, géographie et géomatique, Université Laval, Quebec, QC G1V 0A6, Canada

* Corresponding author. Email address: pcarreau@polymtl.ca

Abstract

The rheological behavior of cellulose nanocrystal (CNC) and modified CNC (mCNC) suspensions in dimethyl sulfoxide (DMSO) was investigated. The efficiency of the surface modification of CNCs by grafting an organic acid chloride to produce hydrophobic CNCs has been verified by X-ray photoelectron spectroscopy (XPS). The thermal degradation temperature of the mCNCs was found to be 165 °C versus 275 °C for CNCs. The CNC suspensions in DMSO at 70 °C underwent gelation at very low concentration (1 wt %) after one day. The network formation was temperature sensitive and did not occur at room temperature. For gels containing 3 wt% CNCs, the complex viscosity at 70 °C increased by almost 4 decades after one day. For the mCNCs in DMSO a weak gel was formed from the first day and temperature did not affect the gelation. Finally, the effect of adding 10 wt% of polylactide (PLA) to the solvent on the rheological properties of CNC and mCNC suspensions was investigated. The properties of suspensions containing 1.9 wt% CNCs and mCNCs increased during the first and second days, and PLA did not prevent gel formation. However, the reduced viscosity and storage modulus of the CNC and mCNC gels with PLA were lower than those of samples without PLA.

Keywords: Cellulose nanocrystals (CNCs), hydrophobic CNCs, dimethyl sulfoxide (DMSO), gel formation, rheology.

---

[3] Accepted with minor revision in Rheologica Acta in April 2017.

7.1 Introduction

Cellulose is biodegradable, non-toxic, renewable, and the most abundant natural biopolymer on earth. Acid hydrolysis of biomass such as bacteria, cotton, and wood pulp can be used to prepare aqueous suspensions of cellulose nanocrystals (CNCs) [1]. Due to the acid that has been utilized to produce CNCs, negative charges from sulfuric acid are introduced on the surface of nanoparticles and stabilize their aqueous suspensions [2-4]. The hydrophilic nature of CNCs limits their use to the reinforcement of mostly water-soluble polymers or water-based emulsions such as latex [5], starch [6], polyvinyl alcohol (PVOH) [7] and polyethylene oxide (PEO) [8]. Different surface modifications of CNCs like acetylation [9], TEMPO-mediated oxidation [10], and grafting [11-15] have been investigated. Gwon et al. [16] modified the surface of CNCs with toluene diisocyanate and used the modified CNCs in PLA-based nanocomposites. These modified particles could be dispersed in chloroform and PLA solutions, and tensile strength of the resulting PLA nanocomposites was improved in comparison with unmodified CNCs [16]. One of the interesting one-step methods to graft aliphatic carbon chains with different lengths on the surface of CNCs is esterification. In this method an organic acid chloride is added to the suspension of CNCs in the presence of a catalyst [13]. It has been reported that such surface modification can improve the dispersion and mechanical properties of LDPE nanocomposites [14].

Using organic solvents like dimethyl formamide (DMF) or dimethyl sulfoxide (DMSO) in order to disperse CNCs has been proven successful [4, 17-19]. Viet et al. [18] observed that re-dispersing freeze-dried CNCs in DMSO and DMF containing a small amount of water (0.1%) was feasible. The apparent hydrodynamic radius of re-dispersed CNC in DMF and DMSO was 170 ± 153 nm and 160 ± 48 nm, respectively and it was concluded that DMSO was a better solvent than DMF for dispersing CNCs. Chang et al. [19] prepared suspensions of CNCs in DMF, water and mixtures of these two solvents. The co-solvent systems containing 25-75% water were more efficient than water and DMF alone in dispersing CNCs. This was attributed to the fact that water and DMF have good interactions so that the H_2O/DMF complex could diffuse in CNC agglomerates and disperse them better. The negatively charged $O\text{-}SO_3^-$ groups on the surface of CNC particles are required to disperse freeze-dried nanoparticles in water or aprotic organic solvents like DMSO and DMF [4]. It has been observed that, since protic solvents like formic acid and m-cresol are well-known

for their ability to break hydrogen bonds between particles, they are able to re-disperse CNCs that have been prepared via HCl hydrolysis and which do not have negative groups on their surface [4]. Toluene has also been used to disperse CNCs in an atactic polypropylene by solvent casting [20]. Since toluene was not able to break the agglomerates, the resulting mechanical properties and dispersion were not improved. This emphasizes the importance of choosing the appropriate solvent for a given polymer, in which the CNC nanoparticles can be dispersed individually. Bagheriasl et al. [17] used CNC/DMF suspensions to prepare CNC/PLA nanocomposites. The rheological properties of PLA/CNC nanocomposites prepared by solvent casting confirmed a strong network formation and good dispersion of CNCs in PLA, whereas samples prepared by melt mixing did not show significant improvements in rheological and mechanical properties.

In addition to forming equilibrium chiral nematic phases above some critical concentration, CNC suspensions tend to gel or aggregate due to different chemical and physical processes: change of surface charges via decreases of the half-ester sulfate groups at the surface of CNCs [21], modification of the ionic strength of the suspension medium [22] and charge reversal through surface functionalization of CNCs [21]. Lewis et al. [23] reported hydrothermally formed gels from aqueous suspensions when CNC concentration was about 4 wt% and the suspensions heated up to 110 °C for 20 h. They attributed this gelation to desulfation or partial removal of sulfate half-ester groups on the surface of CNCs [23, 24].

Dorris and Gray [21] observed that glycerol/CNCs alone did not produce a gel or even a stable suspension. However by mixing an aqueous suspension of an acid form of CNCs with glycerol, and removing excess water by evaporation under controlled conditions, thixotropic gels could be obtained [19]. They also claimed that the reason behind this gel formation was desulfation. Which was slow at room temperature, but a significant level of desulfation was observed for the CNC suspensions kept at 60 °C for 3 days [25]. This desulfation was also observed at temperatures above 50 °C for CNC with half ester sulfate groups on the surface [24].

The aim of the present work is to compare the rheological properties of CNCs and hydrophobic CNCs suspended in an organic solvent, which to the best of our knowledge have not been reported previously. Using solvents such as dimethyl sulfoxide (DMSO) can help to produce high-performance nanocomposites with non-water soluble polymers like PLA. Also DMSO, used in pharmaceutical applications, is much safer than DMF that has been used so far to prepare

PLA/CNC nanocomposites [17, 18]. The use of this solvent opens new possibilities for applications of these particles in the biomedical field.

7.2 Experimental

Freeze-dried CNCs were kindly supplied by FPInnovations (Pointe-Claire, QC, Canada). The details of the CNC preparation are provided elsewhere [26]. The average particle width, length and aspect ratio of these nanoparticles were reported by Bagheriasl et al. [17] to be 16±3 nm, 90±17 nm and 6±2, respectively. Dimethyl sulfoxide (DMSO), certified ACS assay percent 99.9%, was purchased from Fisher Scientific Canada Co. (Ottawa, ON, Canada). Chloroform, 1,4-dioxane, 1-methylimidazole (99%) and myristoyl chloride (97%), a 14-carbon acid chloride, have been purchased from Sigma Aldrich Canada Co. (Oakville, ON, Canada). The PLA (Ingeo Biopolymer 4060D) was obtained from NatureWorks LLC (Minnetonka, MN, USA): its weight average molecular weight is 190 kg/mol and polydispersity index of 1.9, as indicated by the manufacturer. The surface of CNCs has been chemically modified by grafting an organic acid chloride via an esterification reaction to produce hydrophobic CNCs. The reaction aims at grafting carbon chains with ionic bonds being created and replacing most of the surface O-H and $O\text{-}SO_3^-$ groups of the CNCs by hydrophobic moieties [13]. In the present case, myristoyl chloride (246.8 mmol) was grafted on the surface of freeze dried CNCs (6 g), catalyzed with 1-methylimidazole (6.1 mmol) in 120 mL of 1,4-dioxane. Prior to adding the reactants, CNCs were sonicated in a sonicator bath in 1,4-dioxane for 30 min. The reaction was performed in a round-bottomed flask during 7 h and with constant mechanical stirring under a nitrogen atmosphere at 50 °C. All products were obtained after centrifugation at 6000 × G for 10 min (Thermo IEC), supernatant removal, and five washing cycles with warm distilled water to remove excess of unreacted CNCs, and with chloroform to remove unreacted myristoyl chloride. Finally, after the last supernatant removal, the product was dried in a vacuum oven at 30 °C for 24 h. These modified particles are referred to as mCNCs in this work.

7.2.1 Sample preparation

To prepare the suspensions, a water-bath sonicator (FS30 100 Watts Ultrasonic Cleaner, Fisher Scientific, Pittsburgh, PA) was used. Desired amounts of CNCs or mCNCs were dispersed in DMSO during 90 min. Then mechanical mixing was carried out in vials with a magnetic stirrer at 60 rpm for 30 min prior to the tests. To obtain a uniform temperature, the vials were placed in a water bath at 25 or 70 °C. The concentration of CNCs and mCNCs in DMSO was varied between

0.5 to 3 wt%. In order to prepare the samples containing polylactide, half the solvent was used to prepare a PLA solution containing 10 wt% PLA and stirred at 70 °C for 2 h in a water-bath; the CNC/DMSO suspension prepared separately by sonication was added to the PLA/DMSO solution and stirred at 70 °C for 30 min. These composite samples have "PLA" in their nomenclature. For the purpose of comparison, a solution of 10 wt% PLA in DMSO was prepared using magnetic stirring in a water-bath at 70 °C. Nomenclature and composition are listed in Table 7.1. "Day 1" refers to a fresh sample and "day 2" refers to a sample prepared 24 h ago. The first number in the nomenclature represents the weight % of CNC in the suspension.

Table 7.1 Composition of different systems. "X" stands for either CNC or mCNC.

	CNC/mCNC	**DMSO**	**PLA**
1.0X	1	99	0
1.9X	1.9	98.1	0
3.0X	3	97	0
PLA	0	90	10
1.9X/PLA	1.9	88.3	9.8

7.2.2 Characterization

X-ray photoelectron spectroscopy (XPS)

XPS is a powerful tool to investigate chemical changes resulting from surface modification, as it provides quantitative analysis of the atomic composition of a surface by detecting the characteristic binding energies associated with each element. XPS measurements were conducted on a VG ESCALAB 3 MKII spectrometer with a Mg-K-α ray source. The pass energy for survey scans was 100 eV to identify all components. The surface elemental stoichiometry was obtained from the ratios of peak areas corrected with the Wagner empirical sensitivity factors [27] and Shirley background subtraction [28].

Elemental analysis

Elemental analysis can be used to determine the content of specific elements in a sample. Unlike XPS that scans the surface of material, in this method the content of elements in the whole samples is determined. This analysis was carried out at University of Montreal with a Fisons EA-1108, CHNS elemental analyzer. To determine the percentage of C, H, N and S, the dynamic flash combustion method was used.

Thermogravimetric analysis (TGA)

Thermogravimetric analysis was carried out using a TGA Q500 from TA Instruments. The measurements were done at a heating rate of 2°C /min in high resolution mode under a nitrogen atmosphere, with a flow rate of 60 mL/min. Temperature ranged from 50 to 600 °C. The samples weights were 10-15 mg.

Rheometry

A stress-controlled Anton Paar rheometer (MCR 502) was used to carry out the rheological measurements at 25 and 70 °C. Couette and double-Couette flow geometries were used for different samples. The region of linear viscoelasticity was first determined by performing strain-sweep tests. In order to monitor the structure evolution of the samples, time sweep tests at the angular frequency of 1 (rad/s) were carried out. The viscoelastic behavior of the suspensions was determined from frequency sweep tests in the linear regime. The reproducibility of all data was investigated by repeating the tests three times. To avoid solvent evaporation, especially at 70 °C, heavy mineral oil was placed on the top of the sample in the flow geometries. To assure the oil did not affect the rheology of samples, neat DMSO was tested with and w/o oil and no difference was detected. In order to eliminate the history effect, all samples were pre-sheared with decreasing shear rate from 100 to 0. 1 s^{-1} during 10 min prior to the frequency sweep tests.

7.3 Results and discussion

7.3.1 Characterization of modified CNCs

The elemental surface composition (%) and the oxygen-to-carbon ratios of the different samples are summarized in Table 7.2. The oxygen-to-carbon ratio decreases from 0.52 for the unmodified CNCs to 0.32 for mCNCs. Also as mentioned earlier as a result of surface modification, most of the O-SO_3^- groups on the surface have been replaced by carbon chains and, consequently, the content of sulfur (S) decreases to almost zero.

Table 7.2 XPS analysis of CNCs and mCNCs.

sample	S (%)	O/C	C_1 C-C/C-H	C_2 C-O	C_3 O-C-O/C=O	C_4 O-C=O
CNCs	0.81	0.52	26.4	57.8	15.1	0.63
mCNCs	0.07	0.32	57.5	30.7	6.97	4.75

In order to calculate the number of sulfate groups (n) per 100 bulk anhydroglucose units, Equation (7.1) has been used [29]:

$$n = \frac{100 \times 162.14 \times S}{32.065 - 80.065 \times S} \quad (7.1)$$

where S corresponds to the weight ratio of sulfur on the surface. Based on the XPS results the number of sulfate half-ester groups per 100 bulk anhydroglucose units decreases from 4.18 for CNCs to 0.35 for mCNCs. This means that 91% of these groups have been substituted by carbon chains, confirming the success of the surface modification to produce partial hydrophobic CNC. The decrease in the S% has been validated via elemental analysis and the results are presented in Supporting Information (Table 7.S1).

The peak corresponding to carbons was deconvoluted for each sample using curve fitting software. The decomposition of C1s signal into its constituent contributions is illustrated in Figure 7.1. The C1 peak corresponds to C–C/C–H linkages, C2 peak to C–O, C3 peak to O–C–O and C=O and C4 peak corresponds to O–C=O and represents the ester carbon contribution. Considerable changes can be observed in the intensity of the C1 peak for modified CNCs compared to pristine CNCs. The C1 area increases from 26.4 for CNCs to 57.5 for mCNCs. Also the C2 area decreases. This behavior can be attributed to the 14-carbon chain grafting on the CNC surface and provides proof of successful grafting of aliphatic chains on CNCs [14]. Values of the C1, C2, C3 and C4 contributions are reported in Table 7.2.

Equation (7.2) was used to determine the surface coverage by long alkane chains (θ_{SC}), as estimated by the C1 relative area [30]:

$$\theta_{SC} = A_{C1m} - A_{C1um} \quad (7.2)$$

where A_{C1m} and A_{C1um} refer to the areas of the modified and pristine CNCs, respectively. The surface coverage for the mCNCs is 31.1%.

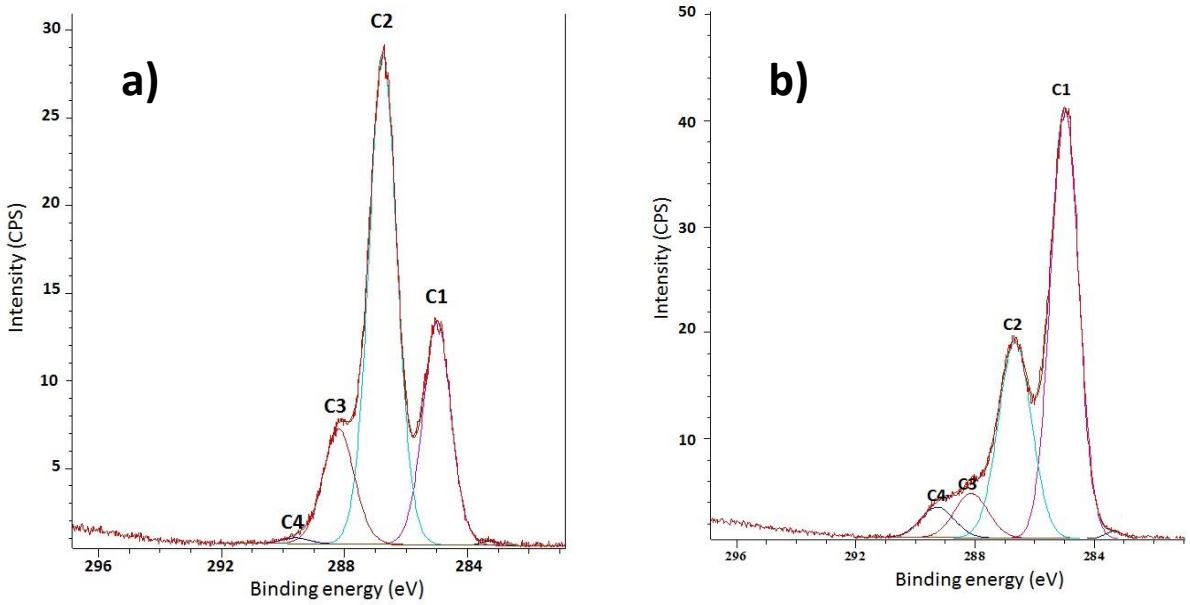

Figure 7.1 Decomposition of C1s signal into its constituent contributions for a) CNCs and b) mCNCs.

7.3.2 Thermal stability

The thermal stability of mCNCs is compared with CNCs using TGA results in Figure 7.2, which reports the relative weight (left ordinate) and the weight drop first derivative (right ordinate) as functions of temperature in nitrogen. For mCNCs three different rapid weight loss regions can be identified, whereas for CNCs two regions can be seen. As CNCs were not dried in the oven prior to the test, the first weight loss is associated with the evaporation of residual moisture from room temperature up to about 100 °C. This bonded water is essential to disperse CNCs in polar solvents like DMF and DMSO [18, 19]. Even though mCNCs were not dried in an oven prior to TGA measurements, they did not absorb moisture due to their partial hydrophobic nature and, consequently, there is no corresponding weight loss. The second important weight loss for CNCs, accounting for more than 50%, takes place between 270 and 280 °C. This weight loss region is shown as a sharp peak in the weight drop first derivative curve. It has been reported [3] that the existence of a small amount of sulfate half-ester groups on the surface of CNCs, resulting from the acid hydrolysis during CNC production, can induce a considerable decrease in the degradation

temperature of CNCs in comparison with other cellulose fibers. In contrary to what has been reported previously, since other natural fibers like flax contain hemicelluloses, which starts degrading at around 240 °C, the degradation temperature for CNCs is higher than that of these fibers [31]. The weight loss for mCNCs breaks into two consecutive peaks. The first weight loss takes place between 155 to 220 °C, which can be related to the degradation of grafted chains on the surface of mCNCs. Accordingly T_{95} for mCNCs is 165 °C. The third region occurs between 265 to 320 °C. This last region is associated with the final stage of cellulose degradation [32].

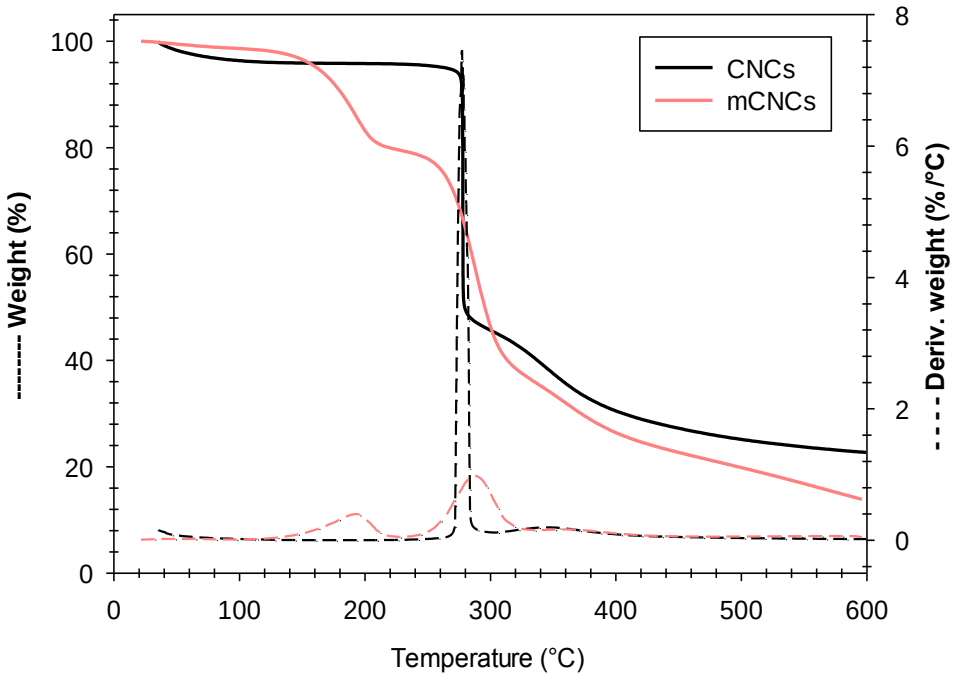

Figure 7.2 TGA results of as-received CNCs and mCNCs in nitrogen.

7.3.3 Rheological behavior in neat DMSO

The viscoelastic properties of materials can give useful information on the network formation in suspensions and quality of dispersion of nanoparticles. Figure 7.3 reports the complex viscosity as a function of time for three different CNC and mCNC suspensions in DMSO at 25 and 70 °C. All the tests have been carried out at the constant angular frequency of 1 rad/s. During a period of 12 h the complex viscosity, η*, of 1.0CNC at 70 °C increases by about 3 decades, whereas for the 1.9 and 3 wt% CNC suspensions η* increases by about a factor of 10^4 (Fig. 7.3a). Higher CNC concentrations speed up the gelation process, but on the other hand the plateau region for η*, which is a sign of a stable gel, is reached faster for lower concentrations. The gelation time, taken as the

crossover of the storage modulus, G', and the loss modulus, G", (data not shown) could not be determined with accuracy, but the final plateau for η* was reproducible. The average gelation times for the 1, 1.9 and 3 wt% CNC suspensions were about 305±25, 260±20 and 240±20 min, respectively. Figure 7.3b presents the variations of η* with time for the suspensions containing 3 wt% of CNCs at 25 °C and mCNCs at 25 and 70 °C. The complex viscosity of the 3.0CNC suspension at 25 °C is very low and increases very little over the 12 h period compared to data of Figure 7.3a and, consequently, no gel is formed. The effect of temperature on gelation will be explained later. The mCNC suspension in DMSO forms a weak gel during the first day at room temperature and 70 °C and its complex viscosity does not increase much with time. The η* value is larger at 25 °C than at 70 °C. The initial complex viscosity of 3.0CNC at 70 °C is much lower than that of 3mCNC, but after one day its final η* value is larger by about two decades. At 25 °C, η* of 3.0mCNC is higher than that of 3.0CNC and changes are negligible for both suspensions over the period of 12 h.

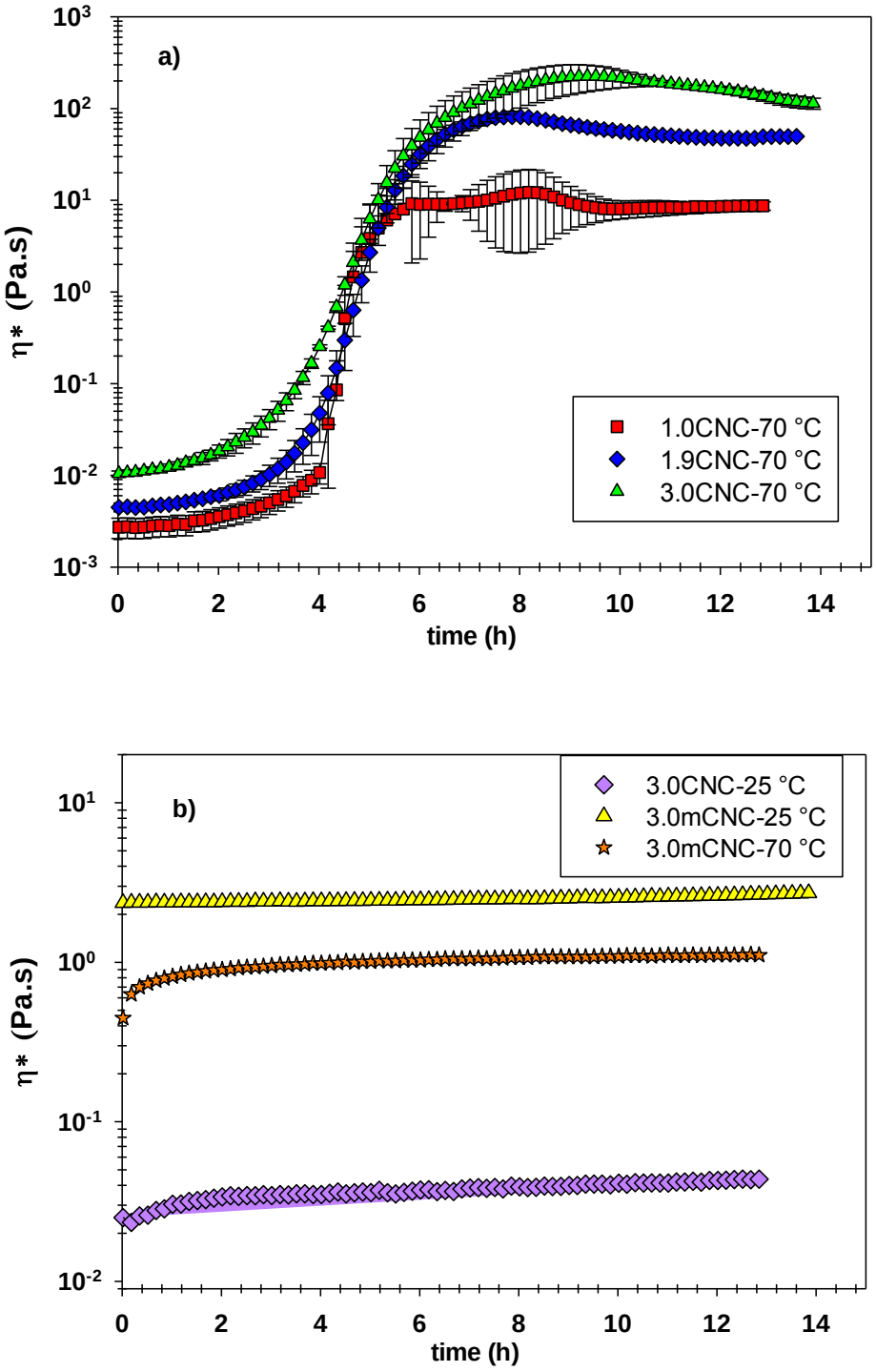

Figure 7.3 Complex viscosity as a function of time at ω = 1 rad/s for a) CNC suspensions; T = 70 °C, b) 3CNC (25 °C) and 3mCNC suspensions at 25 and 70 °C.

Figure 7.4 presents the small amplitude oscillatory shear (SAOS) data of the CNC suspensions on days 1 and 2 at 70 °C as functions of frequency. The three samples on the first day exhibit the

typical Newtonian behavior with a constant complex viscosity over the entire range of frequency (Fig. 7.4a) and no significant elastic modulus, *G*', could be measured. For all concentrations on day 2, the behavior is that of a strong gel or viscoelastic solid [33], where *G*' >> *G"* (loss modulus) and both moduli are relatively independent of frequency, as illustrated by Figure 7.4b. As expected a stronger gel structure is formed at higher concentrations: *G'* of 3.0CNC-day2 is almost five folds that of *G"*. The critical concentration for gel formation in DMSO after one day at 70 °C is between 0.5 and 1 wt% (Figure 7.S1 of Supporting Information). Also it should be mentioned that the rheological behavior of a 3.0CNC-day2 sample gently stirred in the water-bath was comparable to the 3.0CNC sample that has been gelled in the rheometer following the time sweep test.

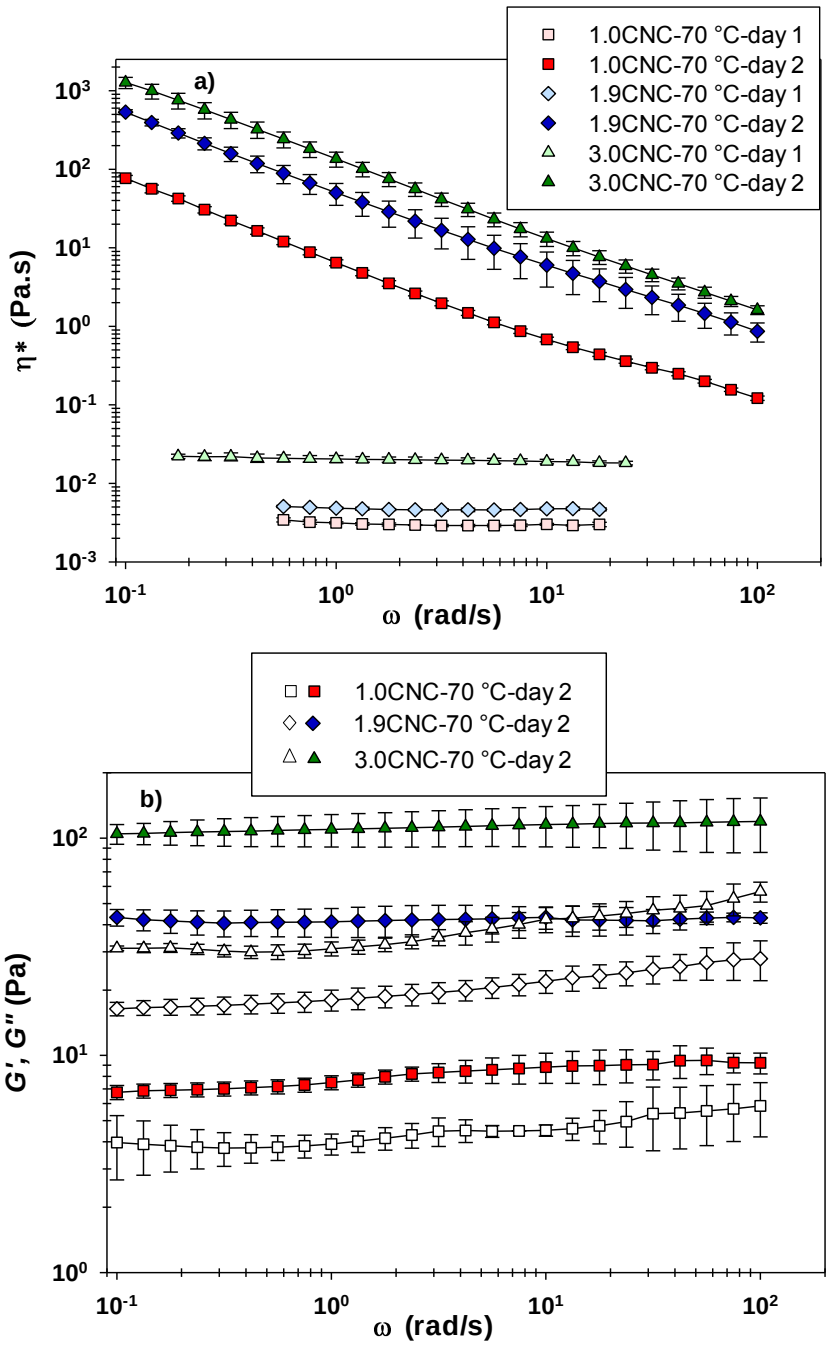

Figure 7.4 SAOS data of CNC suspensions at 70 °C. (a) Complex viscosity vs. angular frequency at days 1 and 2; (b) storage (filled symbols) and loss moduli (open symbols) vs. angular frequency on day 2.

A possible explanation for the gel formation of CNCs in DMSO at higher temperature is the partial desulfation of CNCs. The suspension of CNCs is stabilized by O-SO_3^- groups on the surface, which

cause electrostatic repulsion between particles. During desulfation, the loss of these negatively charged groups from the surface decreases the repulsive force and results in gelation. Since the desulfation is time-dependent, gel formation takes a few hours to occur [23]. In order to investigate desulfation, the pH of the different systems diluted in water before and after gelation was measured (Table 7.S2 of Supporting Information). For the 3 wt% CNC suspension, we determined a pH decrease after gelation at 70 °C from 6.9±0.1 to 6.1±0.1 attributed to desulfation, whereas no significant pH decrease was obtained for the same suspension at 25 °C. Further investigation of desulfation is reported in the Supporting Information. Using XRD, the CNC crystalline structure was shown to be unaffected by the gel formation (results presented in Figure 7.S3 of the Supporting Information).

Figure 7.5 reports the SAOS data of the 1.9 and 3 wt% mCNC suspensions in DMSO at 25 and 70 °C. In contrast to the CNC suspensions, the modified CNC suspensions exhibit a solid-like behavior from the first day at 25 and 70 °C. The shear-thinning behavior with the absence of a Newtonian plateau at low frequencies (Fig. 7.5a) and $G' > G''$ (Fig. 7.5b) are indicative of a network formation in these samples [34]. By increasing the concentration of mCNCs from 1.9 to 3 wt%, the complex viscosity increases by two folds. The complex viscosity of the 3mCNC suspension for both temperatures does not change significantly over the period of 24 h, but it decreases as the temperature is increased from 25 to 70 °C. G' for the 3mCNC suspension is of the order of 10 Pa, whereas the storage modulus for the 3CNC gel is 100 Pa (Fig. 7.4b). The ratio of the loss to the storage modulus (tan $\delta = G''/G'$) can be used to differentiate strong from weak gels [35]. Tan δ values are 0.43±0.04 and 0.46±0.03 for 3.0mCNC-25 °C-day 2 and 3.0mCNC-70 °C-day 2, respectively, over all angular frequencies, whereas tan δ is 0.28±0.03 for 3CNC-70 C-day 2, indicative of a much stronger gel. As explained earlier, these modified CNCs have lost about 91% of $O\text{-}SO_3^-$ groups on their surface in comparison to CNCs. These surface groups provide repulsive interactions between nanoparticles and help their dispersion. For mCNC some short chains of 14 carbons of the myristoyl chloride have substituted the sulfate half-ester and hydroxyl groups on the surface of CNC. These short carbon chains on the surface of mCNCs can help forming the structure right on the first day via physical interactions between chains, but as these chains are not long enough to entangle with each other the formed gel is not strong. As there is no significant desulfation in mCNC suspension these gels are stable and do not change with time since the

degradation temperature of mCNCs is around 165 °C and these chains will not degrade or leave the surface of mCNCs at 70 °C.

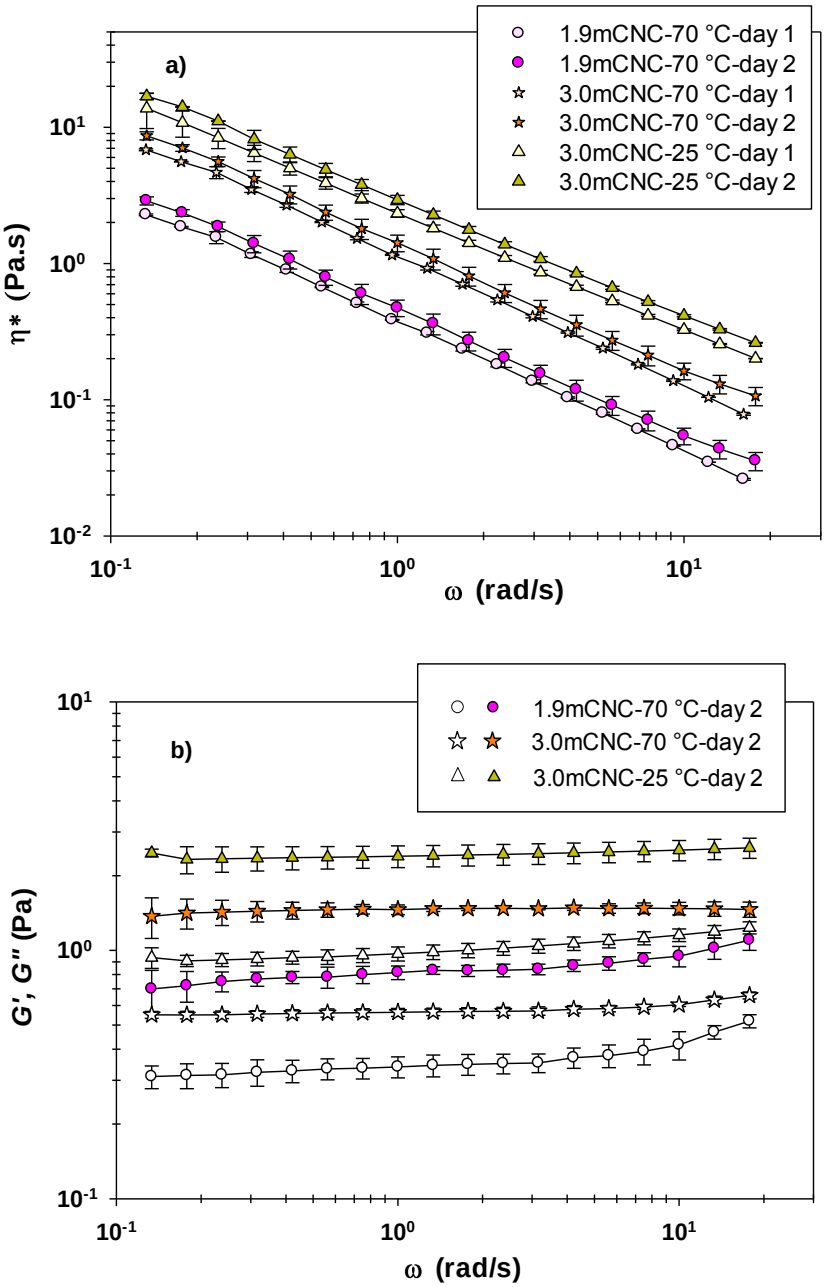

Figure 7.5 SAOS data of 3mCNC suspensions at 25 and 70 °C. (a) Complex viscosity vs. angular frequency on days 1 and 2; (b) storage (filled symbols) and loss moduli (open symbols) vs. angular frequency on day 2.

7.3.4 Rheological behavior in the PLA solution in DMSO

The SAOS data of the CNC and mCNC suspensions in the 10 wt% PLA solution in DMSO are presented in Figure 7.6. All tests have been carried out at 70 °C since PLA would precipitate in DMSO at lower temperatures. The PLA solution alone exhibits a Newtonian behavior for the entire range of frequency and does not show any aging effect (Fig. 7.6a). However, for the 1.9CNC/PLA suspension a slight shear-thinning behavior can be observed on the first day. A similar behavior was observed for dilute CNC suspensions and for polymer/CNC mixtures such as poly (ethylene oxide) [36, 37], polyacrylonitrile [38] and polyurethane [39]. CNCs are believed to be well distributed in the PLA solution. Adding mCNCs increased the overall complex viscosity of the system in comparison to the PLA solution from day 1 (data not shown), and a marginal increase in rheological properties could be observed after 24 h. The shear thinning for 1.9mCNC/PLA is less pronounced than for 1.9mCNC and the behavior tends toward a Newtonian behavior at high frequencies with a viscosity value approaching that of the PLA solution. Figure 7.6b reports the storage (G') and the loss (G'') moduli responses as functions of angular frequency for the 1.9CNC and 1.9CNC/PLA suspensions on day 2. The storage modulus increases by almost two folds as PLA is added to the system. As for the neat 1.9CNC system, the suspension in the PLA solution exhibits a gel-like behavior with G' almost independent of ω and $G'>>G''$; its moduli are somewhat larger than those for the neat CNC suspension, but, the difference in the loss modulus is relatively small. Somehow adding PLA chains to the system contributes more to the storage modulus than to the loss modulus.

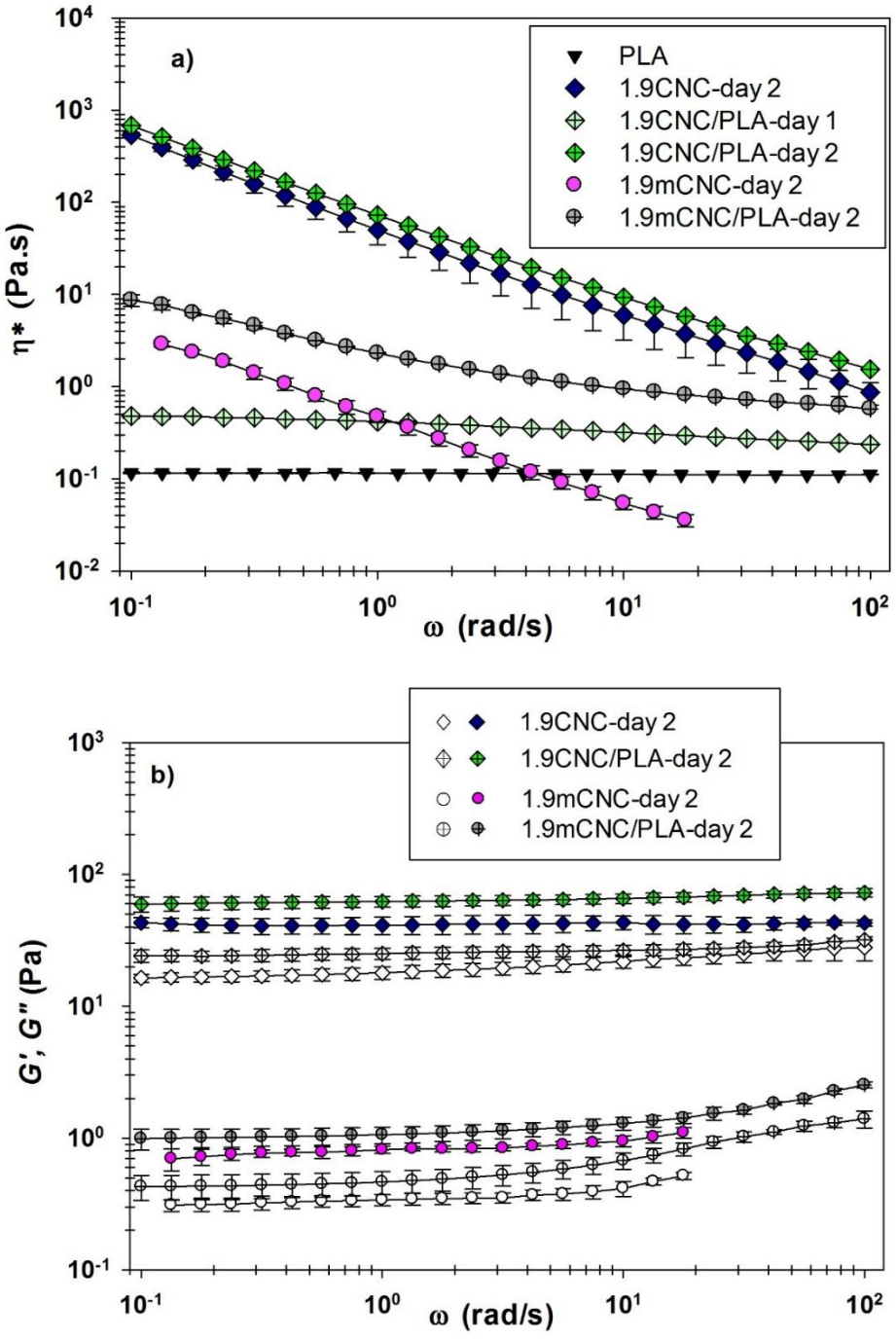

Figure 7.6 SAOS data of 1.9 wt % CNC and mCNC suspensions in DMSO and in PLA solution at 70 °C. (a) Complex viscosity (b) storage (filled symbols) and loss moduli (open symbols) vs. angular frequency.

For mCNC w/o PLA, in the range of 0.1 to 10 rad/s both suspensions show a solid-like gel behavior with *G'* and *G"* almost independent of ω and *G'*>>*G"*. At higher frequencies slight increases with frequency can be observed for both *G'* and *G"*. As expected the storage modulus is larger in the suspensions containing PLA.

The complex modulus ($G^* = G' + iG''$) characterizes the rigidity of a gel subjected to deformation [35]. Table 7.3 summarizes the rheological characteristics of the gels: *G'*, *G"*, *G** and tan δ for the CNC gels at the angular frequency of 1 rad/s. For all these samples tan δ is smaller than unity, confirming that they all form gels on the second day at 70 °C. As expected, for CNC gels *G** increases more than 15 times as the CNC content increases from 1 to 3wt%, with corresponding decreases of tan δ from 0.5 to 0.28. *G** for the CNC nanocomposite systems is considerably larger than the mCNC systems (almost fifty folds), which confirms much stronger gel for CNC nanocomposite suspension in comparison with mCNC.

Table 7.3 Rheological properties of CNC and mCNC gels w/o PLA on day 2 at 70 °C. The data are for angular frequency of 1 rad/s.

	***G'* (Pa)**	***G"* (Pa)**	**tan δ**	***G** (Pa)**
1.0CNC	7.4	3.7	0.50	8.3
1.9CNC	41.2	17	0.40	44.6
3.0CNC	110	31	0.28	114.3
1.9CNC/PLA	61	22	0.36	64.8
1.9mCNC	0.75	0.35	0.47	0.8
3.0mCNC	1.7	0.76	0.46	1.9
1.9mCNC/PLA	1.2	0.46	0.38	1.3

The effects of CNCs and mCNCs on the viscosity and complex modulus of the suspension media are compared in Figure 7.7 in terms of the reduced viscosity, defined by:

$$\eta_{RED} = \frac{\eta^* - \eta^*_{sol}}{\eta^*_{sol}} \tag{7.3}$$

where η^*_{sol} is the complex viscosity of DMSO or 10 wt% PLA solution in DMSO. Equation 7.4 was used to calculate the reduced storage modulus (G'_{RED}):

$$G'_{RED} = \frac{G' - G^*_{sol}}{G^*_{sol}} \tag{7.4}$$

where G^*_{sol} is the complex modulus of DMSO or 10 wt% PLA solution in DMSO. Figure 7.7a compares the reduced viscosity of different systems on day 2 at 70 °C. As expected the reduced viscosity of the 1.9CNC suspensions is larger than that of the 1.9mCNC suspensions. However, and surprisingly, the presence of PLA considerably lowers the reduced viscosity, by factors close to 60 and 25 for the CNC and mCNC systems, respectively, at low frequencies. This suggests that PLA chains interact negatively with CNC and mCNC particles to form weaker networks. This is confirmed by the reduced storage modulus presented in Figure 7.7b.

As discussed earlier, mCNCs form a network from the first day in DMSO. Adding PLA to the system increases the complex viscosity of the 1.9CNC suspension, but the reduced viscosity is lower from the first day for this sample. The relative viscosity, like η*, did not change significantly for samples with and without PLA. The reduced viscosity at low frequencies shows a steep shear thinning, but at higher frequencies the behavior is closer to that of the DMSO/PLA solution and relative viscosity becomes almost independent of frequency.

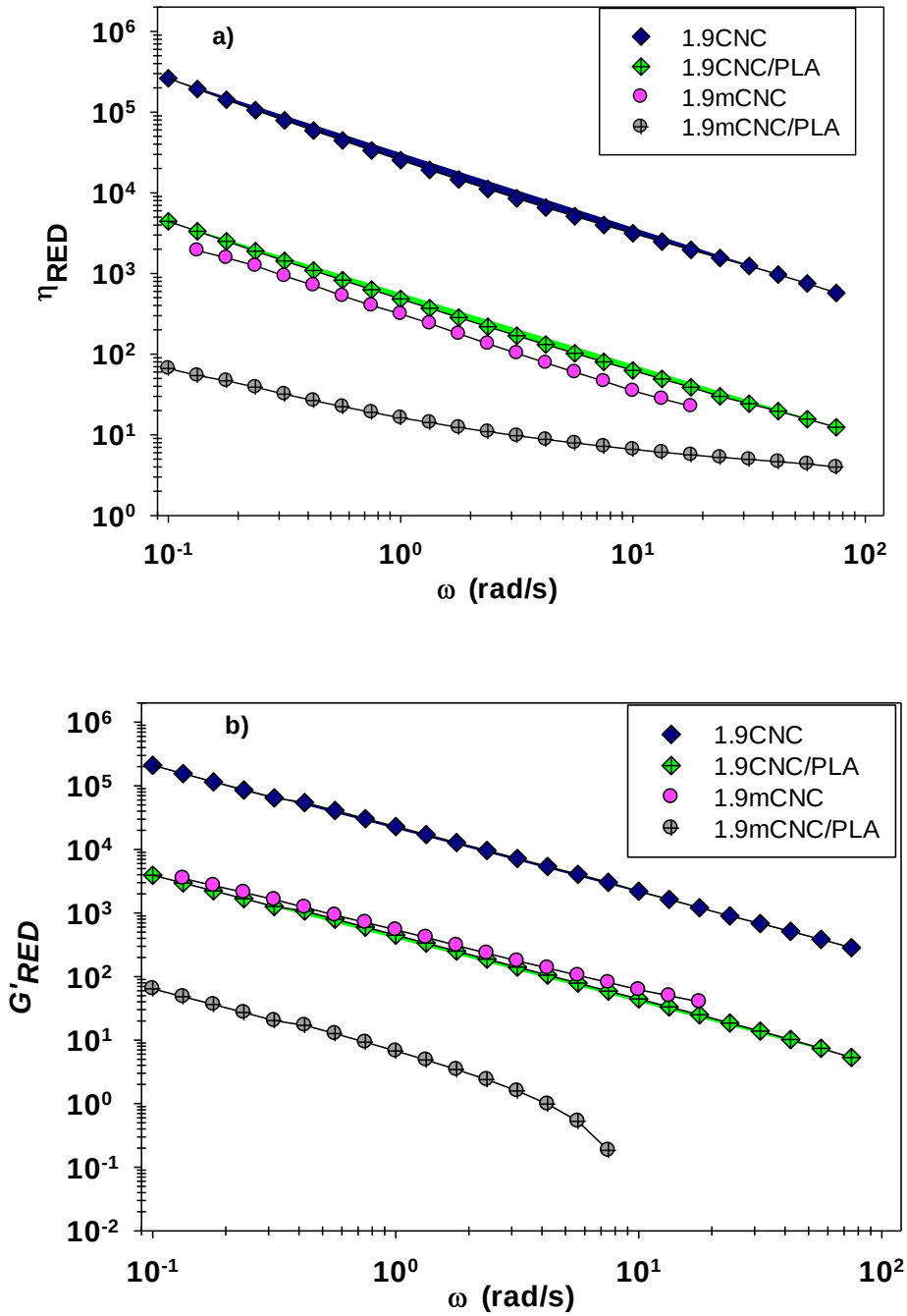

Figure 7.7 Reduced (a) complex viscosity and (b) storage modulus vs. angular frequency of different systems on day 2 at 70 °C.

By adding PLA to the suspensions, the reduced storage modulus markedly decreases. Since G'_{RED} is representative of the strength of the network formed by the nanoparticles and polymer chains, it can be concluded that the negative interactions between PLA and CNC do not promote gelation

and network formation of CNCs and mCNCs. This is possibly due to the increased viscosity of the PLA solution compared to that of the solvent, which hinders the influence of the Brownian motion on the network formation. We note that the effect of PLA on mCNCs is relatively similar although we expected less negative interactions due to the grafted myristoyl chloride chains on their surface. These chains on the surface of mCNCs are, however, not long enough to entangle with PLA chains and help gel formation. Also it should be noted that not all the hydroxyl groups of mCNCs were altered during surface modification and these groups have weak interactions with PLA chains.

7.4 Conclusion

Cellulose nanocrystals have been modified via grafting an organic acid chloride on the surface of the nanoparticles. The efficiency of surface modification has been confirmed by XPS. The rheological properties of CNC and mCNC suspensions in DMSO have been studied. The effect of two different temperatures on the aging of the suspensions has been investigated. Rheological characterization showed that aging of CNC suspensions in DMSO at 70 °C caused gel formation of nanoparticles at very low concentration (1 wt %). The aging process at room temperature did not change the rheological properties of the suspensions significantly. On the other hand, for modified CNCs a weak gel was formed from the first day at low and high temperatures and changes in complex viscosity after one day were marginal. The rheological properties of the mCNC suspensions at 70 °C were found much lower than those of the CNC suspensions. Addition of PLA to CNC and mCNC suspensions increased the complex viscosity and storage modulus of the samples, but the reduced viscosity and reduced storage modulus of CNC/PLA were considerably lower than those of the suspensions in the neat DMSO. This has been ascribed to negative interaction of the PLA chains with the nanoparticles and decreased influence of the Brownian motion due the increased viscosity of the suspending medium. CNC [40-42] and DMSO [43] have been used previously in drug delivery systems. The gelation of CNC and mCNC suspensions at very low content in a polar non-aqueous, safe solvent like DMSO can favor the use of these nanoparticles for biomedical applications.

7.5 Acknowledgments

The authors gratefully acknowledge the Natural Sciences and Engineering Research Council of Canada (NSERC) for funding. We are also thankful to Dr. Jean Bouchard of FPInnovations who provided the CNCs used in this project.

7.6 Supporting Information

The elemental analyses of both pristine and modified samples are given in Table 7.S1. As observed before in XPS results, the content of S% was decreased considerably (around 93%) after surface modification.

Table 7.S1 Elemental analysis of cellulose nanocrystals before and after chemical surface modification.

sample	S (%)	H (%)	C (%)	N (%)	O (%)
CNC	0.7	6.24	41.14	0	51.92
mCNC	0.05	11.84	70.20	0.14	17.77

In a qualitative study of gelation of CNC suspensions, the transition from a liquid suspension to gels induced by the addition of CNCs to DMSO at 70 °C is revealed in Figure 7.S1. Even though 1.0CNC-day 2 forms a gel, its structure is not strong enough to hold the sample up against gravity. The gels from the 1.9CNC and 3.0CNC suspensions are stronger than that of 1.0CNC. As can be seen, of the 0.5CNC suspension did not form a gel. It can be concluded that minimum gelation concentration for CNC suspensions at 70 °C is between 0.5 to 1 wt%.

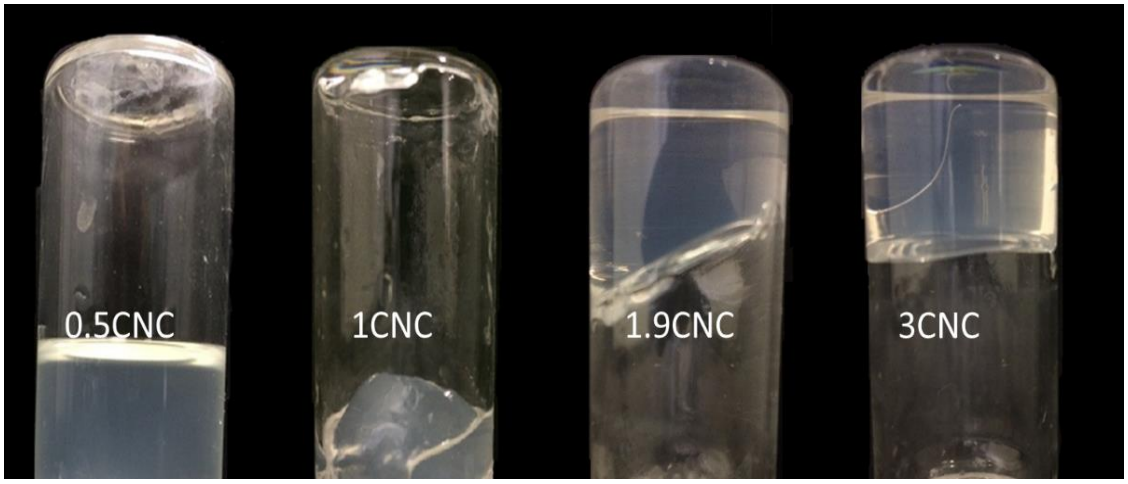

Figure 7.S1 CNC suspensions at different concentrations in DMSO after 24h at 70 °C.

The stability of CNC suspensions with sulfate half-esters on the surface is due to the electrostatic repulsion between negatively charged surface groups, consequently conditions that decrease the repulsive interactions between CNCs will tend to cause gelation.

The decreases of surface charges and increases in ionic strength would destabilize the suspensions. Desulfation would generate sulfuric acid, which would lead to a decrease in the pH of the medium. The pH of the suspensions before and after gelation at 70 °C was measured, and the results are reported in Table 7.S2. Samples with different concentrations were examined, and all the pH values decreased. For the 3.0CNC-25 °C sample, for which no gelation was observed, the pH did not change after 1 day as expected.

Table 7.S2 Change of pH as the result of gelation at different concentrations of CNC.

Sample	Day1	Day2
DMSO	8.1±0.1	8.1±0.1
1.0CNC-70 °C	7.4±0.2	6.7±0.1
1.9CNC-70 °C	7.1±0.2	6.3±0.1
3.0CNC-70 °C	6.9±0.1	6.1±0.1
3.0CNC-25 °C	6.9±0.1	6.8±0.1

Figure 7.S2 reports the complex viscosity of t CNC suspensions at 70 °C on day 1 and 2 as functions of the CNC concentration. These data are in accordance with the observations of Figure 7.S1 and show that the viscosity of the sample containing 0.5 wt% did not change significantly after 24 h, whereas an increase of about 4 decades occurred for sample containing 1 wt% CNCs. It can be concluded that the minimum gelation concentration for CNC in DMSO after one day at 70 °C is between 0.5 and 1 wt% as mentioned before.

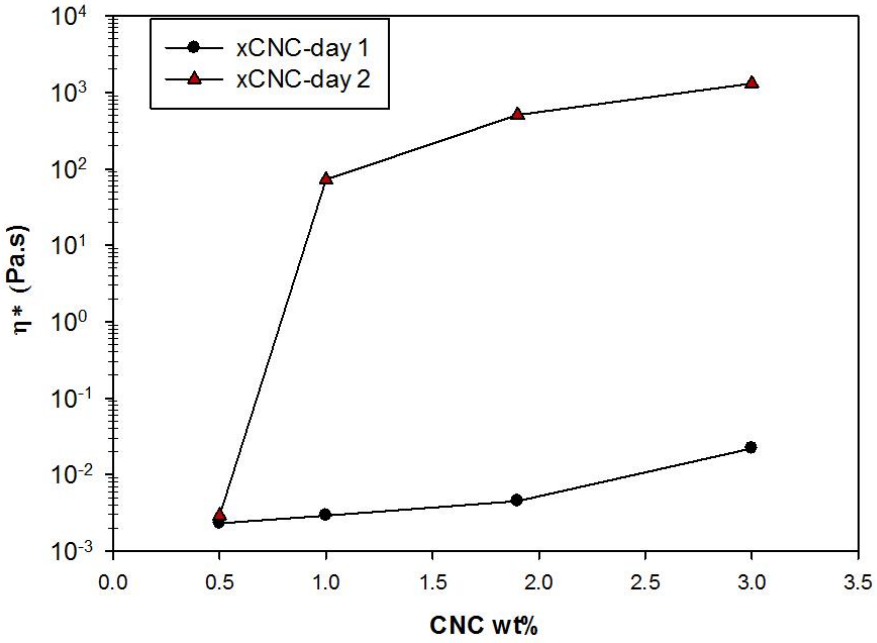

Figure 7.S2 Complex viscosity of CNC suspensions at 70 °C on the first and second days at the frequency of 0.1 rad/s.

Three different CNC suspensions are compared in Figure 7.S3: freeze-dried CNCs, dw-CNCs (dried from an aqueous suspension) and dg-CNCs (dried from gel). The dw-CNCs were prepared by drying a 3 wt% aqueous suspension of CNCs in a vacuum oven at 50 °C for two days. In order to prepare the dg-CNCs, a gel of 3 wt% CNCs in DMSO has been prepared at 70 °C. In the next step, acetone was added to the CNC gel at room temperature to precipitate the particles. The suspension was centrifuged at 6000 × G for 10 min (Thermo IEC) and the supernatant was dried in a vacuum oven at 50 °C for two days. Aqueous suspensions of freez-dried CNCs, dw-CNCs and dg-CNCs were prepared via sonication, all 3 wt% CNCs. As expected, the freeze-dried CNCs were dispersed easily in water and formed a homogeneous suspension after a brief ultrasound treatment (Figure 7.S3 a). For the dw-CNC suspensions the particles formed a stable homogenous suspension, but sonication during a longer time was necessary (Figure 7.S3 b). The dg-CNCs did not re-disperse in water, even under a strong ultrasound treatment, and no homogeneous suspension could be obtained (Figure 7.S3 c). This can be attributed to partial desulfation during gelation in DMSO. The surface charges are responsible for forming a stable suspension of CNCs in water.

Partial desulfation can remove the surface charges on the CNC surface and consequently the aggregates cannot be broken in water.

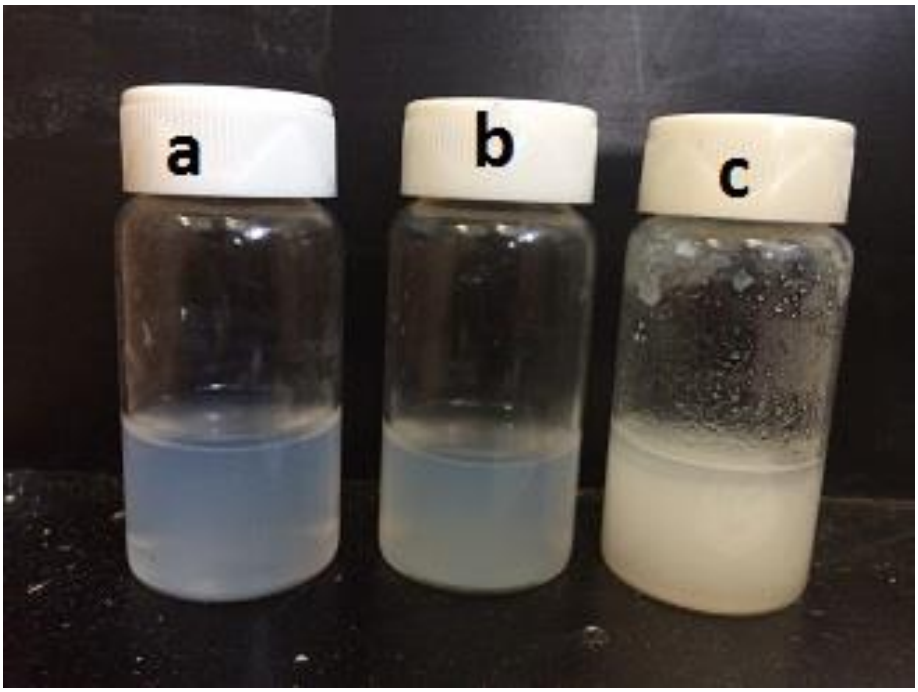

Figure 7.S3 Re-dispersion of a) freeze dried CNCs b) dw-CNCs and c) dg-CNCs, in water after sonication.

CNCs derived from plants can have 12-45% of amorphous parts, depending on the source and duration of the acid hydrolysis [99]. Cellulose molecules are very stiff and have a large intrinsic viscosity so a low content of amorphous cellulose can bridge CNCs.

Figure 7.S4 shows the X-ray diffraction patterns of freeze-dried CNCs and CNCs dried from a DMSO gel. These patterns confirm that the CNCs remain crystalline after gelation. The crystallinity (χ_c) of CNCs based on XRD has been calculated using Equation 7.S1. The crystallinity changed from 76.5 for freeze-dried CNCs to about 77.8% for dried CNCs from the DMSO gel. This is a negligible difference and is in the error range. Thus, the thermal treatment in DMSO can cause desulfation of CNCs, without causing significant crystal degradation of the CNCs.

$$\chi_c = \frac{I_{22.7} - I_{18}}{I_{22.7}} \times 100 \qquad (7.S1)$$

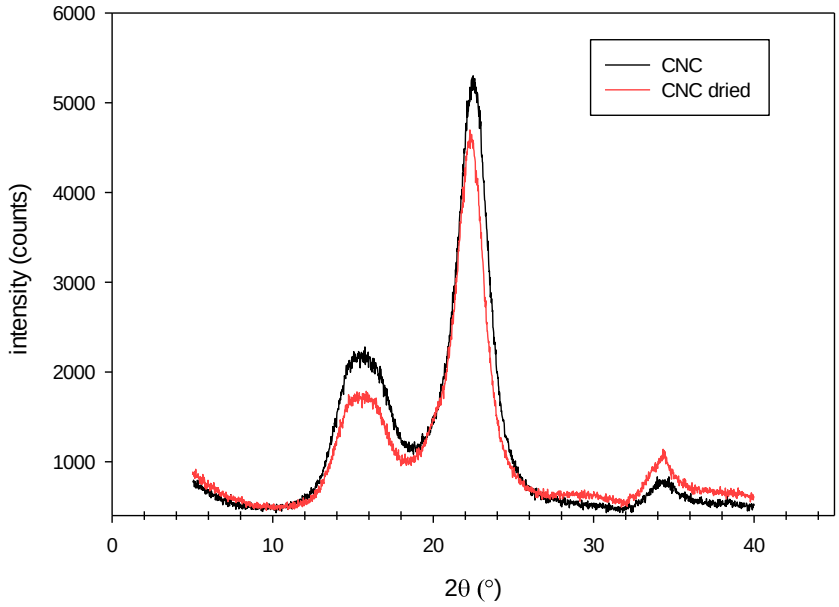

Figure 7.S4 X-ray diffraction pattern for CNCs and CNC dried from DMSO gel.

7.7 References

1. Liu, D., X. Chen, Y. Yue, M. Chen, and Q. Wu, Structure and rheology of nanocrystalline cellulose. Carbohydrate Polymers, 2011. **84**(1): p. 316-322.

2. Peng, B.L., N. Dhar, H.L. Liu, and K.C. Tam, Chemistry and applications of nanocrystalline cellulose and its derivatives: A nanotechnology perspective. The Canadian Journal of Chemical Engineering, 2011. **89**(5): p. 1191-1206.

3. Roman, M. and W.T. Winter, Effect of Sulfate Groups from Sulfuric Acid Hydrolysis on the Thermal Degradation Behavior of Bacterial Cellulose. Biomacromolecules, 2004. **5**(5): p. 1671-1677.

4. van den Berg, O., J.R. Capadona, and C. Weder, Preparation of Homogeneous Dispersions of Tunicate Cellulose Whiskers in Organic Solvents. Biomacromolecules, 2007. **8**(4): p. 1353-1357.

5. Hajji, P., J.Y. Cavaillé, V. Favier, C. Gauthier, and G. Vigier, Tensile behavior of nanocomposites from latex and cellulose whiskers. Polymer Composites, 1996. **17**(4): p. 612-619.

6. Anglès, M.N. and A. Dufresne, Plasticized Starch/Tunicin Whiskers Nanocomposites. 1. Structural Analysis. Macromolecules, 2000. **33**(22): p. 8344-8353.

7. Roohani, M., Y. Habibi, N.M. Belgacem, G. Ebrahim, A.N. Karimi, and A. Dufresne, Cellulose whiskers reinforced polyvinyl alcohol copolymers nanocomposites. European Polymer Journal, 2008. **44**(8): p. 2489-2498.

8. Azizi Samir, M.A.S., F. Alloin, J.-Y. Sanchez, and A. Dufresne, Cellulose nanocrystals reinforced poly(oxyethylene). Polymer, 2004. **45**(12): p. 4149-4157.

9. Braun, B. and J.R. Dorgan, Single-Step Method for the Isolation and Surface Functionalization of Cellulosic Nanowhiskers. Biomacromolecules, 2009. **10**(2): p. 334-341.

10. Goffin, A.L., J.M. Raquez, E. Duquesne, G. Siqueira, Y. Habibi, A. Dufresne, and P. Dubois, Poly(ε-caprolactone) based nanocomposites reinforced by surface-grafted cellulose nanowhiskers via extrusion processing: Morphology, rheology, and thermo-mechanical properties. Polymer, 2011. **52**(7): p. 1532-1538.

11. Habibi, Y., A.-L. Goffin, N. Schiltz, E. Duquesne, P. Dubois, and A. Dufresne, Bionanocomposites based on poly(ε-caprolactone)-grafted cellulose nanocrystals by ring-opening polymerization. Journal of Materials Chemistry, 2008. **18**(41): p. 5002-5010.

12. Morandi, G., L. Heath, and W. Thielemans, Cellulose Nanocrystals Grafted with Polystyrene Chains through Surface-Initiated Atom Transfer Radical Polymerization (SI-ATRP). Langmuir, 2009. **25**(14): p. 8280-8286.

13. Poaty, B., V. Vardanyan, L. Wilczak, G. Chauve, and B. Riedl, Modification of cellulose nanocrystals as reinforcement derivatives for wood coatings. Progress in Organic Coatings, 2014. **77**(4): p. 813-820.

14. Junior de Menezes, A., G. Siqueira, A.A.S. Curvelo, and A. Dufresne, Extrusion and characterization of functionalized cellulose whiskers reinforced polyethylene nanocomposites. Polymer, 2009. **50**(19): p. 4552-4563.

15. Spinella, S., C. Samuel, J.-M. Raquez, S.A. McCallum, R. Gross, and P. Dubois, Green and Efficient Synthesis of Dispersible Cellulose Nanocrystals in Biobased Polyesters for Engineering Applications. ACS Sustainable Chemistry & Engineering, 2016. **4**(5): p. 2517-2527.

16. Gwon, J.-G., H.-J. Cho, S.-J. Chun, S. Lee, Q. Wu, M.-C. Li, and S.-Y. Lee, Mechanical and thermal properties of toluene diisocyanate-modified cellulose nanocrystal nanocomposites using semi-crystalline poly(lactic acid) as a base matrix. RSC Advances, 2016. **6**(77): p. 73879-73886.

17. Bagheriasl, D., P.J. Carreau, B. Riedl, C. Dubois, and W.Y. Hamad, Shear rheology of polylactide (PLA)–cellulose nanocrystal (CNC) nanocomposites. Cellulose, 2016. **23**(3): p. 1885-1897.

18. Viet, D., S. Beck-Candanedo, and D.G. Gray, Dispersion of cellulose nanocrystals in polar organic solvents. Cellulose, 2007. **14**(2): p. 109-113.

19. Chang, H., J. Luo, A.A. Bakhtiary Davijani, A.-T. Chien, P.-H. Wang, H.C. Liu, and S. Kumar, Individually Dispersed Wood-Based Cellulose Nanocrystals. ACS Applied Materials & Interfaces, 2016. **8**(9): p. 5768-5771.

20. Ljungberg, N., C. Bonini, F. Bortolussi, C. Boisson, L. Heux, and Cavaillé, New Nanocomposite Materials Reinforced with Cellulose Whiskers in Atactic Polypropylene: Effect of Surface and Dispersion Characteristics. Biomacromolecules, 2005. **6**(5): p. 2732-2739.

21. Dorris, A. and D.G. Gray, Gelation of cellulose nanocrystal suspensions in glycerol. Cellulose, 2012. **19**(3): p. 687-694.

22. Chau, M., S.E. Sriskandha, D. Pichugin, H. Thérien-Aubin, D. Nykypanchuk, G. Chauve, M. Méthot, J. Bouchard, O. Gang, and E. Kumacheva, Ion-Mediated Gelation of Aqueous Suspensions of Cellulose Nanocrystals. Biomacromolecules, 2015. **16**(8): p. 2455-2462.

23. Lewis, L., M. Derakhshandeh, S.G. Hatzikiriakos, W.Y. Hamad, and M.J. MacLachlan, Hydrothermal Gelation of Aqueous Cellulose Nanocrystal Suspensions. Biomacromolecules, 2016. **17**(8): p. 2747-2754.

24. Beck, S. and J. Bouchard, Auto-catalyzed acidic desulfation of cellulose nanocrystals. Nordic Pulp & Paper Research Journal, 2014. **29**: p. 006-014.

25. Dong, X.M. and D.G. Gray, Effect of Counterions on Ordered Phase Formation in Suspensions of Charged Rodlike Cellulose Crystallites. Langmuir, 1997. **13**(8): p. 2404-2409.

26. Miao, C. and W.Y. Hamad, Cellulose reinforced polymer composites and nanocomposites: a critical review. Cellulose, 2013. **20**(5): p. 2221-2262.

27. Wagner, C.D., L.E. Davis, M.V. Zeller, J.A. Taylor, R.H. Raymond, and L.H. Gale, Empirical atomic sensitivity factors for quantitative analysis by electron spectroscopy for chemical analysis. Surface and Interface Analysis, 1981. **3**(5): p. 211-225.

28. Repoux, M., Comparison of background removal methods for XPS. Surface and Interface Analysis, 1992. **18**(7): p. 567-570.

29. Li, M.-C., Q. Wu, K. Song, S. Lee, Y. Qing, and Y. Wu, Cellulose Nanoparticles: Structure–Morphology–Rheology Relationships. ACS Sustainable Chemistry & Engineering, 2015. **3**(5): p. 821-832.

30. Freire, C.S.R., A.J.D. Silvestre, C. Pascoal Neto, A. Gandini, P. Fardim, and B. Holmbom, Surface characterization by XPS, contact angle measurements and ToF-SIMS of cellulose fibers partially esterified with fatty acids. Journal of Colloid and Interface Science, 2006. **301**(1): p. 205-209.

31. Sojoudiasli, H., M.-C. Heuzey, and P.J. Carreau, Rheological, morphological and mechanical properties of flax fiber polypropylene composites: influence of compatibilizers. Cellulose, 2014. **21**(5): p. 3797-3812.

32. Shafizadeh, F. and A.G.W. Bradbury, Thermal degradation of cellulose in air and nitrogen at low temperatures. Journal of Applied Polymer Science, 1979. **23**(5): p. 1431-1442.

33. Nijenhuis, K.T. and W. Mijs, Chemical and Physical Networks: Formation and Control of Properties. Vol. 1. 1998, Chichester: John Wiley and Sons.

34. Hasani, M., E.D. Cranston, G. Westman, and D.G. Gray, Cationic surface functionalization of cellulose nanocrystals. Soft Matter, 2008. **4**(11): p. 2238-2244.

35. Mezger, T., The Rheology Handbook: For Users of Rotational and Oscillatory Rheometers. 2006, Hannover, Germany: Vincentz Network.

36. Zhou, C., R. Chu, R. Wu, and Q. Wu, Electrospun Polyethylene Oxide/Cellulose Nanocrystal Composite Nanofibrous Mats with Homogeneous and Heterogeneous Microstructures. Biomacromolecules, 2011. **12**(7): p. 2617-2625.

37. Pereda, M., N.E. Kissi, and A. Dufresne, Extrusion of Polysaccharide Nanocrystal Reinforced Polymer Nanocomposites through Compatibilization with Poly(ethylene oxide). ACS Applied Materials & Interfaces, 2014. **6**(12): p. 9365-9375.

38. Chang, H., A.-T. Chien, H.C. Liu, P.-H. Wang, B.A. Newcomb, and S. Kumar, Gel Spinning of Polyacrylonitrile/Cellulose Nanocrystal Composite Fibers. ACS Biomaterials Science & Engineering, 2015. **1**(7): p. 610-616.

39. Marcovich, N.E., M.L. Auad, N.E. Bellesi, S.R. Nutt, and M.I. Aranguren, Cellulose micro/nanocrystals reinforced polyurethane. Journal of Materials Research, 2006. **21**(04): p. 870-881.

40. Mohan Yallapu, M., M. Ray Dobberpuhl, D. Michele Maher, M. Jaggi, and S. Chand Chauhan, Design of Curcumin loaded Cellulose Nanoparticles for Prostate Cancer. Current Drug Metabolism, 2012. **13**(1): p. 120-128.

41. Ndong Ntoutoume, G.M.A., R. Granet, J.P. Mbakidi, F. Brégier, D.Y. Léger, C. Fidanzi-Dugas, V. Lequart, N. Joly, B. Liagre, V. Chaleix, and V. Sol, Development of curcumin–cyclodextrin/cellulose nanocrystals complexes: New anticancer drug delivery systems. Bioorganic & Medicinal Chemistry Letters, 2016. **26**(3): p. 941-945.

42. Dash, R. and A.J. Ragauskas, Synthesis of a novel cellulose nanowhisker-based drug delivery system. RSC Advances, 2012. **2**(8): p. 3403-3409.

43. Basnet, P. and N. Skalko-Basnet, Curcumin: An Anti-Inflammatory Molecule from a Curry Spice on the Path to Cancer Treatment. Molecules, 2011. **16**(6): p. 4567.

CHAPTER 8 GENERAL DISCUSSION

The major problem encountered at the beginning of this work was to obtain the cellulose nanocrystals (CNCs) required to carry out the initial objectives of this project. Because of intellectual property issues, it took almost two years for the agreement between FPInnovations and Polytechnique Montreal to be signed. Hence the first part of the project was carried out on developing polypropylene (PP) flax fiber composites. The first challenge was choosing appropriate coupling agents to prepare composites of flax fibers and hydrophobic PP. The hydrophilicity of the coupling agent could not be too high if not it would be incompatible with PP. PPMAs were chosen as the main compatibilizers. They had to be commercially available grades with a wide range of maleic anhydride content and MFI to be qualified for a systematic study of the coupling agent. After the first phase of the project, one of these compatibilizers was chosen to be used with CNCs. Even though the PPMA with highest MA content was the most effective compatibilizer, in order to avoid plasticizing effect, a high molecular weight grade of Orevac was chosen. The higher viscosity of this polymer could help applying more mechanical energy to break the CNC agglomerates in melt mixing, but at the same time less MA groups would be available to interact with the surface of CNCs.

One other problem that may limit using lignocellulosic fibers as reinforcing agent in industry is the variable properties of different batches. Since these fibers are from natural sources they can have different length, aspect ratio and mechanical properties depending on the source, cultivation and harvest time and also preparation methods. Using different batches of these fibers can produce composites with different mechanical properties, which is not desirable on an industrial scale. In this study, all the samples were prepared from the same batch.

One of the drawbacks of cellulosic fillers for reinforcing conventional hydrophobic polymers like PP or PE is their hydrophilicity. Even though the inter-particle and intra-particle hydrogen bonding is one of the reasons of their extraordinary mechanical properties, they cause re-aggregation of particles and their high tendency to absorb moisture. CNCs are produced in aqueous suspensions. In order to make CNCs suitable for melt mixing they have to be dried. Despite using freeze-dryer or spray-dryer the final samples consist of agglomerates that cannot be dispersed to the level of individual CNCs without using appropriate solvents and high mechanical forces. Using compatibilizers like PPMA can be an effective method to disperse CNCs in PP. The compatibilizer should diffuse into the large agglomerates of CNCs and break them, which is a time consuming

process and also needs high mechanical forces. On the other hand as the size of the agglomerates is decreased, the required energy for their dispersion drastically increases. This results in a composite of bundles of a few CNC whiskers. Due to the limitation in mechanical shear force, further dispersion of CNCs will not be possible in an internal mixer or typical extruder.

Another parameter that can decrease the surface energy of CNCs is a higher process temperature, which also results in a decrease of the interfacial tension between the polymer and CNCs and improves compatibility and dispersion [89]. The degradation temperature of CNCs is around 275 °C, which limits using these particles with polymers like polyamide or PET. Increasing the temperature increases the chance of degradation for the polymer and nanoparticles. Also the decreased viscosity of the matrix results in a lower mechanical force to break the agglomerates. Finding the optimum process temperature based on the molecular weight of the matrix without degrading CNCs is a key issuer in developing CNC composites via melt mixing.

In order to have a good dispersion of CNCs in the polymer matrix without surface modification using a solvent-based approach and the choice of the solvent are crucial. For hydrophobic polymers like PP or polyethylene (PE) finding a common polar solvent with CNCs is not an option. Even the compatibilizers like PPMA of typical molecular weight do not have a conventional polar solvent. This makes solvent casting an impossible option to prepare masterbatches. For other non-water soluble polymers like PLA some aprotic solvents like N, N-dimethylformamide (DMF) or dimethyl sulfoxide (DMSO) can be used to prepare a masterbatch. DMF has an evaporating temperature of 152-154 °C, whereas the evaporation temperature of DMSO is around 189 °C under atmospheric pressure. DMF can be an easier solvent to evaporate in preparing CNC nanocomposites, but it can be adsorbed through the skin and cause liver damage and other adverse health problems. On the other hand, DMSO has been widely used in pharmaceutical applications, which can open new windows of opportunities for using CNCs in biomedical applications. For the samples prepared via solvent casting of DMSO, a small trace of the solvent stays in the nanocomposite, but it doesn’t present hazard risks. The problem that makes the solvent casting method non-favorable on an industrial scale is the cost of solvent evaporation and recovery; also for cases where a solvent beside water is used, the risks of pollution and health problems come into the picture.

Chemical surface modification of cellulosic filler is another option for compatibilizing them with hydrophobic polymers. Most of the surface modifications include using solvent and expensive chemicals, which increases the cost of production for CNCs. Since most surface modifications

change partially the surface, they can cause heterogeneity in surface properties of the particles, especially if the degree of substitution is low. Besides, in some surface modifications the sulfate half-ester groups will be substituted by chains of few carbons. This desulfation can cause difficulty in re-dispersing the particles in a solvent after surface modification since the electrostatic repulsion, which helps stabilizing CNC suspension, does not exist anymore. Also, the short chains grafted to the surface of CNCs can decrease the degradation temperature of the modified particles. For our modified CNCs (mCNCs) the degradation temperature decreased from 275 to 165 °C, which limits incorporating mCNCs in different polymeric matrices like PP. In order to improve the stress transfer between the matrix and particles, it is important to have long enough chains grafted to the CNC surface to entangle with the matrix chains.

CHAPTER 9 CONCLUSION AND RECOMMENDATIONS

9.1 Conclusions

This aim of this research was to investigate different cellulosic-based particles and their potential uses in reinforcing biocomposites. To do so, polypropylene as a common, commercial matrix was chosen to prepare composites via melt mixing, and polylactide, which is the most well-known biopolymer, was employed to study the CNC behavior in suspensions. In the first phase the compatibility between flax fibers and PP was improved by using PPMA and PPAA. Different grades of PPMA with different MA contents and molecular weights were chosen. The rheological, mechanical and morphological behavior of different samples were compared. The main conclusions of this phase are:

1- Melt mixing decreases the length of flax fibers by almost 70%.
2- Compatibilizers like PPMA and PPAA can have a plasticization effect. The balance between enhanced polymer/filler interaction and extent of plasticization determines the overall rheological behavior of the composite.
3- The optimum content for PPMA to have the most efficient compatibilization depends on MA content and MFI of the compatibilizer.
4- Using low molecular weight PPMA with high MA content besides giving better mechanical properties can reduce the energy consumption during mixing.

The second phase focused on composites of CNCs and PP prepared via melt mixing. Like the first phase, PPMA was used as the compatibilizer. Two different temperatures were chosen for the compounding and two different molecular weight PPs were used. For the sake of comparing different melt mixing methods, a twin-screw extruder was used to prepare one of the samples. The transparency and mechanical properties of composites based on CNCs and flax fibers were compared. The main conclusions of this phase are:

1- Rheological properties showed that processing at high temperature (210 $^{\circ}$C) cause the degradation of the matrix in the presence of CNCs.
2- PPMA is an effective compatibilizer for PP/CNC composite. The composites prepared via melt mixing with aid of PPMA consisted of small fibrillar particles composed of few nanowhiskers.
3- For the higher molecular weight PP-based composites, a lower processing temperature favors the dispersion of CNCs and by adding 2 wt% CNC Young modulus increases by

35% in comparison to the matrix. For the lower molecular weight PP, processing at higher temperature results in better dispersion and tensile strength and modulus increased by 10 and 23 %, respectively in comparison to the neat matrix.

4- CNCs increase the crystal content of high molecular weight PP by 15% by acting as a heterogeneous nucleating agent.
5- The composite prepared via twin-screw extrusion exhibits an improved dispersion and incorporating 2 wt% CNC results in 20 and 15% increase in tensile modulus and strength in comparison to unfilled matrix, respectively.
6- The normalized modulus of the composites containing 2 wt% CNCs is equivalent to the composite reinforced with 10 wt% flax fibers. Strain at break is improved considerably from 0.06 of the matrix for brittle PP/ flax composites to 43 and 73% of the matrix for high and low molecular weight PP/CNC composites, respectively.

In the last phase the rheological properties of CNCs and modified CNCs (mCNCs) in suspension of a polar solvent were compared. PLA, as the most known biobased polymer was used to study the change in rheological properties of CNC and mCNC suspensions. A sonicator bath was used to prepare CNC and mCNC samples in DMSO. The main conclusions of this phase are:

1- Cellulose nanocrystals can be modified via grafting an organic acid chloride on the surface of the nanoparticles.
2- Aging of CNC suspensions in DMSO at 70 °C causes gel formation of nanoparticles at very low concentration (1 wt%) after one day, but aging at room temperature does not change the rheological properties significantly.
3- For modified CNCs a weak gel is formed from the first day at low and high temperatures and the change in the viscosity after 24 hours is marginal for both temperatures.
4- Adding PLA to CNC and mCNC suspensions increases the complex viscosity and storage modulus of the samples.
5- The reduced complex viscosity and storage modulus of CNC/PLA and mCNC/PLA with respect to the properties of the solvent are considerably lower compared to suspensions in the neat DMSO. This can be due to negative interaction of the PLA chains with the nanoparticles and decreased influence of the Brownian motion.

9.2 Original contributions

In the first phase of this project PP grafted acrylic acid and different PP grafted maleic anhydrides were used as compatibilizers for PP/flax fiber composite. The optimum concentration of each compatibilizer was verified. The most crucial parameters affecting quality of dispersion, rheological behavior and mechanical properties were determined separately. Taking into consideration the fiber morphology, rheological behavior, mechanical properties and quality of dispersion and correlating all of them in different systems is the originality of this phase.

In the second phase PP/CNC composites were prepared via melt mixing. PPMA was used as the compatibilizer for this system. Besides compatibilization by surface modification or using a compatibilizer, other parameters like process temperature or molecular weight of the matrix can play an important role on the quality of dispersion and mechanical properties of the composite. Increasing the temperature can decrease the surface energy of the particles. The molecular weight of the matrix can affect the chain mobility and mechanical force applied from the matrix to the agglomerates during melt mixing. To the best of our knowledge this is the first study on PP/CNC melt mixing that took into consideration these effects.

The third phase of the project aimed to have a better understanding of CNCs' potential as reinforcement for biocomposites. A successful grafting of an organic acid chloride was performed on the surface of CNC. The rheological properties of CNC and modified CNC were studied in DMSO. Ageing the suspension of very low content of CNC (1 wt%) formed a gel at elevated temperatures. To the best of our knowledge this is the first study on the evolution of rheological properties of CNC suspension in a non-aqueous polar solvent at different temperatures. Also the originality of this work is using DMSO, a safe solvent for pharmaceutical applications, as the media for gel formation of CNC.

Moreover the influence of PLA on gel formation of CNC and mCNC was studied via rheological measurements.

9.3 Recommendations

This study covers a vast domain on the use of cellulosic-based fillers to produce biocomposites. Composites of cellulose nanocrystals were compared to composites prepared from micro-scale cellulosic fibers in melt mixing. The rheological behavior of suspensions of nanoparticles was investigated. However, there are some aspects that can be explored with interest in future studies:

1- Using a commercially available reactive compatibilizer like poly (ethylene-co-glycidyl methacrylate) can improve the dispersion and mechanical properties of composites based on flax fibers and CNCs produced via melt mixing. In order to help the dispersion in PP and avoid phase separation between the matrix and compatibilizer, it will be better to produce PP grafted glycidyl methacrylate in the laboratory.
2- Finding a method to graft longer chains of carbon on the surface of CNCs can help producing modified CNCs interacting more with the polymer matrix. Studying the optimum chain length in order to have the most efficient surface modification can be interesting as well.
3- Studying the physical and chemical properties of new CNC/DMSO gels produced in this study, besides their biocompatibility and toxicity, can help finding CNC applications in the biomedical domain.
4- It has been reported in the third phase of this project, and also previous studies, that the interface of PLA/CNC is not strong. A compatibilizer like PLA grafted maleic anhydride could be used in solvent casting and melt mixing to improve the interface of the PLA/CNC nanocomposites.

REFERENCES

[1] J. Biagiotti, S. Fiori, L. Torre, M. A. López-Manchado, and J. M. Kenny, "Mechanical properties of polypropylene matrix composites reinforced with natural fibers: A statistical approach.," *Polymer Composites,* vol. 25, pp. 26-36, 2004.

[2] K. Oksman, A. P. Mathew, R. Långström, B. Nyström, and K. Joseph, "The influence of fibre microstructure on fibre breakage and mechanical properties of natural fibre reinforced polypropylene.," *Composites Science and Technology,* vol. 69, pp. 1847-1853, 2009.

[3] M. Soleimani, L. Tabil, S. Panigrahi, and A. Opoku, "The Effect of Fiber Pretreatment and Compatibilizer on Mechanical and Physical Properties of Flax Fiber-Polypropylene Composites.," *Journal of Polymers and the Environment,* vol. 16, pp. 74-82, 2008.

[4] B. Wielage, T. Lampke, H. Utschick, and F. Soergel, "Processing of natural-fibre reinforced polymers and the resulting dynamic–mechanical properties.," *Journal of Materials Processing Technology*, vol. 139, pp. 140-146, 2003.

[5] A. K. Bledzki and J. Gassan, "Composites reinforced with cellulose based fibres.," *Progress in Polymer Science,* vol. 24, pp. 221–274, 1999.

[6] N. M. Barkoula, S. K. Garkhail, and T. Peijs, "Effect of Compounding and Injection Molding on the Mechanical Properties of Flax Fiber Polypropylene Composites.," *Journal of Reinforced Plastics and Composites,* vol. 29, pp. 1366-1385, 2009.

[7] P. Mingzhu, S. Y. Zhang, and Z. Dingguo, "Preparation and Properties of Wheat Straw Fiber-polypropylene Composites. Part II. Investigation of Surface Treatments on the Thermo-mechanical and Rheological Properties of the Composites.," *Journal of Composite Materials,* vol. 44, pp. 1061-1073, 2009.

[8] P. Hajji, J. Y. Cavaillé, V. Favier, C. Gauthier, and G. Vigier, "Tensile behavior of nanocomposites from latex and cellulose whiskers.," *Polymer Composites,* vol. 17, pp. 612-619, 1996.

[9] M. Roohani, Y. Habibi, N. M. Belgacem, G. Ebrahim, A. N. Karimi, and A. Dufresne, "Cellulose whiskers reinforced polyvinyl alcohol copolymers nanocomposites.," *European Polymer Journal,* vol. 44, pp. 2489-2498, 2008.

[10] M. A. S. Azizi Samir, F. Alloin, J.-Y. Sanchez, and A. Dufresne, "Cellulose nanocrystals reinforced poly(oxyethylene)." *Polymer,* vol. 45, pp. 4149-4157, 2004.

[11] B. Braun and J. R. Dorgan, "Single-Step Method for the Isolation and Surface Functionalization of Cellulosic Nanowhiskers," *Biomacromolecules,* vol. 10, pp. 334-341, 2009/02/09 2009.

[12] A. L. Goffin, J. M. Raquez, E. Duquesne, G. Siqueira, Y. Habibi, A. Dufresne, *et al.*, "Poly(ε-caprolactone) based nanocomposites reinforced by surface-grafted cellulose nanowhiskers via extrusion processing: Morphology, rheology, and thermo-mechanical properties," *Polymer,* vol. 52, pp. 1532-1538, 3/23/ 2011.

[13] Y. Habibi, A.-L. Goffin, N. Schiltz, E. Duquesne, P. Dubois, and A. Dufresne, "Bionanocomposites based on poly(?-caprolactone)-grafted cellulose nanocrystals by ring-opening polymerization," *Journal of Materials Chemistry,* vol. 18, pp. 5002-5010, 2008.

[14] G. Morandi, L. Heath, and W. Thielemans, "Cellulose Nanocrystals Grafted with Polystyrene Chains through Surface-Initiated Atom Transfer Radical Polymerization (SI-ATRP)," *Langmuir,* vol. 25, pp. 8280-8286, 2009/07/21 2009.

[15] B. Poaty, V. Vardanyan, L. Wilczak, G. Chauve, and B. Riedl, "Modification of cellulose nanocrystals as reinforcement derivatives for wood coatings," *Progress in Organic Coatings,* vol. 77, pp. 813-820, 2014.

[16] A. Junior de Menezes, G. Siqueira, A. A. S. Curvelo, and A. Dufresne, "Extrusion and characterization of functionalized cellulose whiskers reinforced polyethylene nanocomposites," *polymer,* vol. 50, pp. 4552-4563, 2009.

[17] S. Spinella, C. Samuel, J.-M. Raquez, S. A. McCallum, R. Gross, and P. Dubois, "Green and Efficient Synthesis of Dispersible Cellulose Nanocrystals in Biobased Polyesters for Engineering Applications," *ACS Sustainable Chemistry & Engineering,* vol. 4, pp. 2517-2527, 2016/05/02 2016.

[18] S. Kalia, A. Dufresne, B. M. Cherian, B. S. Kaith, Av, #233, *et al.*, "Cellulose-Based Bio- and Nanocomposites: A Review," *International Journal of Polymer Science,* vol. 2011, 2011.

[19] E. Twite-Kabamba, A. Mechraoui, and D. Rodrigue, "Rheological properties of polypropylene/hemp fiber composites.," *Polymer Composites,* vol. 30, pp. 1401-1407, 2009.

[20] N. Ljungberg, C. Bonini, F. Bortolussi, C. Boisson, L. Heux, and J. Y. Cavaille, "New Nanocomposite Materials Reinforced with Cellulose Whiskers in Atactic Polypropylene:

Effect of Surface and Dispersion Characteristics.," *Biomacromolecules,* vol. 6, pp. 2732-2739, 2005.

[21] H. M. Hassanabadi, A. Alemdar, and D. Rodrigue, "Polypropylene reinforced with nanocrystalline cellulose: Coupling agent optimization," *Journal of Applied Polymer Science,* vol. 132, p. 42438, 2015.

[22] A. K. Mohanty, M. Misra, and L. T. Drzal, *Natural fibers, biopolymers, and biocomposites*: CRC, 2005.

[23] S. Kalia, B. S. Kaith, and I. Kaur, "Pretreatments of natural fibers and their application as reinforcing material in polymer composites-A review," *Polymer Engineering & Science,* vol. 49, pp. 1253-1272, 2009.

[24] A. Bismarck, S. Mishra, and T. Lampke, "Plant Fibers as Reinforcement for Green Composites.," in *Natural Fibers, Biopolymers, and Biocomposites.*, ed: CRC Press Taylor & Francis Group, 2005, pp. 37-108.

[25] R. Malkapuram, V. Kumar, and Y. S. Negi, "Recent Development in Natural Fiber Reinforced Polypropylene Composites.," *Journal of reinforced plastics and composites,* vol. 28, pp. 1169-1189, 2008.

[26] B. L. Peng, N. Dhar, H. L. Liu, and K. C. Tam, "Chemistry and applications of nanocrystalline cellulose and its derivatives: A nanotechnology perspective.," *The Canadian Journal of Chemical Engineering,* vol. 89, pp. 1191-1206, 2011.

[27] S. K. Garkhail, "Composites Based on Natural Fibers and Thermoplastic Matrices-thesis," PhD, Department of Material,

Queen Mary College University of London, London, 2001.

[28] F. A. My Ahmed Said Azizi Samir, and Alain Dufresne, "Review of Recent Research into Cellulosic Whiskers, Their Properties and Their Application in Nanocomposite Field," *Biomacromolecules,* vol. 6, 2005.

[29] H. C. V. Favier, and J. Y. Cavaille, "Polymer Nanocomposites Reinforced by Cellulose Whiskers," *Macromolecules,* vol. 28, pp. 6365-6367, 1995.

[30] O. van den Berg, J. R. Capadona, and C. Weder, "Preparation of Homogeneous Dispersions of Tunicate Cellulose Whiskers in Organic Solvents," *Biomacromolecules,* vol. 8, pp. 1353-1357, 2007/04/01 2007.

[31] D. Liu, X. Chen, Y. Yue, M. Chen, and Q. Wu, "Structure and rheology of nanocrystalline cellulose.," *Carbohydrate Polymers,* vol. 84, pp. 316-322, 2011.

[32] P. Lu and Y.-L. Hsieh, "Preparation and properties of cellulose nanocrystals: Rods, spheres, and network," *Carbohydrate Polymers,* vol. 82, pp. 329-336, 2010.

[33] F. Alloin, A. D'Aprea, A. Dufresne, N. Kissi, and F. Bossard, "Poly(oxyethylene) and ramie whiskers based nanocomposites: influence of processing: extrusion and casting/evaporation.," *Cellulose,* vol. 18, pp. 957-973, 2011.

[34] B. C. Barkakaty, "Some structural aspects of sisal fibers.," *Journal of Applied Polymer Science,* vol. 20, pp. 2921-2940, 1976.

[35] A. Arias, M.-C. Heuzey, and M. A. Huneault, "Thermomechanical and crystallization behavior of polylactide-based flax fiber biocomposites.," *Cellulose,* vol. 20, pp. 439-452, 2012.

[36] B. Alexander, M. Supriya, and L. Thomas, "Plant Fibers as Reinforcement for Green Composites.," in *Natural Fibers, Biopolymers, and Biocomposites.*, ed: CRC Press, 2005.

[37] S. Garkhail, R. Heijenrath, and T. Peijs, "Mechanical properties of natural-fibre-mat-reinforced thermoplastics based on flax fibres and polypropylene.," *Applied Composite Materials,* vol. 7, pp. 351-372, 2000.

[38] S. M. Luz, A. R. Gonçalves, and A. P. Del'Arco, "Mechanical behavior and microstructural analysis of sugarcane bagasse fibers reinforced polypropylene composites.," *Composites Part A: Applied Science and Manufacturing,* vol. 38, pp. 1455-1461, 2007.

[39] H. Hagen, J. Boersma, and G. van Koten, "Homogeneous vanadium-based catalysts for the Ziegler-Natta polymerization of [small alpha]-olefins," *Chemical Society Reviews,* vol. 31, pp. 357-364, 2002.

[40] S. K. Nayak, S. Mohanty, and S. K. Samal, "Influence of short bamboo/glass fiber on the thermal, dynamic mechanical and rheological properties of polypropylene hybrid composites.," *Materials Science and Engineering: A,* vol. 523, pp. 32-38, 2009.

[41] D. Puglia, A. Terenzi, S. E. Barbosa, and J. M. Kenny, "Polypropylene-natural fibre composites. Analysis of fibre structure modification during compounding and its influence on the final properties.," *Composite Interfaces,* vol. 15, pp. 111-129, 2008.

[42] G. Kalaprasad, G. Mathew, C. Pavithran, and S. Thomas, "Melt Rheological Behavior of Intimately Mixed Short Sisal–Glass Hybrid Fiber-Reinforced Low-Density Polyethylene

Composites. I. Untreated Fibers.," *Journal of Applied Polymer Science,* vol. 89, pp. 432-442, 2003.

[43] C. Mobuchon, P. J. Carreau, M.-C. Heuzey, M. Sepehr, and G. Ausias, "Shear and extensional properties of short glass fiber reinforced polypropylene.," *Polymer Composites,* vol. 26, pp. 247-264, 2005.

[44] J. K. Kim and J. H. Song, "Rheological properties and fiber orientations of short fiber-reinforced plastics.," *Journal of Rheology,* vol. 41, pp. 1069-1078, 1997.

[45] C. González-Sánchez, C. Fonseca-Valero, A. Ochoa-Mendoza, A. Garriga-Meco, and E. Rodríguez-Hurtado, "Rheological behavior of original and recycled cellulose–polyolefin composite materials.," *Composites Part A: Applied Science and Manufacturing,* vol. 42, pp. 1075-1083, 2011.

[46] G. M. G. Kalaprasad, C. Pavithran, Sabu Thomas, "Melt Rheological Behavior of Intimately Mixed Short Sisal–Glass Hybrid Fiber-Reinforced Low-Density Polyethylene Composites. I. Untreated Fibers," *Journal of Applied Polymer Science,* vol. 89, 2003.

[47] Y.-H. Feng, D.-W. Zhang, J.-P. Qu, H.-Z. He, and B.-P. Xu, "Rheological properties of sisal fiber/poly(butylene succinate) composites," *Polymer Testing,* vol. 30, pp. 124-130, 2011.

[48] J. George, R. Janardhan, J. S. Anand, S. S. Bhagawan, and S. Thomas, "Melt rheological behaviour of short pineapple fibre reinforced low density polyethylene composites," *Polymer,* vol. 37, pp. 5421-5431, 1996.

[49] T. Q. Li and M. P. Wolcott, "Rheology of wood plastics melt. Part 1. Capillary rheometry of HDPE filled with maple.," *Polymer Engineering & Science,* vol. 45, pp. 549-559, 2005.

[50] J. Ferec, M. Heuzey, G. Ausias, and P. Carreau, "Rheological behavior of fiber-filled polymers under large amplitude oscillatory shear flow," *Journal of Non-Newtonian Fluid Mechanics,* vol. 151, pp. 89-100, 2008.

[51] A. Arias, H. Sojoudiasli, M.-C. Heuzey, M. A. Huneault, and P. Wood-Adams, "Rheological study of crystallization behavior of polylactide and its flax fiber composites," *Journal of Polymer Research,* vol. 24, p. 46, 2017.

[52] V. Hristov and J. Vlachopoulos, "Influence of Coupling Agents on Melt Flow Behavior of Natural Fiber Composites.," *Macromolecular Materials and Engineering,* vol. 292, pp. 608-619, 2007.

[53] N. Le Moigne, M. van den Oever, and T. Budtova, "Dynamic and capillary shear rheology of natural fiber-reinforced composites.," *Polymer Engineering & Science,* vol. 53, pp. 2582-2593, 2013.

[54] M. Khalid, A. Salmiaton, T. Chuah, C. Ratnam, and S. T. Choong, "Effect of MAPP and TMPTA as compatibilizer on the mechanical properties of cellulose and oil palm fiber empty fruit bunch–polypropylene biocomposites.," *Composite Interfaces,* vol. 15, pp. 251–262, 2008.

[55] X. Tu, R. A. Young, and F. Denes, "Improvement of bonding between cellulose and polypropylene by plasma treatment," *Cellulose,* vol. 1, pp. 87-106, 1994.

[56] H. P. Rensch and B. Riedl, "Characterization of chemically modified chemithermomechanical pulp by thermal analysis. Part 1. Treatment with anhydrides.," *Thermochimica Acta,* vol. 205, pp. 39-49, 1992.

[57] A. Arbelaiz, B. Fernández, J. A. Ramos, A. Retegi, R. Llano-Ponte, and I. Mondragon, "Mechanical properties of short flax fibre bundle/polypropylene composites: Influence of matrix/fibre modification, fibre content, water uptake and recycling.," *Composites science and technology,* vol. 65, pp. 1582-1592, 2005.

[58] P. Jandura, B. V. Kokta, and B. Riedl, "Cellulose Fibers/Polyethylene Hybrid Composites: Effect of Long Chain Organic Acid Cellulose Esters and Organic Peroxide on Rheology and Tensile Properties," *Journal of Reinforced Plastics and Composites,* vol. 20, pp. 697-717, 2001.

[59] P. Uschanov, L.-S. Johansson, S. L. Maunu, and J. Laine, "Heterogeneous modification of various celluloses with fatty acids," *Cellulose,* vol. 18, pp. 393-404, 2010.

[60] J. George, M. S. Sreekala and T. Sabu, "A Review on Interface Modification and Characterization of Natural Fiber Reinforced Plastic Composites," *POLYMER ENGINEERING AND SCIENCE,* vol. 41, 2001.

[61] R. Li, L. Ye, and Y.-W. Mai, "Application of plasma technologies in fibre-reinforced polymer composites: a review of recent developments," *Composites Part A,* vol. 28A, pp. 73-86, 1997.

[62] G. Siqueira, J. Bras, and A. Dufresne, "New process of chemical grafting of cellulose nanoparticles with a long chain isocyanate," *Langmuir : the ACS journal of surfaces and colloids,* vol. 26, pp. 402-411, 2010.

[63] A. Arbelaiz, B. Fernández, G. Cantero, R. Llano-Ponte, A. Valea, and I. Mondragon, "Mechanical properties of flax fibre/polypropylene composites. Influence of fibre/matrix modification and glass fibre hybridization.," *Composites Part A: Applied Science and Manufacturing,* vol. 36, pp. 1637-1644, 2005.

[64] G. Cantero, A. Arbelaiz, R. Llano-Ponte, and I. Mondragon, "Effects of fibre treatment on wettability and mechanical behaviour of flax/polypropylene composites.," *Composites Science and Technology,* vol. 63, pp. 1247-1254, 2003.

[65] K. Oksman and C. Clemons, "Mechanical Properties and Morphology of Impact Modified Polypropylene-Wood Flour Composites.," *Journal of Applied Polymer Science,* vol. 67, pp. 1503-1513, 1998.

[66] K. V. d. Velde and P. Kiekens, "Influence of Fibre and Matrix Modifications on Mechanical and Physical Properties of Flax Fibre Reinforced Poly(propylene)." *Macromolecular Materials and Engineering,* vol. 4, pp. 237-242, 2001.

[67] T. Paunikallio, J. Kasanen, M. Suvanto, and T. T. Pakkanen, "Influence of Maleated Polypropylene on Mechanical Properties of Composite Made of Viscose Fiber and Polypropylene.," *Journal of Applied Polymer Science,* vol. 87, pp. 1895–1900, 2003.

[68] T. J. Keener, R. K. Stuart, and T. K. Brown, "Maleated coupling agents for natural fibre composites.," *Composites Part A: Applied Science and Manufacturing,* vol. 35, pp. 357-362, 2004.

[69] W. Qiu, T. Endo, and T. Hirotsu, "Interfacial interaction, morphology, and tensile properties of a composite of highly crystalline cellulose and maleated polypropylene.," *Journal of Applied Polymer Science,* vol. 102, pp. 3830-3841, 2006.

[70] R. Gauthier, C. Joly, A. C. Coupas, H. Gauthier, and M. Escoubes, "Interfaces in polyolefin/cellulosic fiber composites: Chemical coupling, morphology, correlation with adhesion and aging in moisture.," *Polymer Composites,* vol. 19, pp. 287-300, 1998.

[71] M. Roman and W. T. Winter, "Effect of Sulfate Groups from Sulfuric Acid Hydrolysis on the Thermal Degradation Behavior of Bacterial Cellulose.," *Biomacromolecules,* vol. 5, pp. 1671-1677, 2004.

[72] B. Derakhshandeh, G. Petekidis, S. Shafiei Sabet, W. Y. Hamad, and S. G. Hatzikiriakos, "Ageing, yielding, and rheology of nanocrystalline cellulose suspensions," *Journal of Rheology,* vol. 57, pp. 131-148, 2013.

[73] J. Araki, M. Wada, S. Kuga, and T. Okano, "Flow properties of microcrystalline cellulose suspension prepared by acid treatment of native cellulose," *Colloids and Surfaces A: Physicochemical and Engineering Aspects,* vol. 142, pp. 75-82, 11/30/ 1998.

[74] S. Onogi and T. Asada, "Rheology and Rheo-Optics of Polymer Liquid Crystals," in *Rheology: Volume 1: Principles*, G. Astarita, G. Marrucci, and L. Nicolais, Eds., ed Boston, MA: Springer US, 1980, pp. 127-147.

[75] M. Bercea and P. Navard, "Shear Dynamics of Aqueous Suspensions of Cellulose Whiskers," *Macromolecules,* vol. 33, pp. 6011-6016, 2000/08/01 2000.

[76] S. Shafiei-Sabet, W. Y. Hamad, and S. G. Hatzikiriakos, "Rheology of Nanocrystalline Cellulose Aqueous Suspensions," *Langmuir,* vol. 28, pp. 17124-17133, 2012/12/11 2012.

[77] M. Hasani, E. D. Cranston, G. Westman, and D. G. Gray, "Cationic surface functionalization of cellulose nanocrystals," *Soft Matter,* vol. 4, pp. 2238-2244, 2008.

[78] D. Bagheriasl, P. J. Carreau, B. Riedl, C. Dubois, and W. Y. Hamad, "Shear rheology of polylactide (PLA)–cellulose nanocrystal (CNC) nanocomposites," *Cellulose,* vol. 23, pp. 1885-1897, 2016.

[79] D. Viet, S. Beck-Candanedo, and D. G. Gray, "Dispersion of cellulose nanocrystals in polar organic solvents," *Cellulose,* vol. 14, pp. 109-113, 2007.

[80] H. Chang, J. Luo, A. A. Bakhtiary Davijani, A.-T. Chien, P.-H. Wang, H. C. Liu, *et al.*, "Individually Dispersed Wood-Based Cellulose Nanocrystals," *ACS Applied Materials & Interfaces,* vol. 8, pp. 5768-5771, 2016.

[81] L. C. Fidale, N. Ruiz, T. Heinze, and O. A. E. Seoud, "Cellulose Swelling by Aprotic and Protic Solvents: What are the Similarities and Differences?," *Macromolecular Chemistry and Physics,* vol. 209, pp. 1240-1254, 2008.

[82] N. Ljungberg, C. Bonini, F. Bortolussi, C. Boisson, L. Heux, and Cavaillé, "New Nanocomposite Materials Reinforced with Cellulose Whiskers in Atactic Polypropylene: Effect of Surface and Dispersion Characteristics," *Biomacromolecules,* vol. 6, pp. 2732-2739, 2005/09/01 2005.

[83] M. N. Anglès and A. Dufresne, "Plasticized Starch/Tunicin Whiskers Nanocomposites. 1. Structural Analysis.," *Macromolecules,* vol. 33, pp. 8344-8353, 2000.

[84] L. Zhou, H. He, M.-C. Li, K. Song, H. N. Cheng, and Q. Wu, "Morphological influence of cellulose nanoparticles (CNs) from cottonseed hulls on rheological properties of polyvinyl alcohol/CN suspensions," *Carbohydrate Polymers,* vol. 153, pp. 445-454, 11/20/ 2016.

[85] I. Kvien, B. S. Tanem, and K. Oksman, "Characterization of Cellulose Whiskers and Their Nanocomposites by Atomic Force and Electron Microscopy.," *Biomacromolecules,* vol. 6, pp. 3160-3165, 2005.

[86] A. Arias, M.-C. Heuzey, M. A. Huneault, G. Ausias, and A. Bendahou, "Enhanced dispersion of cellulose nanocrystals in melt-processed polylactide-based nanocomposites.," *Cellulose,* vol. 22, pp. 483-498, 2014.

[87] N. Ljungberg, J. Cavaille, and L. Heux, "Nanocomposites of isotactic polypropylene reinforced with rod-like cellulose whiskers.," *Polymer,* vol. 47, pp. 6285-6292, 2006.

[88] M. R. Kamal and V. Khoshkava, "Effect of Cellulose Nanocrystals (CNC) on Rheological and Mechanical Properties and Crystallization Behavior of PLA/CNC Nanocomposites.," *Carbohydrate Polymers,* vol. 123, pp. 105-114, 2015.

[89] V. Khoshkava and M. R. Kamal, "Effect of surface energy on dispersion and mechanical properties of polymer/nanocrystalline cellulose nanocomposites.," *Biomacromolecules,* vol. 14, pp. 3155-63, 2013.

[90] A. C. Corrêa, E. de Morais Teixeira, V. B. Carmona, K. B. R. Teodoro, C. Ribeiro, L. H. C. Mattoso, *et al.*, "Obtaining nanocomposites of polyamide 6 and cellulose whiskers via extrusion and injection molding.," *Cellulose,* vol. 21, pp. 311-322, 2013.

[91] K. Ben Azouz, E. C. Ramires, W. Van den Fonteyne, N. El Kissi, and A. Dufresne, "Simple Method for the Melt Extrusion of a Cellulose Nanocrystal Reinforced Hydrophobic Polymer.," *ACS Macro Letters,* vol. 1, pp. 236-240, 2012/01/17 2011.

[92] N. L. Garcia de Rodriguez, W. Thielemans, and A. Dufresne, "Sisal cellulose whiskers reinforced polyvinyl acetate nanocomposites.," *Cellulose,* vol. 13, pp. 261-270, 2006.

[93] A. Junior de Menezes, G. Siqueira, A. A. S. Curvelo, and A. Dufresne, "Extrusion and characterization of functionalized cellulose whiskers reinforced polyethylene nanocomposites.," *Polymer,* vol. 50, pp. 4552-4563, 2009.

[94] V. Favier, J. Y. Cavaille, G. R. Canova, and S. C. Shrivastava, "Mechanical Percolation in Cellulose Whisker Nanocomposites.," *Polymer Engineering & Science,* vol. 37, pp. 1732-1739, 1997.

[95] V. Khoshkava and M. R. Kamal, "Effect of Cellulose Nanocrystals (CNC) Particle Morphology on Dispersion and Rheological and Mechanical Properties of Polypropylene/CNC Nanocomposites," *ACS Applied Materials & Interfaces,* vol. 6, pp. 8146-8157, 2014/06/11 2014.

[96] D. Bagheriasl, P. J. Carreau, B. Riedl, and C. Dubois, "Enhanced properties of polylactide by incorporating cellulose nanocrystals," *Polymer Composites,* 2016.

[97] D. Bondeson and K. Oksman, "Polylactic acid/cellulose whisker nanocomposites modified by polyvinyl alcohol," *Composites Part A: Applied Science and Manufacturing,* vol. 38, pp. 2486-2492, 2007.

[98] D. Bagheriasl, P. J. Carreau, C. Dubois, and B. Riedl, "Properties of polypropylene and polypropylene/poly(ethylene-co-vinyl alcohol) blend/CNC nanocomposites," *Composites Science and Technology,* vol. 117, pp. 357-363, 9/29/ 2015.

[99] R. J. Moon, A. Martini, J. Nairn, J. Simonsen, and J. Youngblood, "Cellulose nanomaterials review: structure, properties and nanocomposites," *Chemical Society Reviews,* vol. 40, pp. 3941-3994, 2011.

[100] J.-G. Gwon, H.-J. Cho, S.-J. Chun, S. Lee, Q. Wu, M.-C. Li, *et al.*, "Mechanical and thermal properties of toluene diisocyanate-modified cellulose nanocrystal nanocomposites using semi-crystalline poly(lactic acid) as a base matrix," *RSC Advances,* vol. 6, pp. 73879-73886, 2016.

[101] A. Dorris and D. G. Gray, "Gelation of cellulose nanocrystal suspensions in glycerol," *Cellulose,* vol. 19, pp. 687-694, 2012.

[102] M. Chau, S. E. Sriskandha, D. Pichugin, H. Thérien-Aubin, D. Nykypanchuk, G. Chauve, *et al.*, "Ion-Mediated Gelation of Aqueous Suspensions of Cellulose Nanocrystals," *Biomacromolecules,* vol. 16, pp. 2455-2462, 2015/08/10 2015.

[103] G. Lenfant, M.-C. Heuzey, T. G. M. van de Ven, and P. J. Carreau, "A comparative study of ECNC and CNC suspensions: effect of salt on rheological properties," *Rheologica Acta,* vol. 56, pp. 51-62, 2017.

[104] X. M. Dong and D. G. Gray, "Effect of Counterions on Ordered Phase Formation in Suspensions of Charged Rodlike Cellulose Crystallites," *Langmuir,* vol. 13, pp. 2404-2409, 1997/04/01 1997.

[105] S. Beck and J. Bouchard, "Auto-catalyzed acidic desulfation of cellulose nanocrystals," *Nordic Pulp & Paper Research Journal*, vol. 29, pp. 006-014, 2014.

[106] L. Lewis, M. Derakhshandeh, S. G. Hatzikiriakos, W. Y. Hamad, and M. J. MacLachlan, "Hydrothermal Gelation of Aqueous Cellulose Nanocrystal Suspensions," *Biomacromolecules*, vol. 17, pp. 2747-2754, 2016.